Experimental Evaluation of Roll Stability Control System Effectiveness for A-double Commercial Trucks

Zachary R. Van Kat

Thesis submitted to the faculty of the Virginia Polytechnic Institute and State University in partial fulfillment of the requirements for the degree of

Master of Science
In
Mechanical Engineering

Mehdi Ahmadian, Chair
Oumar Barry
Steve C Southward

November 11th, 2021
Blacksburg, Virginia

Keywords: Articulated Heavy Vehicles, Roll Stability Control, Trailer roll angle, Lateral acceleration, Rollover

Experimental Evaluation of Roll Stability Control System Effectiveness for A-double Commercial Trucks

Zachary R. Van Kat

ABSTRACT

Some of the results of an extensive track testing program at the Center for Vehicle Systems and Safety (CVeSS) at Virginia Tech for evaluating the roll stability of commercial trucks with 33-ft A-double trailers are evaluated. The study includes straight-rail trailers with heavy and light loading conditions. Commercial trucks are more susceptible to rollovers than passenger cars because of their higher center of gravity relative to their track width. Multi-trailer articulated heavy vehicles, such as A-doubles, are particularly prone to rollovers because of their articulation and rearward amplification.

Electronic stability control (ESC) has been mandated by the National Highway Safety Administration (NHSTA) for Class 8 trucks and busses since 2017. When detecting oversteer or understeer, ESC automatically activates the brakes at the correct side of the steer and/or drive axle(s) to regain steering stability. ESC, however, often cannot sense the likelihood of trailer rollover in multi-trailer articulated heavy vehicles because of the articulation between the trailers and tractors. As a result of this, trailers are often equipped with roll stability control (RSC) systems to mitigate speed-induced rollovers. Sensing the trailer lateral acceleration, RSC activates the trailer brakes to reduce speed and lower the likelihood of rollover. However, a limited number of past studies have shown that the trailer roll angle may provide an earlier indication of a pending rollover than the lateral acceleration. This study intends to provide further analysis in this regard in an effort to improve the effectiveness of RSC systems for trailers.

An extensive amount of data from track testing with a 33-ft A-double under heavy and light loading is evaluated. Particular attention is given to lateral accelerations and trailer roll angles prior to rollover and relative to RSC activation time. The study's results indicate that the trailer roll angle provides a slightly earlier indication of rollover than lateral acceleration during dynamic driving conditions, potentially resulting in a timelier activation of RSC. Of course, detecting the roll angle is often more challenging than lateral acceleration, which can be detected with an accelerometer. Additionally, the roll angle measurement may be subjected to errors and possibly unwanted RSC engagement. The study's results further indicate that the trailer-based RSC systems effectively mitigate rollovers in both quasi-steady-state and dynamic driving conditions.

Experimental Analysis of the Effectiveness of Roll Stability Control for A-double Commercial Trucks

Zachary R. Van Kat

GENERAL AUDIENCE ABSTRACT

Some of the results of an extensive track testing program at the Center for Vehicle Systems and Safety (CVeSS) at Virginia Tech for evaluating the roll stability of commercial trucks with 33-ft A-double trailers are evaluated. "33-ft A-doubles" commonly refer to a commercial truck that has a tractor with two trailers (in this case 33-ft in length) that are connected by an A-dolly. Their modularity and ease of connecting and disconnecting at various drop stations have made such commercial vehicles a common scene on U.S. highways due to the proliferation of e-commerce cargo. Compared to a single-unit or tractor semi-trailer combination, the double- or triple-trailer configurations offer several logistical benefits that make them more advantageous. The multi-trailer vehicles can carry more cargo per driver, lowering driver, fuel, and equipment costs significantly. There are, however, some challenges to operating multi-trailer articulated vehicles. On average, their accidents are more expensive than single-trailer or single-unit trucks. Additionally, they are more susceptible to rolling over and causing property damage, injuries, and at times fatalities. To reduce rollovers, systems with automated braking, called roll stability control (RSC), are often installed on the trailers. RSC applies the trailer brakes if it senses that the vehicle speed — the primary cause of most commercial vehicle accidents — exceeds the safe limit for negotiating a turn.

In this study, we intend to evaluate the effectiveness of roll stability control (RSC) systems for reducing the likelihood of speed-induced rollovers. We will also explore ways of improving their performance. Namely, we will evaluate whether sensing the lateral acceleration of the trailer or its roll angle would provide a better means for timely activation of RSC. The study's results indicate that, although more challenging to measure, the trailer roll angle provides a slightly sooner indication of a pending rollover than lateral acceleration. The results also suggest that RSC systems vastly reduce the number of speed-induced rollovers in trucks with 33-ft A-double trailers under different trailer configurations and cargo weights.

Acknowledgements

First and foremost, I would like to thank my parents, grandparents, girlfriend, and the rest of my family for giving me their endless support throughout the years. To my parents, Karen and Ray, I cannot thank you enough. Thank you for being wonderful parents and supporting all of my ambitions and dreams since I was a young child. Additionally, I would also like to thank all my friends at CVeSS who have made my years here a great experience. In particular, I want to thank the Roll-Stability Team for all of their help and advice during my time here. I am very grateful for having the opportunity to work with such a great group of people over the last two years. Furthermore, I would like to thank Dr. Barry and Dr. Southward for serving on my committee. Last but not least, I would like to thank Dr. Ahmadian for being an amazing advisor and mentor. Without him, none of this would have been possible. Thank you for accepting me as a summer volunteer, an undergraduate research assistant, a graduate research assistant, and for teaching me so much along the way.

Contents

List of Figures

List of Tables

1. Introduction

1.1. Motivation

A vehicle overturning on the road, commonly known as rollover, is one of the most dangerous and costly accident types. Heavy vehicles, because of their heavy loads and high center of gravity relative to their track width, are especially prone to rollover compared to passenger vehicles. Rollovers are the first harmful event in 15% of fatal single-vehicle crashes involving vehicles over 10,000 lb. [1]. Furthermore, there was either a fatality or injury in 41% of all large vehicle accidents where rollover was the first harmful event [1]. Although rollover is not the most common cause of heavy vehicle accidents, a large proportion of accidents involving rollover result in either a fatality or injury. For vehicles greater than 10,000 lb., rollover is the first harmful event in 2.0% of all accidents; however, it is the cause of 4.2% of fatal accidents [1]. While rollovers are dangerous to both the driver and occupants of other vehicles, they also result in large amounts of property damage. A rollover has the potential to severely damage the overturned vehicle, the vehicle's cargo, other vehicles, road infrastructure, and the environment. Because of the large amounts of property damage and high percentages of injury and death, rollover accidents can be costly. In 2007, an FMCSA report was released stating that the estimated average cost (in 2021 U.S. dollars) of police-reported crashes from 2001-2003 involving vehicles with GVWR greater than 10,000 lb. was $127,557 [2]. The average cost of non-fatal injury crashes was $273,361 and fatal crashes was $5,046,325 [2]. Because of the high percentage of injury or death in rollover crashes, a rollover crash is more likely to have a high cost than other types of heavy vehicle accidents. For these reasons, there has been a lot of focus on mitigating the occurrence of heavy vehicle rollovers in the last 50 years.

Rollover mitigation efforts have focused on increasing the static roll stability of heavy vehicles, passive electronic warning systems to alert the driver of an impending rollover, and active electronic control systems that will manipulate the vehicle dynamics to avoid rollover. The first method to reduce rollover was passive road signs. These road signs alert the vehicle to turns with a high rollover probability if taken at excessive speeds. In later

years, active road signs were used to alert drivers that they were moving too fast into the turn and must slow down to complete the turn without rolling over. Some of these systems consider vehicle speed and weight when issuing warnings to individual vehicles [3]. Another innovation in heavy vehicle stability was tractor-based electronic stability control (ESC) systems. In 2015, the NHSTA passed FMVSS 136, which required all new truck/tractors to be equipped with ESC systems [4]. Some ESC systems are comprised of two subsystems, roll stability control and yaw stability control. In a 2009 study, it was determined that if all 5-axle tractor-semitrailers operating on US roads were fitted with ESC, the rollover safety benefits are a reduction in 3,489 crashes, 106 fatalities, and 4,384 injuries, and the yaw instability safety benefits are a reduction in 4,659 crashes, 126 fatalities, and 5,909 injuries [5]. In recent years, trailer-based roll stability control (RSC) was introduced to actively mitigate the rollover probability of trailers, the most susceptible unit of a heavy vehicle train to rollover. The trailer-based RSC seeks to diminish the rollover propensity of a tractor-semitrailer by acting on the trailer rather than the tractor. As articulated vehicles with multiple trailers become more common on roads today, the importance of effective trailer-based RSC systems increases.

Multiple trailer articulated heavy vehicles (AHVs) are becoming increasingly common on roads today because of the increase in cargo capacity per driver, lower driver, equipment, and gasoline costs, lower environmental impact, as well as a lower probability of accidents [6]. Although crashes with multiple trailer AHVs are the rarest of all heavy vehicle accidents, the average cost is the highest at $405,369 [2]. As the number of these vehicles on roads increases, the number of accidents can be expected to increase, as the probability of accidents is directly related to the number of miles traveled. One of the most significant issues regarding AHVs, especially when there are two or more trailers, is the decoupling of the driver from the trailer dynamics. Even professional drivers with years of experience have difficulty sensing when trailers are approaching rollover before it is too late. With additional trailers, the time delay from the tractor to the rearmost trailer and the amplification of roll dynamics increases. Multiple trailer AHVs are becoming more common, so the need for effective rollover mitigation techniques is as present as ever, in particular trailer-based, active roll stability controllers.

1.2. Objectives

This study aims to:

- Characterize semi-trailer roll dynamics under different loading conditions when connected in an A-double configuration
- Provide quantitative benefits for the implementation of trailer-based roll stability control for articulated heavy vehicles
- Determine the rollover thresholds in terms of lateral acceleration and trailer roll angle for trailers under different loading conditions
- Compare the robustness of lateral acceleration and trailer roll angle as roll indicators for RSC systems
- Compare the time-domain response of lateral acceleration and trailer roll angle in quasi-steady-state and dynamic maneuvers until the rollover limit
- Compare the consistency of lateral acceleration and trailer roll angle values at the time of RSC engagement for a commercially-available lateral-acceleration-based RSC system

1.3. Approach

To achieve the above objectives, an experimental analysis on the roll dynamics of Class 8 A-doubles was performed. A tractor and four trailers were instrumented and tested at the Transportation Research Center (TRC) in East Liberty, Ohio. In total, seven different trailer combinations, including different loading conditions and trailer configurations, were tested on track. Four unique maneuvers were used to evaluate the roll stability of the trailers, including two quasi-steady-state and two dynamic maneuvers. The maneuvers were designed to either imitate or idealize real-world rollover driving scenarios. During the testing, a commercially-available trailer RSC system was installed on both of the trailers to allow for the evaluation of the effectiveness of trailer-based RSC systems.

To evaluate the effects of different loading conditions on the rollover propensity of the A-double, the maneuver entry speeds or steering percentages at which a trailer rolled over were compared between the different loading conditions. Outriggers installed on the trailers were used to prevent complete rollover, but were also equipped with load cells,

allowing the definition of rollover for this study to be an outrigger wheel contact greater than or equal to 400 lbf. It is believed that the outrigger contact force is more indicative of absolute instability rather than relative instability as compared to unmeasured outrigger contact or wheel lift. To evaluate the effectiveness of RSC, the improvements in entry speed or steering percentage at rollover were used. Lastly, the trailers were equipped with both accelerometers and string potentiometers, measuring lateral acceleration and trailer roll angle, respectively. The robustness, time-response, and consistency of lateral acceleration and trailer roll angle were compared up to and at the rollover limits of the trailers as well as when the RSC system engaged.

1.4. Contributions

This study presents results based on the scientific evaluation of A-double roll dynamics. This study provides:

- Experimental data detailing the differences in rollover thresholds of trailers connected in an A-double configuration under different loading conditions
- Quantitative evidence showing the effectiveness of trailer-based roll stability control on trailers connected in an A-double configuration under different loading conditions
- Investigation of the effects of different trailer couplings on the rollover threshold of trailers in an A-double configuration.
- Examination of the differences in rollover threshold between quasi-steady-state maneuvers and dynamic maneuvers for semi-trailers under different loading conditions.
- Determination of the effects of semi-trailer loading on lateral acceleration and trailer roll angle at rollover
- Comparison of lateral acceleration and body roll angle as real-time indicators of semi-trailer rollover for use in trailer-based roll stability control modules
- Comparison of lateral acceleration and trailer roll angle distributions at the time of trailer-based RSC intervention for a commercially-available lateral-acceleration-based RSC system

1.5. Outline

Chapter 1 first introduces the motivation and objectives for this study. It then discusses the approach and contributions of this thesis.

Chapter 2 provides background on heavy vehicles, heavy vehicle dynamics, and electronic stability devices used on tractors and trailers. The chapter first introduces non-articulated heavy vehicles and roll dynamics, then moves forward into articulated heavy vehicle components and the dynamics of such vehicles. Lastly, the chapter discusses the electronic safety equipment utilized on heavy vehicles and how those devices affect the vehicle's stability.

Chapter 3 explains the high-speed testing study performed at the Transportation Research Center (TRC) in East Liberty, Ohio. The chapter begins with an overview of the instrumentation installed on-board the test vehicle, calibration procedures for each sensor type, the data acquisition device, the signal routing process, and the steering robot used on the test vehicle. Next, the chapter discusses the safety systems and structural components installed on the test vehicle and provides the tractor, trailer, and dolly properties with all additional systems installed. After giving an overview of the test setup, the chapter describes the maneuvers, test configurations, test environment, and the tests completed at TRC. Lastly, the data analysis and signal processing techniques used to draw conclusions from the data are discussed.

Chapter 4 first illustrates the effect of different loading conditions on the rollover thresholds of an A-double without roll stability control. Then, the chapter presents the benefits of a trailer-based RSC system by comparing the stock test results with results from RSC-equipped trailers. Lastly, the effect of different loading conditions on the effectiveness of RSC is evaluated.

Chapter 5 compares lateral acceleration and trailer roll angle as rollover indicators for use in trailer-based RSC systems. First, the effects of different trail-couplings, trailer loading, trailer type, and maneuver type on both lateral acceleration and trailer roll angle are investigated. Next, a time-domain comparison between the two roll indicators is performed to evaluate the differences in their response to excitations. Lastly, the distributions of the

lateral acceleration and trailer roll angle are compared at the time of RSC engagement to prove that despite being related, they are distinct indicators of roll instability.

Chapter 6 presents the conclusions of this study and recommendations for future work.

2. Background and Literature Review

This chapter defines heavy vehicles and presents the dynamic instabilities that they experience on roadways. First, the general definition of a heavy vehicle is introduced, and the roll instabilities that heavy vehicles are prone to are discussed. After introducing rollover, static rollover threshold estimation techniques for heavy vehicles are explained. Additionally, the geometric properties of trailers that affect the static rollover threshold and the advances in heavy vehicle design that increase the static rollover threshold are discussed. Building on the static rollover threshold models, dynamic rollover models and methods to calculate the proximity to rollover in real-time are discussed. Next, articulated heavy vehicles (AHVs) are defined, and the yaw instabilities that arise from the articulation between units are discussed. The different combination types of articulated heavy vehicles and the implications of each different configuration on the overall dynamics of the vehicle are explained. Lastly, electronic control systems that increase the safety and stability of heavy vehicles are introduced. Both passive and active methods of mitigating the rollover propensity of trucks in motion will be provided, including roadway infrastructure, truck/tractor-based electronic stability control (ESC), trailer-based roll stability control (RSC).

2.1. Introduction to Heavy Vehicles

In the United States, heavy-duty vehicles are vehicles with gross vehicle weight ratings (GVWR) greater than or equal to 26,001 lb. Within the group of heavy vehicles, there are two different weight classes, Class 7 (26,001-33,000 lb.) and Class 8 (>33,000 lb.) [7]. In addition to the weight classes, heavy vehicles are also characterized by the number of axles and the number of trailers attached in the train. There are 13 vehicle categories within this classification method used by the FHWA, in which classes 8-13 are the most relevant to this study [8]. The focus of this thesis is commercial trucks in the A-double configuration, which commonly refers to a tractor with two trailers connected with an A-dolly. The particular configuration used has a GVWR greater than 33,000 lb., contained two single-axle semitrailers, a single-axle A-converter dolly, and a tri-axle tractor; therefore, the test

vehicle is categorized in Class 8 by GVWR and in Class 12 by the number of trailers and axles. More information about this particular AHV combination is discussed in the following sections.

The primary function of heavy vehicles is to transport goods from one location to another. In 2018, 67% of the domestic freight tonnage in the United States was transported by trucks as the sole transportation method [9]. Because heavy vehicles are designed to carry and transport heavy loads, the unloaded CG height of heavy vehicles is typically higher than that of passenger cars; however, because heavy vehicles travel within the same lane size as passenger cars, the ratio of track width to CG height is much smaller. Currently, the maximum width limit for commercial vehicles in the United States is 102 in [10]. This width limit restricts the maximum allowable track width of the vehicle. The common dual tire configuration used on tractors and semi-trailers restricts the track width to approximately 78 in., much less than the federal width limit. When heavy vehicles are loaded, the center of gravity height increases with the increasing load, decreasing the CG height to track width ratio and further decreasing the roll stability. This low ratio negatively affects the roll stability of heavy vehicles and makes them prone to rolling over.

2.2. Estimating Heavy Vehicle Rollover

Classified by cause, there are two different types of rollovers: tripped and untripped rollovers [11]. A tripped rollover occurs when an external force is applied to the vehicle, causing it to roll over. This could result from a tire hitting a curb, the tire digging into soil, or hitting some other object that may cause the vehicle to rollover [11]. An untripped rollover occurs when the vehicle is subjected to intense dynamics, typically during evasive maneuvers or when maintaining a curve at an excessive speed. For an untripped rollover, an external force is not necessary to cause rollover, as the forces between the tire and the road are sufficient to cause rollover [11]. Although tripped rollovers are more common, they are nearly impossible to detect ahead of time; therefore, untripped rollovers are the main focus of rollover mitigation techniques [12]. This thesis will focus on the characterization and minimization of untripped, also known as maneuver induced, rollovers only.

As shown on the simplified free-body diagram in Figure 2-1, an untripped rollover occurs when the overturning moments acting on the vehicle reach a magnitude greater than the restoring moments acting on the vehicle [12]. Two distinct overturning moments are acting on the vehicle. The first is a result of lateral forces acting through the CG, and the second is a moment applied from gravity due to the lateral offset of the CG [12]. The single restoring moment is due to the transfer of vertical load on the tires and has a maximum value equal to the combined weight of the sprung and unsprung masses [12]. Following the simplified model in Figure 2-1, the balance of forces at the equilibrium point is

$$W \cdot h \cdot a_y = (F_2 - F_1) \cdot \frac{T}{2} - W \cdot \Delta y \tag{2.1}$$

where W is the weight of the vehicle, h is the CG height, a_y is the lateral acceleration, F_i are the vertical tire loads, T is the track width, and Δy is the lateral offset of the CG position from the center of the track.

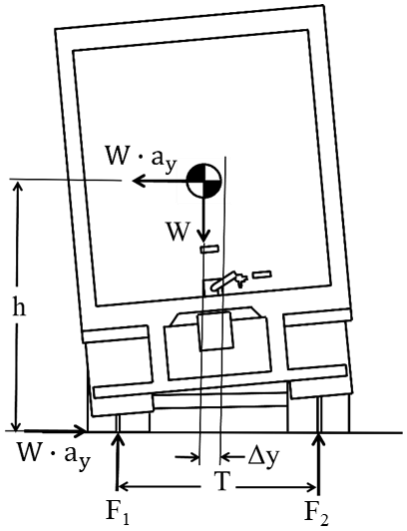

Figure 2-1. Simplified freebody diagram of heavy vehicle approaching rollover (Adopted from [12]).

The vehicle/trailer type and geometry govern the baseline roll stability of the vehicle. Vehicle type refers to the build and purpose of the heavy vehicle, such as a flatbed trailer, tanker, reefer, straight-rail (box) trailer, or drop-frame trailer. Flatbed trailers, in particular, have more torsional compliance than other trailer types, which negatively affects the roll stability of the trailer. Additionally, vehicle types are typically designed to transport a particular load, which further impacts the roll stability of the vehicle. A tanker with a partial

liquid load will experience side-to-side load transfer due to the sloshing of the liquid, while a box trailer may be filled with a fixed load that does not shift during operation. This study focuses on straight-rail (box) trailers that are assumed to have fixed loads. Geometry refers to the vehicle properties that can be adjusted within the construction type, such as track width, wheelbase, unloaded gross vehicle weight rating (GVWR), and suspension type. The trailer's loading can vary and is not considered a fixed property of the trailer; yet, it has a significant effect on the roll stability of the trailer as it raises the CG height from the unloaded position and determines the lateral and longitudinal offset of the CG position.

The most basic methods of determining the rollover threshold for a given vehicle assume static or steady-state conditions. A simple yet widely used method for determining the theoretical rollover threshold, including by the NHSTA, is the static stability factor (SSF) [11]. The SSF assumes that the vehicle is rigid and gives the maximum lateral acceleration applied at the CG for which a vehicle will rollover. The SSF is equal to the half of the track width divided by the CG height

$$SSF = a_{y,crit} = \frac{T}{2h} \tag{2.2}$$

where T and h are equal to the track width and CG height, respectively [11]. By increasing the track width or effective track width, the SSF increases. Law and Janajreh found that adopting wide single tires on the tractor drive-axle and trailer axles rather than the conventional dual tires can increase the lateral acceleration required for rollover [13]. The wide single tires increased the effective track width, increasing the roll stability of the vehicle even though the wide single tires had less vertical stiffness than the conventional dual tires. When the maximum width of heavy vehicles was increased from 96 in. to 102 in. in 1982, the corresponding increase in track width increased the roll stability of vehicles, as proven in a study conducted by Ervin in 1983 [10, 14]. Additionally, by decreasing the CG height, the rollover threshold of the vehicle increases, as shown by the SSF and verified by Ervin [14].

Even though the SSF is a simple measure, the SSF is related to the rollover rate of heavy vehicles. As the SSF decreases, the probability of rollover based on total miles driven increases exponentially, as illustrated in Figure 2-2 [12]. Thus, heavy vehicles with lower static rollover thresholds have more accidents per million km traveled than vehicles with

higher static thresholds, highlighting the importance of this basic predictive measure on the roll stability of heavy vehicles.

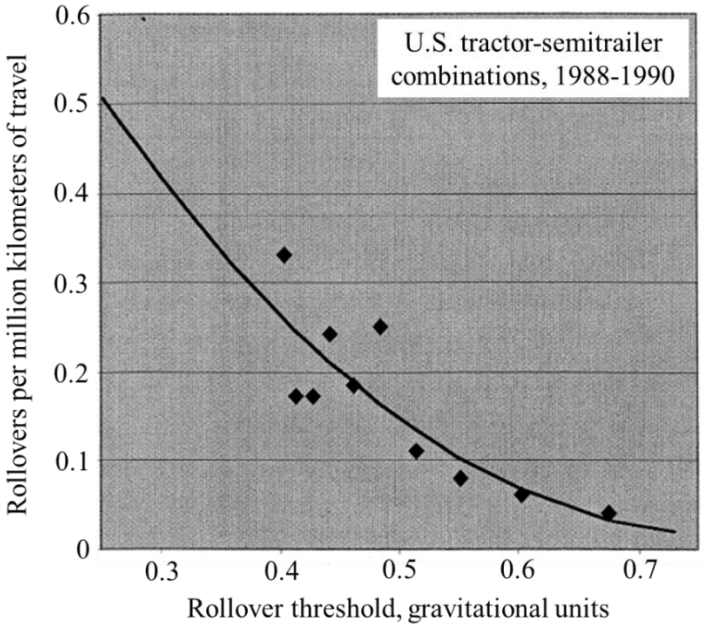

Figure 2-2. The number of rollover incidents increases as the SSF decreases (Adopted from [12]).

The SSF provides a basic measure based on the vehicle properties for roll stability that can represent the vehicle well in quasi-static or quasi-steady-state maneuvers; therefore, in ideal situations the SSF provides a maximum rollover threshold for a given vehicle. As more compliance is added to the vehicle model, the value of the rollover threshold will decrease from the value reported by the SSF. In actual vehicles, tire compliance, suspension compliance, fifth-wheel lash, spring lash, body lateral compliance, and multiple suspensions lower the vehicle's static rollover threshold from the SSF value, as shown in Figure 2-3 [12].

A method used to determine the rollover threshold of vehicles that includes the various compliances present is the tilt table test. The tilt table exposes the vehicle to a constant lateral acceleration as the vehicle is gradually tilted in roll [12]. The appropriate weighting of the tilt-table response to a simulated lateral acceleration is

$$a_y = \tan(\varphi_T) \tag{2.3}$$

where φ_T is equal to the roll angle of the tilt table [12]. Additionally, the tilt table test can be used to determine the suspension properties that affect the roll stability of trailers, such as the roll center height, total roll stiffness, lateral compliance, and suspension height [15].

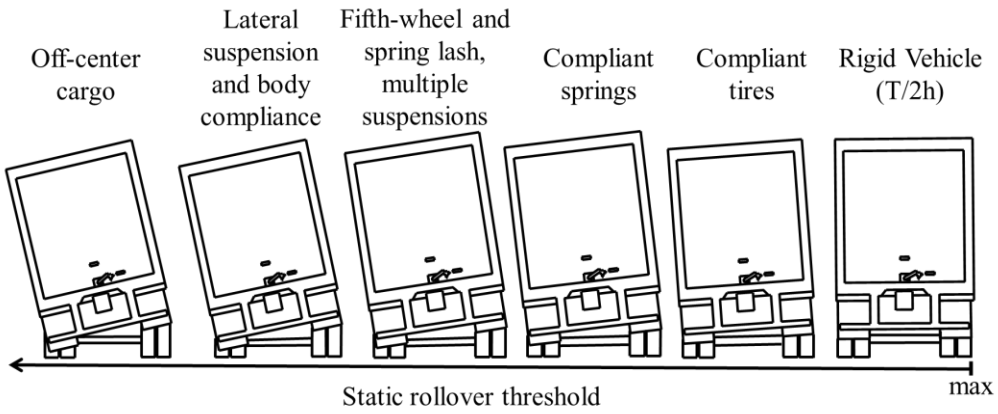

Figure 2-3. Decrease in static rollover threshold corresponding to additional vehicle compliance (Adopted from [12]).

Although the tilt table test captures the compliances of the vehicle in its determination of the rollover threshold, mathematical models with additional compliances also exist to predict the rollover threshold without the need for expensive equipment. Roll models with additional compliances represent rollover thresholds that are lower than that predicted by the SSF. The first non-rigid model includes tire compliance. When considering a single degree of freedom roll plane model that includes tire compliance, as shown in Figure 2-4, the lateral acceleration limit is equal to

$$a_{y,lim} = \frac{T}{2h} - \frac{W}{K_t T} \tag{2.4}$$

where K_t is equal to the vertical tire stiffness [16]. When the rigid vehicle assumption is not made, the roll angle of the sprung mass and unsprung mass are also considered in roll-plane models. In models with only tire compliance present, the sprung mass and unsprung mass are lumped together into a single body with a single roll angle. The roll angle in this scenario is equal to:

$$\varphi_{lim} = \frac{W}{K_t T} \tag{2.5}$$

where φ_{lim} represents the roll angle limit for the combined sprung and unsprung mass [16]. If, instead of considering tire compliance, suspension compliance is considered, then the

roll center height of the sprung mass must be included in the equations. This separates the sprung mass from the unsprung mass, making the trailer roll angle equal to the overall roll angle of the vehicle. An illustration of the suspended mass model is shown in Figure 2-5. For the analysis in this study, the road bank angle is assumed to be zero.

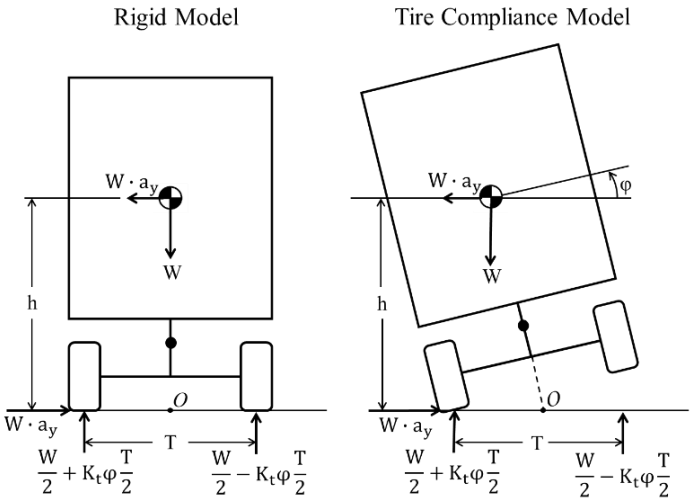

Figure 2-4. Roll-plane model with tire compliance compared to rigid roll-plane model (Adopted from [16]).

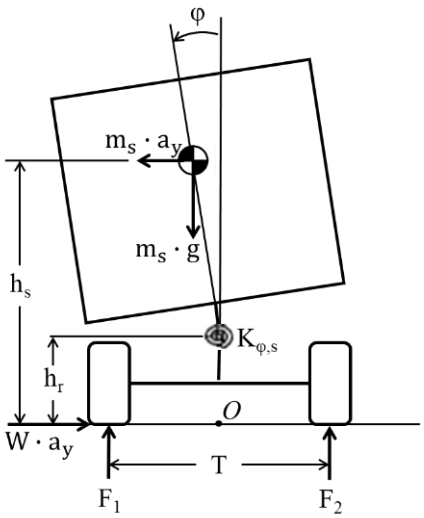

Figure 2-5. Suspended mass roll-plane model (Adopted from [17]).

The sprung mass is assumed to rotate about a roll center with resistance equal to the suspension roll stiffness. The model now includes suspension properties as well as additional geometric properties such as the roll center height. In reality, the roll center position varies during actual vehicle motion and roll, so the roll center concept is idealized

and does not represent the instantaneous point of rotation [15]. Typical assumptions made with this model include that the sprung mass is much greater than the unsprung mass and that the chassis and tire stiffnesses are much greater than the suspension stiffness. From these assumptions, the unsprung mass and tire effects are neglected [17]. A common equation derived from this model is the roll gain. For a flat road, the roll gain is defined as:

$$R_{\varphi} = \frac{\varphi}{a_y/g} = \frac{m_s g(h_s - h_r)}{K_{\varphi,s} - m_s g(h_s - h_r)} \tag{2.6}$$

where m_s is the mass of the sprung mass, h_s is the sprung mass cg height, h_r is the roll center height, and $K_{\varphi,s}$ is the suspension roll stiffness [17]. Using the roll gain definition, the lateral acceleration limit value is equal to

$$\frac{a_{y,lim}}{g} = \frac{T/2}{h_s + (h_s - h_r)R_{\varphi}} \tag{2.7}$$

and the trailer roll angle limit is [17]

$$\varphi_{lim} = \frac{T/2}{h_s/R_{\varphi} + h_s - h_r} \tag{2.8}$$

Another roll plane model combines the previous two models, including both tire and suspension compliance [16]. This model no longer assumes that the unsprung mass and chassis and tire stiffness are much greater than the sprung mass and the suspension stiffness. The effects of the sprung mass and the tires are now included in the model, introducing the unsprung mass roll angle. The total roll angle becomes the combination of the sprung and unsprung roll angles. Even more complex roll-plane models exist that include the effects of the fifth wheel coupling with the tractor, such as the model introduced by Chen and Peng [16]. In later chapters, the critical lateral acceleration values derived from the rigid roll-plane model and the suspended mass roll-plane model are compared to the experimental results.

Looking beyond the SSF into other geometric factors that affect the roll stability of trailers shows that the SSF is not comprehensive in representing the complete picture of trailer roll dynamics. In reality, in dynamic maneuvers, the roll dynamics are coupled with yaw dynamics, so additional properties affect heavy vehicle roll dynamics. In addition to an increased trackwidth, an increased wheelbase has been found to affect the rollover

threshold of a trailer positively. Chen et al. determined that a longer trailer could slightly increase the roll stability due to the corresponding increase in wheelbase[18]. It should be noted that when the wheelbase of the trailer is increased, roll dynamics are improved, but the amount of low-speed off-tracking is increased. Other improvements in the roll stability of heavy vehicles can be made by improving the systems commonly found in trailers. For example, Chen et al. also found that a balanced heavy truck pneumatic suspension, as opposed to the common in series pneumatic suspension, can improve the roll stability of the trailer by allowing for independent air spring pressure changes on the left and right sides of the trailer [19].

Different trailer loading conditions can also affect the rollover threshold of the vehicle by affecting the CG position. Although not included in the SSF, the longitudinal and lateral center of gravity positions affect a vehicle's or trailer's roll stability. As the longitudinal center of gravity is pushed back from the kingpin towards the rear axle(s) of a trailer, the roll stability of the trailer increases slightly [13]. While the movement of the CG towards the rear of the trailer increases the roll stability of the trailers, it also decreases the yaw stability of the trailers and will generate more trailer swing than if the CG were closer to the kingpin. If the load is laterally offset from the center of gravity, the rollover threshold towards the more heavily loaded side of the trailer will decrease. This effect is witnessed by Garcia et al. during testing with an offset load; the load generated more suspension compression on the heavier side of the trailer, which in turn generated more lateral displacement of the CG and caused rollover at lower lateral accelerations, especially to the heavier side of the trailer [20]. Even when the trailer loading does not affect the CG position, the vehicle's rollover threshold still decreases. As shown in Figure 2-6, when the loading on each axle of the vehicle was increased, the CG height remained relatively constant, yet the rollover threshold of both trailers decreased significantly [14].

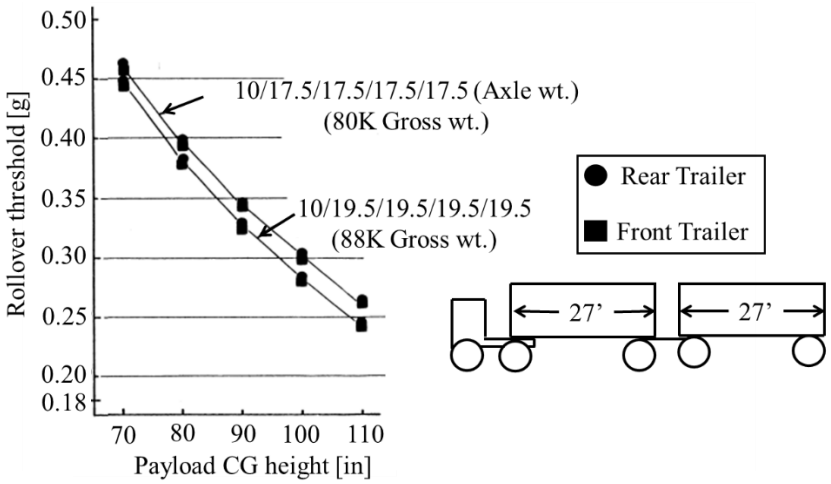

Figure 2-6. Effect of axle load and CG height on lateral acceleration rollover threshold (Adopted from [14]).

While the static rollover thresholds can provide relatively realistic estimations of rollover thresholds of heavy vehicles, in reality, whenever a vehicle is in motion, there is momentum present that affects the rollover threshold of the vehicle and causes it to deviate from the static rollover threshold. Dynamic rollover thresholds were developed to portray the rollover thresholds of moving vehicles more accurately than the static or steady-state rollover thresholds. Using a roll energy analysis, Dahlberg proposed a dynamic rollover threshold (DRT) to provide such a measure, as follows:

$$DRT(\zeta) = \frac{SSRT}{1 + e^{-\zeta\pi}\left(\frac{SSRT}{DRT_{\zeta=0}} - 1\right)} \tag{2.9}$$

where ζ is equal to

$$\zeta = \frac{C_\varphi}{2\sqrt{J_x\left(K_\varphi - m_s g H\right)}} \tag{2.10}$$

and $SSRT$ is the steady state rollover threshold, C_φ is the roll damping, J_x is the roll moment of inertia, K_φ is the roll stiffness, and m_s is the sprung mass [21]. While the SSF indicates the theoretical maximum lateral acceleration before rollover, the DRT presents the minimum value of lateral acceleration at which a vehicle can rollover [21]. Although two heavy vehicles may have the same SSF, the DRT may vary because of the differing properties of the vehicles. For example, if the suspension roll stiffness of vehicle A is

greater than that of vehicle B and all other vehicle properties are identical, the DRT of vehicle A will be greater than that of vehicle B.

While static and rollover thresholds are important for determining a baseline value at which a vehicle may rollover, there are also predictive measures which measure a vehicle's proximity to rollover. A popular method of determining the proximity of a vehicle to rollover is the lateral transfer ratio (LTR) [22, 23]. The LTR is equal to the difference in loading between the left and right wheels divided by the total loading, as follows:

$$LTR = \frac{F_{zL} - F_{zR}}{F_{zL} + F_{zR}} \tag{2.11}$$

where F_{zL} and F_{zR} are the vertical loads on the left and right wheels, respectively [22, 23]. At a value of 0, the loading of the left and right wheels is equal, and the vehicle is stable. At a value of ±1, one of the wheels is unloaded, signaling that the vehicle is unstable and in danger of rolling over. Estimations of the LTR are commonly found in roll stability control designs to approximate the proximity of the trailer to rollover. One such example of an estimated rollover index is the roll safety factor (RSF) used by Liu et al., which is equal to,

$$RSF = \frac{K_t\left(\delta_0 + \frac{T}{2}\varphi_u\right) - K_t\left(\delta_0 - \frac{T}{2}\varphi_u\right)}{(m_s + m_u)g} \tag{2.12}$$

where δ_0 is the static deflection of the tires, m_u is mass of the unsprung mass, and φ_u is the unsprung mass roll angle [24]. Another proposed method for determining the proximity of a trailer in motion is the time to rollover (TTR) method proposed by Chen and Peng [16]. The TTR metric is a real-time method used by control systems to determine the time until an impending rollover. Similar to the LTR, it is not a measure of the innate rollover threshold of the vehicle, but a measure of the proximity of a vehicle to rollover. In addition to the simple TTR metric, a trained neural-network can enhance the TTR index [16], and more advanced versions have been shown to give earlier and more accurate rollover detections than the simple model [25].

2.3. Introduction to Articulated Heavy Vehicles

Articulated heavy vehicles (AHVs) are an assembly of multiple rigid bodies that are joined together in a train. When a heavy vehicle has two trailing units, it is referred to as a double, and when there are three trailing units, it is referred to as a triple. There are many benefits to adding trailers to a heavy vehicle. By adding additional trailers to the heavy vehicle, there are additional trailers available to carry cargo. Furthermore, if the two trailers have different destinations, a single driver can bring both trailers to their respective locations rather than needing two drivers. This means that the number of drivers per unit cargo will decrease, saving companies costs in salary. Additional cost benefits include savings on fuel from carrying more cargo with a single truck/tractor rather than separating the cargo into two separate shipments. Some additional benefits of articulated heavy vehicles include fewer truck units on the roads for the same amount of cargo, lower emissions per unit cargo, a decrease in miles traveled of heavy vehicles, thereby decreasing the probability of accident occurrence [6].

While there are benefits to articulated heavy vehicles, there are also some downfalls. In addition to being susceptible to rollover, AHVs also commonly experience yaw instabilities such as jack-knifing and rearward amplification from the addition of articulation points. Jack-knifing is a yaw instability that occurs when one unit in the long combination vehicle rotates about the vertical axis of the coupling between units. There are three distinct types of jack-knifing, as illustrated in Figure 2-7. Tractor jack-knifing occurs when the tractor's drive-axle tires slip, rotating the tractor perpendicular to the trailers. If the AHV has two or more trailers, then trailer and dolly jack-knifing can also occur. Dolly jack-knifing occurs when the dolly rotates about the vertical axis of the hitch with the front trailer. Lastly, trailer jack-knifing occurs when the rear trailer swings out into adjacent lanes of traffic or off the road about the vertical axis of the dolly connection.

(a) (b) (c)

Figure 2-7. Three potential jack-knifing events: a) tractor jack-knifing, b) trailer jack-knifing, and c) dolly jack-knifing

In addition to jack-knifing, AHVs also experience the steering-frequency related phenomenon called rearward amplification (RA). When traveling through a turn at a particularly high frequency, the trailing units will typically experience larger lateral accelerations than the lead unit; this is called rearward amplification. RA is generally defined as

$$RA = \frac{a_{y,input}}{a_{y,i}} \tag{2.13}$$

where $a_{y,input}$ is equal to the lateral acceleration of the towing unit and $a_{y,i}$ is the lateral acceleration of the ith trailing unit. The RA phenomenon increases with the number of articulated units in the train; therefore, the last trailer in a triple will have a larger lateral acceleration than the last trailer in a double and so on, assuming the properties of the trailers are equal. As shown in Figure 2-8, RA can significantly increase the lateral acceleration of the rearmost trailer from that of the tractor. While RA is a yaw dynamic, it also has a large effect on the roll dynamics of the vehicle, especially in the rearmost trailer. Because the lateral acceleration of the rearmost trailer is amplified, it is more vulnerable to rolling over in the turn. Through simulation by Chen et al., it has been shown that rearward amplification is greater with more articulated units; therefore, trucks with more articulated units are expected to rollover at lower speeds in dynamic maneuvers because of the rearward amplification phenomenon [18]. This finding is important because of the decoupling of the driver with trailers in articulated vehicles. Because of the nature of interconnection between articulated units, the driver cannot feel the adverse dynamics of the trailing units and is often not aware that the trailers are rolling over until it is too late. The decoupling of the driver from the rearmost trailer while the lateral acceleration of the rearmost trailer is being amplified by RA is an unfavorable combination. While additional

articulation points increase rearward amplification, a longer wheelbase can reduce lateral acceleration by increasing the yaw damping of the trailer [26].

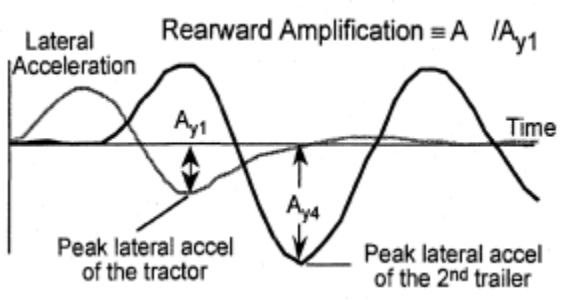

Figure 2-8. Rearward amplification (RA) is a frequency-related phenomenon that amplifies the lateral acceleration of the rearmost trailer [12].

Besides the additional instabilities experienced by articulated heavy vehicles, there are also other disadvantages of AHVs. Firstly, the amount of low-speed off-tracking will increase with the addition of a trailer. A double will experience more off-tracking than a tractor semi-trailer combination, and a triple will experience more off-tracking than a double when all trailers are the same length. As shown in Figure 2-9, each additional articulated unit experiences more off-tracking than the previous unit [27]. However, the addition of articulation points can also decrease off-tracking for the same total length of the vehicle. By adding an articulation point, the rear trailer axles can follow the tractor path more closely than if the trailing units were one rigid body. Therefore, a 28-foot double will have less off-tracking than a 53-foot single. However, the increase in overall vehicle length means that infrastructure may not be spacious enough to fit articulated heavy vehicles. Garages, loading docks, truck stops, and other areas may need to be expanded to be used by AHVs. Some additional disadvantages to using AHVs are that the additional weight of the entire unit could pose a danger to bridges and over-land infrastructure, the additional length of the vehicle requires more space on the road than a single-unit heavy vehicle (considering the same trailer length), and the slower acceleration and deceleration of the AHV due to increased total load could lead to traffic or even accidents [6].

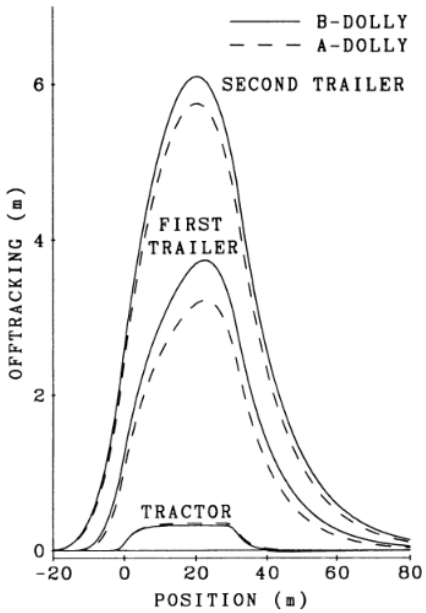

Figure 2-9. Off-tracking of double semi-trailer configuration [27]

Within the AHV classification, there are multiple different configurations available, with units split into lead units and trailing units [26]. The different types of units that typically make up AHV trains are shown in Figure 2-10. The lead unit is responsible for providing power to and steering the vehicle and comes in two different types: trucks and tractors. A truck is permanently equipped with a cargo container, while a tractor is attached to temporary trailing units called trailers. There are also multiple types of trailers: full trailers and semi-trailers. A full-trailer is equipped with both front and rear axle groups to sustain vertical load on both ends of the trailer without the support of another unit. In addition, the full trailer also has a front drawbar, which allows it to connect to another unit in the chain. A semi-trailer only possesses a rear axle group and has no vertical support on the front of the trailer; therefore, a converter dolly must be used to connect the semi-trailer to another unit. Within trailer designs, the number of axles and the locations of axles may vary. A less common type of trailer is the center-axle trailer, in which the axle group is located near the center of the trailer rather than the rear, eliminating the need for a converter dolly [26]. Some trailers may even have a combination of axle locations; for example, some have two axles in the rear and two axles in the center, although these types of constructions are far less common than the standard rear axle group trailers.

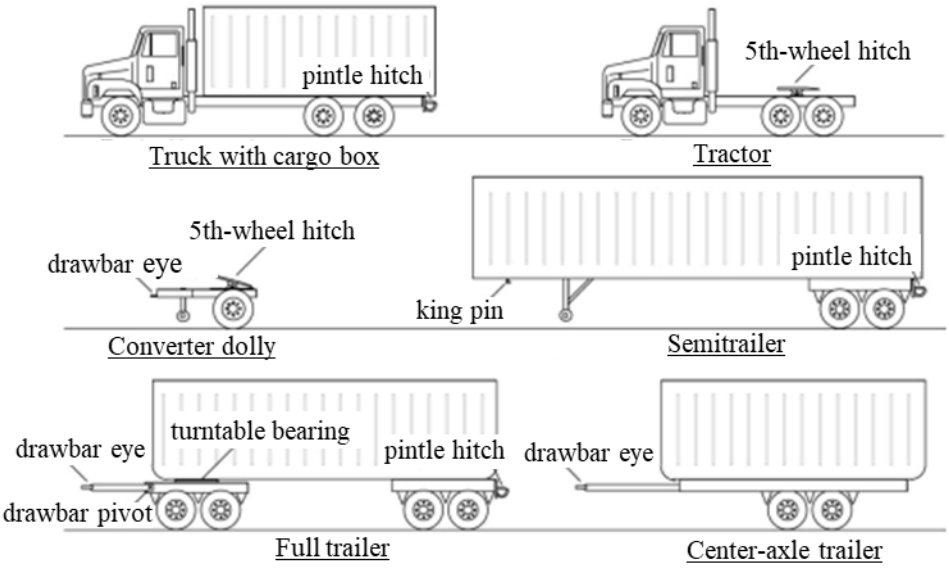

Figure 2-10. Commonly used vehicle units in articulated heavy vehicles (Adopted from [26]).

There are two main types of hitches used for the connecting units of an articulated vehicle: the pintle hitch and the fifth wheel hitch, both shown in Figure 2-11. Both the pintle hitch and the fifth wheel hitch constrain the translational degrees of freedom between the two connected units. However, the pintle hitch connection possesses three degrees of rotational freedom and is not designed to bear a large load, while the fifth wheel hitch only allows yaw and pitch rotation and is designed to withstand heavy loading [26]. Dollies are most commonly attached to the rear of a truck or a trailer using a pintle hitch to drawbar coupling, and semi-trailers are typically connected to a converter dolly or a tractor using a fifth-wheel hitch to kingpin coupling.

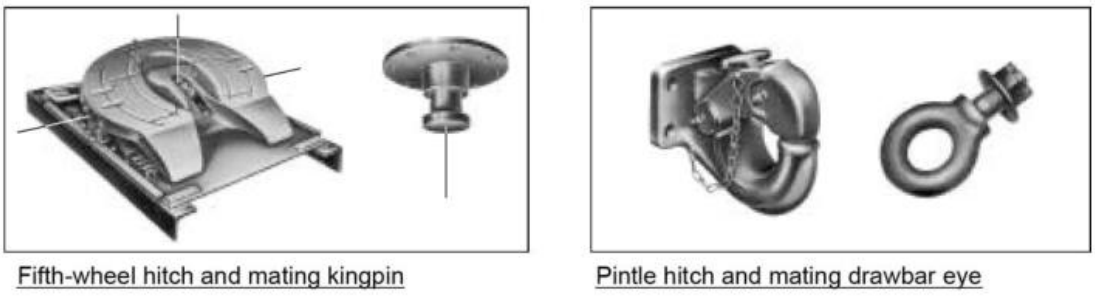

Figure 2-11. Commonly used hitches in articulated heavy vehicles [26].

Lastly, three types of converter dollies are used on roads: an A-dolly, B-dolly, and C-dolly, as shown in Figure 2-12. The A-dolly is the most commonly used of the three in the United States and features a single drawbar connection. The front of the A-dolly connects to the pintle-hitch of the front unit, and the rear of the A-dolly connects to the rear unit using a fifth wheel. AHVs that use A-dollies to connect vehicle units are known as A-trains. Because of the single drawbar design, the dolly has rotational freedom about the pintle hitch, which can cause undesirable yaw dynamics such as rearward amplification, trailer swing, and jack-knifing. The B-dolly, also known as the B-train, was introduced to mitigate these undesirable dynamics by reducing the number of yaw articulation points. The B-train consists of a front trailer with an extended rear frame equipped with a 5th wheel to connect to the trailing unit [26]. In practice, the A-dolly is much easier to connect units with than the B-dolly, as connecting the B-dolly requires significantly more precision. This allowed for the introduction of a C-dolly that was designed to possess some of the A-dolly's ease of use and the B-dolly's yaw stability. The C-dolly also features the double draw-bar design of the B-train, but it requires a wide spread between the towing unit's rear axle and the trailing unit's front axle [26]. C-dollies are commonly equipped with self-steering tires to mitigate tire wear from this extended distance between units [26]. Converter dollies typically possess either one or two axles.

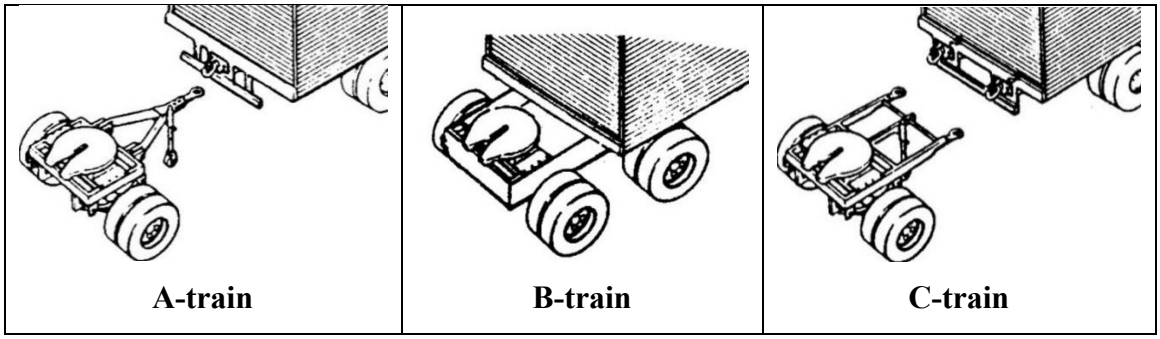

Figure 2-12. Commonly used couplings in articulated vehicle trains [28].

2.4. Heavy Vehicle Stability Control

Because of the severity of heavy vehicle rollover accidents, extensive research has been performed over the last few decades to investigate the most effective means of decreasing these types of accidents. Because it is difficult to sense tripped rollovers sufficiently ahead of time, most methods focus on mitigating the probability of untripped rollovers. Several

methods have been proposed, such as passive road signs, active road signs, passive warning systems, and active warning systems. In addition to electronic roll and yaw stability systems, other innovations like ABS have also increased the safety of heavy vehicles.

The simplest method introduced to reduce rollover accidents was to mark the roads with suggested speed limits and warnings to indicate to heavy vehicle drivers that there is a danger of rollover if the upcoming turn is taken at an excessive speed. Although the signs warn drivers of the impending danger, passive roadway signs can be easily ignored by drivers. Another innovation is active road signs that will encourage drivers to reduce speed if they enter a turn at an excessive speed, such as the one pictured in Figure 2-13. Like passive systems, active systems that report many false rollover warnings can be easily ignored. However, active road infrastructure that tailors to the vehicle, such as with a speed and weight-based warning algorithm, can issue warnings more difficult to ignore. According to Baker, Bushman, and Berthelot, a speed-based rollover system can generate 44-49% more false rollover warnings than a system that employs weight as well [3]. In the three rollover warning sites installed in Virginia and Maryland that are based on speed, deceleration, and weight, there had been no rollover events since the system was installed in 1994 to when the study was completed in 2001 [3].

Figure 2-13. Dynamic road warning sign [29].

One issue with the passive and active road signs is that during driving, the lateral acceleration experienced by heavy vehicles may be greater than the expected values based on the geometric design characteristics of the roadway [20]. External warning devices may issue warnings effectively with a particular factor of safety, but they cannot capture a realistic representation of the actual dynamics of the vehicle. Systems installed on the truck/tractor can also issue warnings to drivers or intervene on the driver's behalf but have

the advantage of measuring dynamics on the vehicle body. A system installed on the vehicle that warns the driver is a passive rollover warning device, while one that intervenes on the driver's behalf is an active rollover prevention device.

A passive warning device called the roll-stability-advisory (RSA) system was proposed by Winkler and Ervin in 1999 [12]. When the system detects that the vehicle's lateral acceleration is close to the predetermined, worst-case static rollover threshold for the vehicle, the device produces an audible warning to the driver. The system also features a live display that shows the driver the estimated rollover thresholds for both right- and left-side rollover along with the current lateral acceleration measurement. One drawback of such a device is that the warning may be issued to the driver with less than enough time to react. Approximately 85% of drivers should be able to respond to a clear stimulus and a straightforward situation – such as applying the brake – in about 1.5 after first being alerted to the stimulus [30]. Assuming the driver is not distracted or fatigued, this response time may not be sufficient to avoid rollover in all scenarios. If the driver is turning to avoid an obstacle, the first reaction may not be to brake to avoid rollover but to steer around the obstacle. Unlike human drivers, controllers' response times to a trigger are nearly instantaneous, leading to the innovation of active roll control systems.

The first active electronic control system introduced to combat both rollover and yaw instabilities was the truck/tractor-based electronic stability control (ESC) system. ESC systems use braking, throttle control, or other methods to mitigate roll and or yaw instabilities. A large bulk of research into the effectiveness of active ESC systems has been performed in the past few decades. Throughout the years of research, ESC has proven that it can assist drivers in preventing vehicles from rolling over as well as oversteering and understeering. In 2015, the NHSTA proposed FMVSS No. 136, which required the installation of ESC on truck tractors and some buses with gross vehicle weight ratings greater than 26,000 lb.; it was estimated that with this requirement, 40-56% of untripped rollovers and 14% of loss-of-control crashes would be prevented [4]. In FMVSS No. 136, the FHSTA also required ESC instead of RSC on truck tractors because the ESC systems encompass RSC and prove to be more effective in mitigating rollover accidents [4].

While every ESC device has the same objective, there are different methods in which the controllers and actuators of the system interact with the vehicle. Among these methods are differential braking [31, 32], active steering [33], active suspension [25], and active anti-roll bars [34].

Differential braking anti-rollover systems modulate brake pressures on the left and right sides of the vehicle to reduce speed, lateral acceleration, and to adjust for undesirable yaw dynamics such as oversteer and understeer. When maneuvering through a turn at an excessive speed, the anti-rollover system will apply the brakes to the outer tires, which are more heavily loaded due to lateral load transfer, to avoid rollover. Examples of such systems in use today are the Bendix Electronic Stability Program and the WABCO ESCsmart^{TM} systems [31, 32]. In addition to applying brake pressures, the ESC systems may also cut the throttle input so that the driver cannot accelerate the vehicle. This assists in slowing down the vehicle and preventing rollover.

Anti-rollover active steering control is used to provide auxiliary steering control in addition to the driver control to maintain a safer path than if the driver had lone control of the vehicle. In a study by Imine, Fridman, and Madani, active steering control minimized the lateral load transfer and lateral acceleration of the vehicle, allowing it to avoid rollover at the same speeds at which the vehicle without the controller had rolled over [33]. However, one major drawback to active steering control exists. Because the driver is no longer in complete control of the vehicle's course, if there are not sufficient sensors on the vehicle to prevent it from steering into an undesirable location, the steering control can cause the vehicle to move off of the road or into adjacent lanes of traffic. Therefore, the driver must always maintain primary control of the steering for the systems to be used safely on roads.

Active suspension control systems manipulate the air spring pressure and/or the suspension travel on opposite sides of the vehicle to reduce the sprung mass body roll during turns. The active suspension roll control system developed by Yu et al. features an additional suspension control torque between the sprung and unsprung mass to tilt the sprung mass inwards on a curve to balance the lateral forces generated during the turn [25]. Active suspensions can be realized through actuators that tilt the sprung mass or, if equipped with a pneumatic suspension, by controlling the air flow in and out of the air springs.

A passive anti-roll bar will reduce body roll by acting as a mechanical linkage between a vehicle's left and right suspensions. During a left turn, the right suspension will compress, and the left suspension will extend. The anti-roll bar will extend with the left suspension and exert a force upward on the right suspension, decreasing the amount that the suspension compresses and reducing body roll. An active anti-roll bar will typically use hydraulic actuators to generate a stabilizing moment and lean the vehicle into turns to minimize the load transfer to the outer wheels [34].

In addition to tractor-based ESC systems, trailer-based roll stability control (RSC) systems are also commercially available, although they are not yet required by a NHSTA standard. The function of trailer-based RSC systems is to mitigate roll instabilities experienced by the trailers. In nearly all cases of untripped rollover in tractor semi-trailer or articulated vehicles, the trailer will be the first unit of a heavy vehicle to experience wheel lift or a rollover because it has a higher CG and greater roll stiffness than the tractor, as shown in Figure 2-14 [35]. The tractor-based roll stability systems are decoupled from the trailers and do not intervene on behalf of the trailer dynamics. Since the trailers will be the first unit to roll over, the trailer-based RSC attempts to attack the rollover problem at its most likely cause. Additionally, the trailers experience delayed dynamics from the tractor, so a rollover may occur after the ESC system has finished intervening. By adding systems to the trailers, the amount of time the brakes are applied on the vehicle can be extended. This is especially important in double and triple configurations where the dynamics of the tractor can be amplified increasingly in each successive trailing unit. As shown in Figure 2-15, there can be a significant delay in the trailer dynamics when more than one trailer is being towed.

In summary, trailer-based anti-rollover systems can more accurately intervene when the trailers are in danger of rolling over than a system on the tractor, which is important as the trailer is more likely than the tractor to rollover. When the RSC system senses that the trailer is approaching rollover conditions, the system applies counter-measures to decrease the roll instabilities encountered by the trailer.

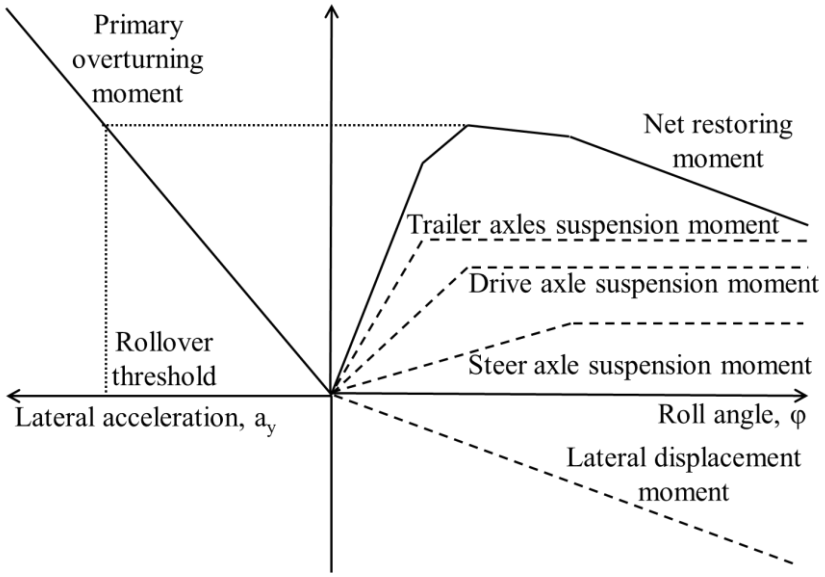

Figure 2-14. Load-transfer moments of articulated heavy vehicle axles (Adopted from [35]).

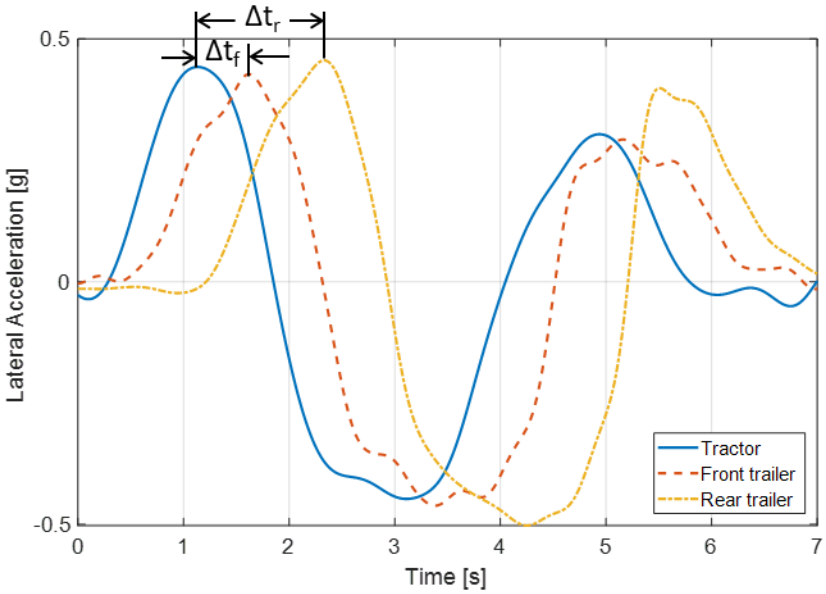

Figure 2-15. Time delay in lateral acceleration response in trailing units.

In 1993, Dunwoody and Froese set out requirements for viable trailer-based RSC systems. It was determined that a good RSC system should decrease the incidence of rollovers, yet not encourage drivers to perform maneuvers at higher speeds, should be reliable, should fail safely, should have insignificant power consumption, and should be self-contained on the trailer [36]. In addition to these requirements, it should also be pointed out that the systems should be able to be employed on different semi-trailer constructions with minimal adjustments needed. The systems should also have minimal complexity such that it can

effectively minimize the roll instabilities of the trailers without being too intrusive or requiring excessive installation and maintenance. The systems should have acceptable costs such that they can be adopted in large fleets and not be seen as a non-necessary luxury to be used in trailers. Finally, the systems should not intervene too often when the roll indicator is significantly lower than the rollover threshold. If the system intervenes too much, the driver will be negatively impacted by the system when driving at lateral accelerations well below the threshold.

RSC systems employ methods similar to ESC systems to mitigate roll instability, such as braking, active suspensions, and anti-roll bars. Roll stability systems that modulate the trailer brakes to slow down a vehicle in danger of impending rollover are the most common commercially available type of trailer-based anti-rollover systems. Examples of such systems in use today are the Bendix® TABS-6 Advanced and TABS-6 Advanced MC systems with trailer roll stability programs (TRSP) technology, the Haldex TRS System, and the WABCO Trailer Electronic Braking System (TEBS) [37-39]. These systems utilize lateral acceleration measurements within the control module, suspension pressure, and wheel speed to monitor the rollover risk of the trailer. If the system senses that the trailer is at high risk of rollover, it will intervene by selectively applying the brakes to the outer, more heavily loaded wheel to maximize braking effort. In addition to sensing lateral acceleration, another possible indicator of rollover that can be measured online is the trailer roll angle. According to Rakheja and Piche, the semi-trailer rearmost axle roll angle allows for a more reliable detection of rollover onset than lateral acceleration does during high-speed dynamic maneuvers, and lateral acceleration provides a reliable indicator of an impending rollover during quasi-steady-state maneuvers [40]. While the study proposes that the rearmost axle roll angle may provide a quicker indicator of rollover than lateral acceleration for dynamic maneuvers, it does not include experimental evidence to bolster this claim, only simulation results from a parametric study. Another study conducted by Liu et al. concluded that roll angle response was more closely correlated and in phase with the determined roll stability factor than lateral acceleration [24].

A second method to reduce rollover risk is to reduce body roll rather than the vehicle's velocity, which can be done through manipulation of the suspension. Active suspension

control for trailers can be performed either using actuators to control the sprung mass roll or – if equipped with a pneumatic suspension – by adjusting the pressure of the air springs to control body roll. Sampson and Cebon suggested an anti-roll system comprised of hydraulic actuators in parallel with the springs and a tiltable fifth-wheel coupling to mitigate the body roll [35]. Dunwoody and Froese investigated the use of such a suspension and estimated that the system could increase the rollover threshold by up to 30% when compared to an identical vehicle with a conventional suspension [36]. Additional research was performed on active air-spring suspensions by Senalik and Medanic. It was found that with the active suspension anti-rollover system that manipulates the relative pressures of the inner and outer air springs can increase the lateral acceleration at rollover by 21% [41].

The last method proposed to decrease trailer rollover propensity is using active anti-roll bars to reduce body roll. In 2012, Huang et al. investigated the use of active anti-roll bars in a tractor semi-trailer configuration and uncovered that a single roll-bar on the trailer axle was more effective than multiple roll bars on both the trailer and the tractor axles [42].

Another important safety system that works in conjunction with ESC and RSC modules is the anti-lock braking system (ABS), one of the first electronic safety systems employed on heavy vehicles. The purpose of ABS is to modulate braking pressure to avoid wheel-lockup during braking. ABS systems use wheel speed sensors to detect tire slip. When tire slip is detected, the system decreases the braking pressure so that the wheel does not lock up but stays rolling on the ground while braking. This maximizes braking forces during the braking action and lets the vehicle stop within a shorter distance than if the wheels had locked up during braking. The avoidance of wheel lock-up also increases the yaw stability of heavy vehicles by reducing the amount of lateral tire slip during braking in turn, thereby decreasing the probability of jack-knifing or tire swing. ABS systems can assist in mitigating rollover risk by preventing wheel lock-up and allowing vehicles to reduce speed by greater amounts before a turn if entering at an excessive speed. If the ESC or RSC module initiates braking, the ABS prevents the tires from locking up during this action, maximizing the positive effects of ESC or RSC systems. During the late 1990s, the Federal Motor Vehicle Safety Standards were passed that required new vehicles to be equipped with ABS systems. In 1997, ABS systems were required new tractors with a GVWR over

10,000 lb., while ABS was required on trailers, single-unit trucks, and buses with GVWR greater than 10,000 lb. starting in 1998 [43]. Lastly, in 1999 all new heavy vehicles with hydraulic brakes were required to be equipped with ABS [44].

3. High-speed Testing Set-up

This chapter describes the high-speed testing study, including the instrumentation and electronics used on the test vehicle, the safety equipment installed, details regarding the tests performed, and data analysis techniques.

3.1. Instrumentation and Electronics

The following section discusses the different sensors installed on the test vehicle, including accelerometers, load cells, pressure transducers, string potentiometers, and LiDAR. A side view of the test vehicle with the locations of all sensors is shown in Figure 3-1. After describing the purpose and installation of the sensors, the calibration method for each sensor is described. The calibration curves for all analog sensors installed on the test vehicle are included in Appendix A.

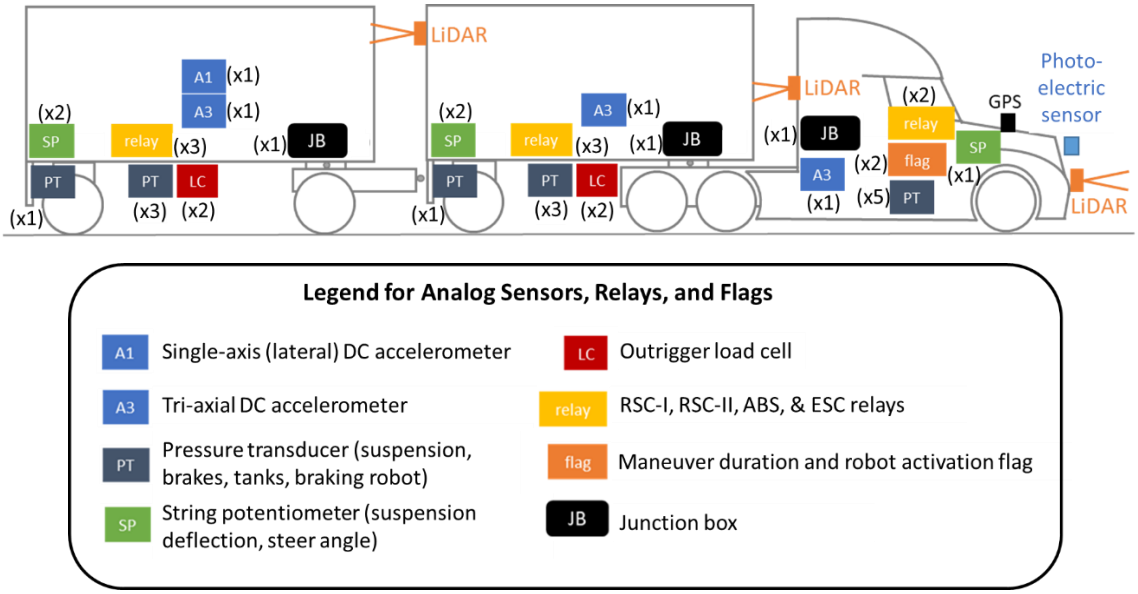

Figure 3-1. Side view of test vehicle with locations of sensors, relays, flags, and junction boxes.

3.1.1. Accelerometers

PCB® Series 3713F11 triaxial accelerometers were installed on both the tractors and the trailers to measure the lateral, longitudinal, and vertical accelerations. The triaxial accelerometer on the tractor was mounted on the frame as close to the CG position as

possible. The accelerometers of the trailers were mounted at the heavily loaded CG position on robust mounts to ensure that there was little to no mount vibration that would degrade data quality. On the rear trailers, PCB® Series 3741F12 single-axis accelerometers were used to measure the lateral acceleration and provide redundancy in the lateral acceleration measurements to ensure high fidelity data. The mounting of the trailer accelerometers, including both the triaxial and single-axis accelerometers, is shown in Figure 3-2.

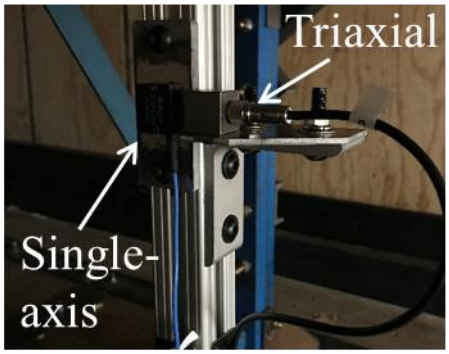

Figure 3-2. Triaxial and single-axis accelerometer mounted inside the trailer.

A redundancy was provided for the rear trailers only because during dynamic obstacle-avoidance maneuvers, the rear trailer is likely to experience larger lateral accelerations than the front trailer due to rearward amplification. Therefore, there were no single-axis accelerometers on the front trailers for the first three test sessions. However, before the fourth testing session, it was determined that high-frequency oscillations on the triaxial accelerometers had become too large. To mitigate this problem, the single-axis accelerometer from a different test trailer was moved to the front trailer. This removed the redundancy of lateral acceleration from the other type of trailer but provided higher accuracy lateral acceleration measurements for the front trailer without degrading the accuracy of the other trailer's lateral acceleration measurements by an undesirable degree.

The accelerometers were purchased with calibration curves provided; therefore, calibration curves were not developed for the sensors. Rather than generate new calibration curves for each accelerometer, the calibration process instead verified that the provided calibration curves were reasonably accurate. After testing each accelerometer against the curve provided by the manufacturer, each was found to match within a reasonable margin.

3.1.2. Load Cells

Although the primary function of an outrigger is to prevent the trailer from rolling over, the outriggers were each equipped with a Forsentek FLP-100t load cell to measure the contact force when the outrigger wheel hit the ground. The contact force measurement allowed for quantitative differentiation between the outrigger grazing the ground, light outrigger wheel contact, and hard outrigger wheel contact, thereby allowing for the categorization of rollovers based on expected severity. The mounting of the load cells within the outrigger inboard beam is shown in Figure 3-3.

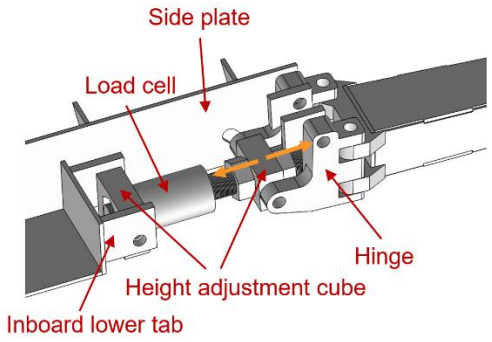

Figure 3-3. Load cell mounted within outrigger inboard beam.

To quantify the relationship between the force measured by the load cell and the force at the outrigger wheel, each load cell was calibrated by applying a known force to the outrigger wheel bearing surface and fitting a curve between the applied force and the measured force. As shown in Figure 3-4, a hoist fitted with a Futek L2900 tension load-cell was used to apply forces up to 3,500 lbf at the outrigger wheel bearing surface. Using the calibration curves provided by the manufacturer, the force measured at the outrigger load cell was compared to the force measured by the hoist load cell, and a curve fit was developed to quantify the relationship. The force on the outrigger wheel was increased from 0-3,500 lbf and then decreased back to 0 lbf a total of three times for each load cell. The data from each of the three trials was then used to develop a curve fit for each outrigger load cell. A piecewise function best approximated the vertical force applied on the outrigger wheel, where the first equation was cubic and the second was linear.

Figure 3-4. Load cell calibration test setup

3.1.3. Pressure Transducers

Four pressure transducers were used on each trailer to measure the air pressure in key parts of the trailer's pneumatic circuit. Air pressure was measured at the air tank, suspension, and both the left and right brake chambers. The brake pressure transducers were installed between the RSC module and the brake chambers. Additional pressure transducers were installed onto the tractor to measure the left and right brake chamber pressures, air tank pressure, and the braking robot auxiliary tank and actuator pressures.

To calibrate the pressure transducers, the output voltage of each transducer was compared against that of a pressure transducer with a known curve fit. The reference pressure transducer output voltage was measured at 0, 20, 40, 60, 80, and 100 psi using a digital pressure gage with ± 0.1 psi accuracy. A curve fit was developed for the relationship between output voltage and pressure for the transducer from this data. To calibrate each test pressure transducer, the output voltage of the pressure transducer was recorded for a slowly changing pressure and simultaneously compared to the reference pressure transducer, which was exposed to the same pressure. The pressure was first increased from 0-100 psi, then decreased back to 0 psi to account for hysteresis. A curve fit was then developed between the measured pressure of the test transducer and the reference transducer. The calibration test setup is shown in Figure 3-5.

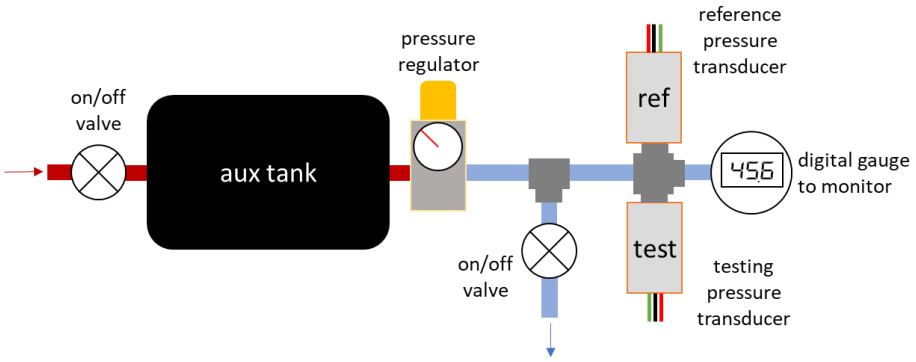

Figure 3-5. Pressure transducer calibration setup.

3.1.4. String Potentiometers

String potentiometers were used to measure the tractor steering wheel angle and the suspension travel on both the passenger and driver sides of the trailers. The steering string potentiometer was wrapped around the steering column, and the measured linear displacement was converted to an angle measurement using the circumference of the steering column. The suspension string potentiometers were installed underneath the trailers and measured the sprung mass deflection at the load-leveling valve bracket. The mounting of each string potentiometer type is shown in Figure 3-6.

(a) (b)

Figure 3-6. String potentiometer mounting locations for the (a) trailer, (b) tractor steering wheel angle.

To develop the calibration curves for the string potentiometers, the output voltage of each sensor was measured at 0, 2.5, 5.0, 7.5, and 10.0 inches both increasing and decreasing through the range. A linear curve fit was developed for each string potentiometer based on the output voltage measurements. The steering wheel angle calibration curve was measured

by rotating the steering wheel to a known angle and comparing that to the output voltage of the sensor.

3.1.5. LiDAR

Multi-segment solid-state LiDAR sensors were used to measure the articulation angle between the units of the articulated heavy vehicle. The sensors utilized were LeddarTech™ IS16 sensors with a 48° total horizontal field of view and 6° vertical field of view over 16 segments. The first LiDAR sensor was installed on the back of the tractor and measured the articulation angle between the tractor and the front trailer. The second LiDAR was mounted on the back of the front trailer and measured the articulation angle between the front and rear trailers. The articulation angle between the dolly and the front trailer and the dolly and the rear trailer were not directly measured and were bypassed by measuring the articulation angle between the two trailers. The installed LiDAR sensors are shown in Figure 3-7. The segmented LiDAR allows for the calculation of articulation angle from the slope of the distance measurements by each segment. Measured values of the LiDAR were calibrated using a linear curve-fit developed from testing the LiDAR at known distances from the front face of a trailer.

(a) (b)

Figure 3-7. LiDAR sensors installed on the rear of the (a) tractor and (b) front trailer.

3.1.6. Relays and Flags

Three relays on each trailer and two relays on the tractor were used to record the activation times of the electronic safety control systems. When the ABS, RSCI, RSCII, and ESC activated, the relays would switch to a high voltage signaling that the safety systems had activated. The use of relays in detecting the on/off times of the safety systems allowed for the determination of roll indicator values at the point in time where the safety system had activated.

A photo-electric sensor was used as a flag to mark the start of each trial. The sensor was mounted on the front of the tractor perpendicular to the path of motion. As the vehicle was entering the maneuver, the sensor would detect a reflective target that marked the maneuver starting point. The flag eased processing the continuous test data by marking points in time at which a test was taking place, thereby allowing the splicing of data to include only relevant data.

3.1.7. Data Acquisition and Signal Routing

A National Instruments CompactRIO (NIcRIO), shown in Figure 3-8, is a real-time embedded industrial controller used to collect and record information from all the analog sensors on the articulated vehicle and the GPS receiver on the tractor during testing. The NIcRIO system consists of a real-time controller, reconfigurable I/O modules, and an FPGA chassis. The setup used two NI 9205 models with up to 16 differential or 32 single-ended voltage analog inputs up to ±10 V. The first module utilized 2 differential and 28 single-ended signals, while the second module used 3 differential signals and 14 single-ended signals. The NIcRIO system is operated through the NI LabVIEW software on a host PC that is connected to the NIcRIO through an ethernet cable. During testing, the live data is viewable on a user interface to observe key data during the tests and ensure data accuracy. The sample rate used for data collection on the NIcRIO modules was 250 Hz, while the GPS transmitted data as a sample rate of 5 Hz.

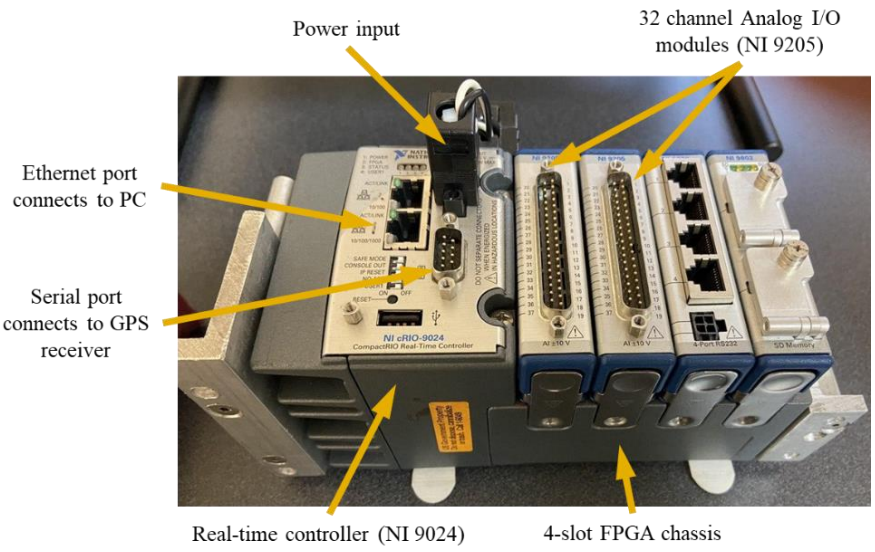

Figure 3-8. National Instruments CompactRIO (NIcRIO).

While all analog sensors were connected to the NIcRIO, the two digital LiDAR sensors used LeddarTech's proprietary software Leddar Configurator™ to record data. Each LiDAR sensor required its own instance of software; therefore, two Leddar Configurator™ programs were running simultaneously. Because a different software was used to connect the LiDAR sensors, the different data files had to be synchronized in post-processing using the start times of all files and the flag data from the NIcRIO. The sample rate of the Leddar Configurator™ was 50 Hz, different than that of the NIcRIO and GPS.

To provide power to the onboard analog sensors and route the voltage signals from the sensors back to the NIcRIO by way of a DB-37 cable, the tractor and each trailer possessed a junction box. The trailer JBs were identical to preserve interchangeability in case of unacceptable noise levels or failure in one of the junction boxes. The tractor junction box was unique because it connected to fewer analog sensors but combined the signal cabling of both the front trailer and the tractor for output into a single module of the NIcRIO. The rear junction box sensor signals were routed directly to the NIcRIO. Each trailer junction box was powered by a 13V 4s1p Lithium-Iron Phosphate ($LiFePO_4$) battery pack that could provide more than 12 hours of power, which is longer than the typical day of testing. The tractor junction box required an additional 10 Ah battery to power the NIcRIO. Additionally, each junction box was connected to a common ground to ensure the same base electric potential and avoid introducing ground loops. In the trailers, the junction

boxes were secured using wooden mounts and bungee cords to ensure that they did not shift and damage any cables during testing. Additionally, all sensor inputs to the junction box were secured with strain relief to guarantee that the cables did not damage the junction box if pulled. The sensor cables also had strain relief on the sensor end to ensure no damage to the sensor if the cable was pulled. The trailer junction boxes' last function was to provide power to the LED flags used for video synchronization with the data.

3.1.8. Video Data

Throughout testing, 8 to 13 GoPro Hero cameras were used simultaneously to observe the key dynamics of the tractor, trailers, and dolly during the maneuvers. The cameras were positioned to observe the articulation between units, wheel lift, outrigger contact, wheel lock-up, oversteer, understeer, and the driver. The layout of the cameras on the articulated vehicle is shown in Figure 3-9. The existence of video data allows for the verification of the analog data and clarification of uncertainties in the analog data. LED flags in the view of each camera were used to synchronize the video data to the analog data in post-processing.

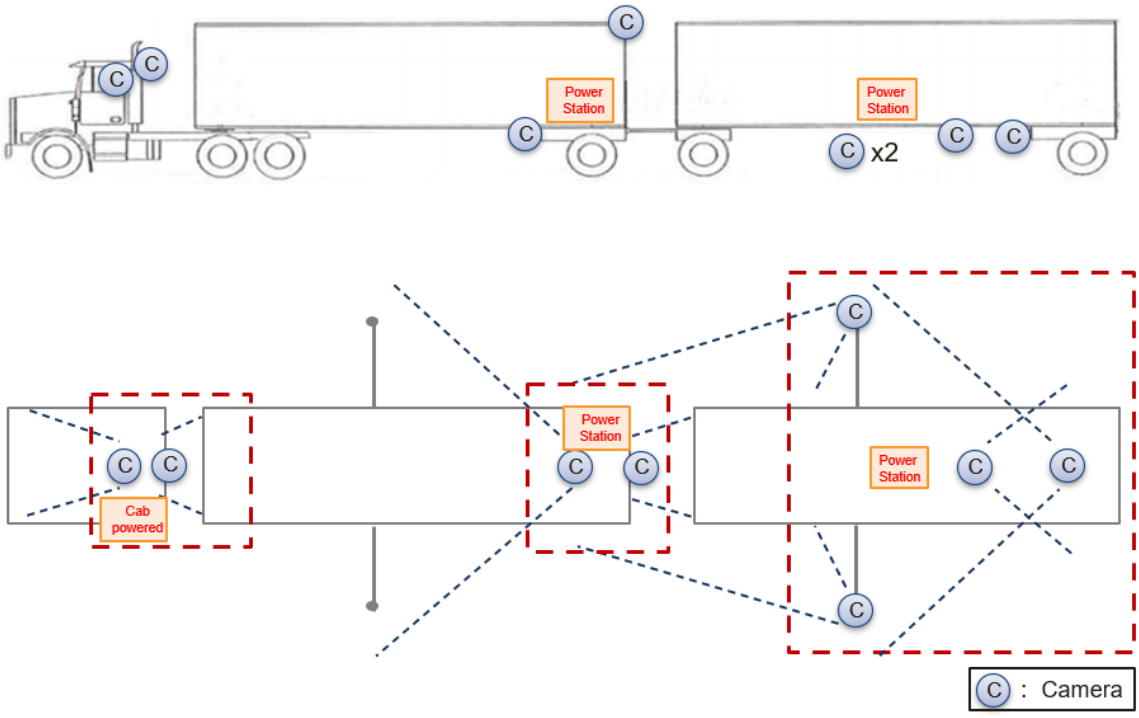

Figure 3-9. Camera layout on tractor and trailers.

3.1.9. Steering Robot

For higher repeatability during complex-steering maneuvers, the tractor was equipped with a programmable open-loop steering robot shown in Figure 3-10. The steering robot uses a servo motor attached to the steering column to control the steering angle of the wheels. The robot is mounted inside of the engine bay so that it does not interfere with the driver's ability to resume steering control of the vehicle if necessary. For the steering robot to engage, a switch must be continuously held. If the switch is disengaged or the emergency stop button is pressed, the robot will relinquish steering control to the driver. The photo-electric sensor attached to the front of the tractor, in addition to marking the start time of the maneuver, is used as a spatial trigger to initiate steering control by the robot. When the sensor passes by the reflective target at the starting gate of the maneuver, the robot begins the open-loop steering script.

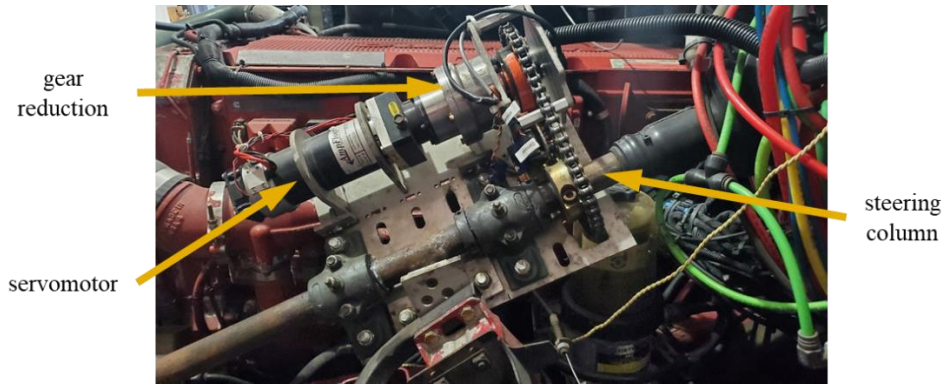

Figure 3-10. Steering robot installed on tractor steering column

3.2. Safety Equipment

To protect the driver, passengers, bystanders, and vehicle structure itself safety equipment was installed on the vehicle to prevent rollover, jack-knifing, and torsion of the trailer frame. Additionally, load frames were installed that were designed to withstand high lateral and longitudinal accelerations and hold heavy loads that could imitate the actual loading of trailers during highway driving. This section will briefly describe the design of the safety equipment installed on the test vehicle, including trailer outriggers, an anti-jack-knifing system, trailer reinforcement structures, and the load frames.

3.2.1. Outriggers

Each trailer was equipped with an outrigger assembly to prevent the trailers from rolling over during testing. The outrigger assembly consists of one inboard beam, a pair of outboard beams, and connecting hinge assemblies, as shown in Figure 3-11.

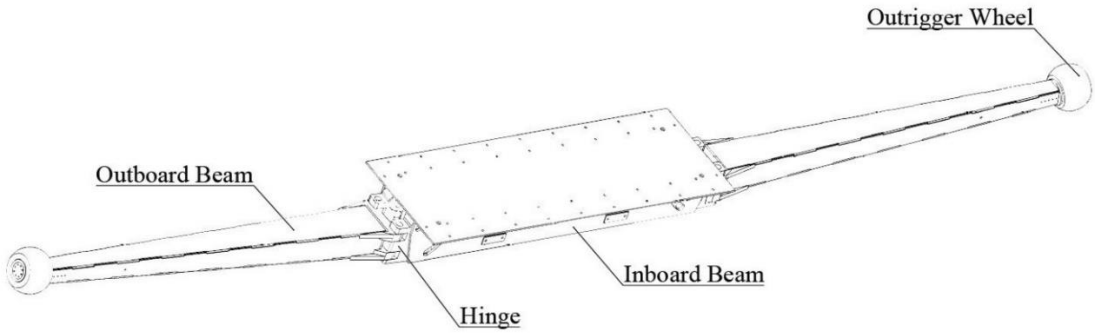

Figure 3-11. CVeSS outrigger assembly

The inboard beam is mounted to the lateral cross beams of the trailers and was fitted with two sets of holes for ease of installation. The outboard beams are connected to the inboard beams through hinge assemblies so that they could be folded underneath the trailer during transport. The outboard beams were equipped with 10' HDPE plastic wheels at the ends to minimize the effects of an extended mass on the inertial properties of the trailer. If the outriggers were equipped with a rubber tire and steel wheel, the impact of the extended mass on the roll properties of the trailer would have been more significant. In addition to the assembly shown above, each outrigger was also outfitted with a load cell so that the contact force of the wheel with the ground could be determined. The load rating of each outrigger is approximately 31,685 lbf.

3.2.2. Anti-jack-knifing System

During aggressive dynamic maneuvers, the articulated units of a combination vehicle are in danger of jack-knifing. To prevent jack-knifing, each connection between the articulated units is equipped with an anti-jack-knifing system consisting of kinetic ropes and metal chains, as illustrated in Figure 3-12.

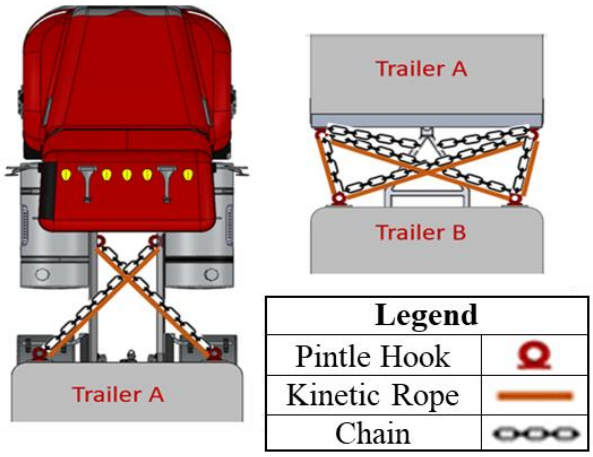

Figure 3-12. Anti-jack-knifing system design

The ropes and chains are connected to pintle hooks installed on the tractor and trailer using shackles and clevis hooks. The pintle hooks installed on the trailer are bolted to both the trailer frame and yaw reinforcement structure of the trailer. The system is designed so that the ropes engage first to remove kinetic energy from the system prior to the engagement of the chains. If the ropes are unable to dissipate enough energy to prevent jack-knifing at the limit of permanent elongation, the chains will engage. In total, the ani-jackknifing system is designed to prevent three types of jack-knifing: tractor jack-knifing, trailer jack-knifing, and dolly jack-knifing. Cross ropes and chains are installed between the tractor and trailer to prevent tractor jack-knifing. Cross chains and ropes are used between the trailers to prevent trailer jack-knifing, along with parallel chains and ropes to prevent dolly jack-knifing. The ropes are designed to elongate by 30% and have a breaking strength of 28,600 lbf., while the rigid chains have a breaking strength of 90,400 lbf.

3.2.3. Trailer Reinforcement

When the trailers roll onto the outriggers, a large force is transmitted from the outrigger to the trailer structure. Since trailers have low torsional strength, roll reinforcement structures, shown in Figure 3-13, were necessary to prevent the trailer frame from bending or twisting during rollover events.

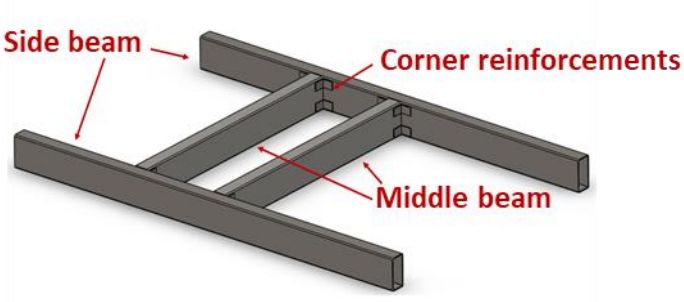

Figure 3-13. Roll reinforcement structure

On the trailers, the roll reinforcement is an "H" shaped assembly of steel beams mounted underneath the trailer. In addition to the roll reinforcement structure, each trailer was also equipped with a yaw reinforcement structure to prevent bending or twisting of the trailer frame if the anti-jack-knifing system engages, as shown in Figure 3-14. The yaw reinforcement structure is installed at the bulkhead of the trailer.

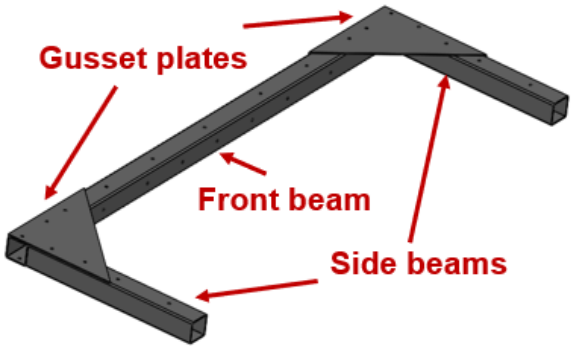

Figure 3-14. Yaw reinforcement structure

3.2.4. Load Frames and Loading Conditions

Each trailer was equipped with a load frame to carry the ballast required for the desired loading and CG position. The load frames consist of a double-layer pallet rack that can carry up to approximately 20,000 lbf of ballast. Bags of gravel and sand weighing 50 lbf were used as ballast during testing. The ballast placed in the pallet racks of the load frame was secured using wooden boards and ratchet straps to prevent the load from shifting during testing. To meet the desired CG position, bags of ballast were also secured on the floor of the trailer during testing. To prevent the ballast on the trailer floor from shifting during the test maneuvers, the bags were secured in place using wooden boards and ratchet

straps. The load frames were designed to withstand high lateral and longitudinal accelerations that may be experienced by the trailer during testing. To verify the strength of the load frames, an FEA analysis of the load frames was performed in which a 1.2g lateral acceleration and 0.4g longitudinal acceleration were simultaneously applied to each pallet at the location of the sandbags. The load frames had a minimum factor of safety of 2.8. The installed load frames are shown in Figure 3-15.

Figure 3-15. Load frame mounted inside the trailers

To approximate realistic trailer loading conditions, two different loading conditions were used: heavy loading and light loading. When the trailers were heavily loaded, each trailer contained an additional 15,000 lb. of load from its stock condition. This weight includes the safety equipment installed within the trailers, load frames, and the additional ballast needed to reach the desired weight. Under light loading conditions, an additional 7,500 lb. of load was contained within each trailer, replicating a scenario in which the trailer is loaded to 40% volumetric capacity with uniform density load. The heavy loading scenario replicates a trailer loaded to 80% volumetric capacity with a uniform density load. Both loading conditions are presented in Figure 3-16.

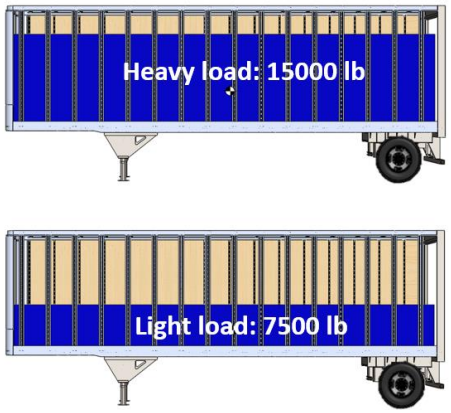

Figure 3-16. Heavy and light loading conditions.

3.3. Class 8 – A-double Test Vehicle

Two different 33 ft box trailer loading conditions were used during testing, as illustrated in Figure 3-16. The trailer under heavy loading and light loading will be referred to as straight(H) and straight(L), respectively. A second trailer type, the drop-frame trailer, was also used during testing. Within the context of this study, the drop-frames themselves were not analyzed; however, the effect of a drop-frame trailer on a straight-rail trailer when coupled is analyzed. The unloaded geometric properties of the test straight-rail trailer are summarized in Table 3-1, while the trailer pneumatic suspension properties are summarized in Table 3-2. The coupled drop-frame trailers had nearly the same geometric properties as the straight-rail trailers, with the exceptions of a 336 in. wheelbase and a tare weight equal to 11,160 lb. The drop-frame trailer possessed a pneumatic suspension with a different architecture and ride height. The drop-frame suspension was an under-slung trailing arm suspension with a ride height of 3.5 in. and a jounce and rebound of 2.6 and 3.0 in., respectively.

Table 3-1. Unloaded trailer properties.

Trailer Type	Manufacturer	Manufacture date	Trailer length	Wheelbase	Track width	Tare weight
Straight-Rail	Hyundai	Sep 2015	396 in	330 in	78 in	10,110 lb.

Table 3-2. Trailer pneumatic suspension properties

Trailer type	Suspension Type	Design Ride Height (in.)	Jounce (in.)	Rebound (in.)
Straight-rail	Top-slung trailing-arm	14	2.9	5.1

A CAD model was used to determine the properties of the test trailers. The CAD model of the stock trailers was verified by comparing the CG position and weight of the model to the actual trailers. The longitudinal location of the CG was determined by performing an incline test with the trailers and measuring the weight distributed underneath the tires. As shown in Table 3-3, the CAD model accurately represented both the CG location and the weight of the empty stock trailers. Therefore, the CAD model could approximate the CG location and inertial properties of the loaded trailers used during testing.

Table 3-3. Comparison of incline test results and trailer CAD model

	33-ft Straight-rail (Empty)		
	Incline test	CAD model	Difference
CG height [in]	60.1	61.2	1.6%
CG longitudinal distance to kingpin [in]	206.9	205.7	1.2%
Tare weight [lb.]	10,110	10,154	0.4%

The safety structures and load frames were added to the CAD model to obtain an accurately modeled representation of the trailers. In addition, for the heavy loading and light loading scenarios, ballast was added to the model to approximate the loading conditions during the actual tests. The final approximate trailer properties, including all safety equipment and ballast load, are shown in Table 3-4.

The tractor used for testing, pictured in Figure 3-17, was a 2004 Volvo VNL 6x4 tractor with a sleeper cab. The front steering axle is equipped with a leaf spring suspension, while the tandem drive axles are equipped with a pneumatic suspension. The physical properties of the tractor are given in Table 3-5. The tractor is equipped with an electronic stability control (ESC) module with both yaw stability control and roll stability control. This particular ESC module uses differential braking to stabilize the vehicle when it is

approaching either yaw or roll instability. In addition to providing differential braking control, the ESC system also has access to the throttle control and can cut the driver throttle demand. Because the driver did not apply throttle and disengaged the clutch during the test maneuvers, the effects of throttle control were not observed during testing. The ESC system was toggled on and off during testing for different test permutations, but no tests involving ESC were analyzed in this study.

Table 3-4. Comparison of CG location and inertial properties of a trailer with a typical load and a trailer with a loaded load-frame

Loading condition	**Parameter**	**33-ft straight-rail**		
		Trailer with typical load (CAD model)	Trailer with load frame (CAD model)	Difference
Heavy load (15,000-lb load)	Total weight [lb.]	25,250	25,022	0.1%
	CG height [in]	79.5	77.8	2.0%
	CG longitudinal [in]	182.8	179.6	1.0%
	Roll inertia [lb·ft^2]	8.4*10^5	8.9*10^5	6.0%
	Yaw inertia [lb·ft^2]	7.1*10^6	7.0*10^6	1.7%
Light load (7,500-lb load)	Total weight [lb.]	17750	17522	1.2%
	CG height [in]	66.8	65.6	1.8%
	CG longitudinal [in]	189.8	183.5	3.3%
	Roll inertia [lb·ft^2]	7.0*10^5	7.6*10^5	8.5%
	Yaw inertia (lb·ft^2)	6.5*10^6	6.6*10^6	1.5%

Figure 3-17. 2004 Volvo VNL 6x4 tractor with sleeper cab

Table 3-5. 2004 Volvo VNL 6x4 tractor with sleeper cab properties

Manufacturer	Manufacture Date	Tare weight	Steer axle track width	Drive axle track width	Wheelbase
Volvo	Jan 2004	~20,000 lb.	82 in	73 in	250 in.

The converter dolly used during testing was an A-dolly, the most common configuration found in the United States. As described in 2.3, the A-dolly connects to the rear of the front trailer using a pintle-hitch and connects to the rear trailer using a fifth-wheel hitch. The A-dolly used during testing, shown in Figure 3-18, was equipped with a pneumatic suspension and did not have self-steering tires. Table 3-6 shows the properties of the A-dolly used during testing.

Figure 3-18. Test converter A-dolly

Table 3-6. A-dolly properties.

A-Dolly	Wheelbase	Track width	Tare weight	Suspension Type
	72 in	78 in	3,000 lbf	Air

3.4. Testing Procedure

This section describes the tests performed at the Transportation Research Center (TRC) to evaluate the stability of articulated heavy vehicles in the A-double configuration. First, the different combinations of trailer conditions that were evaluated during testing are illustrated. Then, the maneuvers used to evaluate and compare trailer stability between the different trailer combinations are specified. Next, the test environment is described. Lastly,

the tests that were completed at the track are listed, and the data processing techniques that were used are described

3.4.1. A-Double Test Vehicle Combinations

Various conditions were evaluated during the high-speed testing phase at TRC, including different loading conditions and different trailer combinations. Three different loading conditions were tested: heavy, mixed, and light loading. Heavy and light loading refer to the cases in which both trailers are either under heavy or light loading conditions, respectively. The mixed loading condition refers to the scenario in which the front trailer is under heavy loading, and the rear trailer is under light loading. In addition to testing the A-double under different trailer loading conditions, the A-double was also tested in mixed trailer tests, with a heavily loaded drop-frame trailer – drop(H) – coupled to either the front or the rear of the straight(H) trailer. To summarize the different test combinations in Figure 3-19, the following naming convention is used: heavy: "Straight (H)," mixed: "Straight (M)," and light: "Straight (L)." Note that straight(H) refers to a single straight-rail trailer that is heavily loaded, while Straight(H) refers to the combination of two heavily loaded straight-rail trailers.

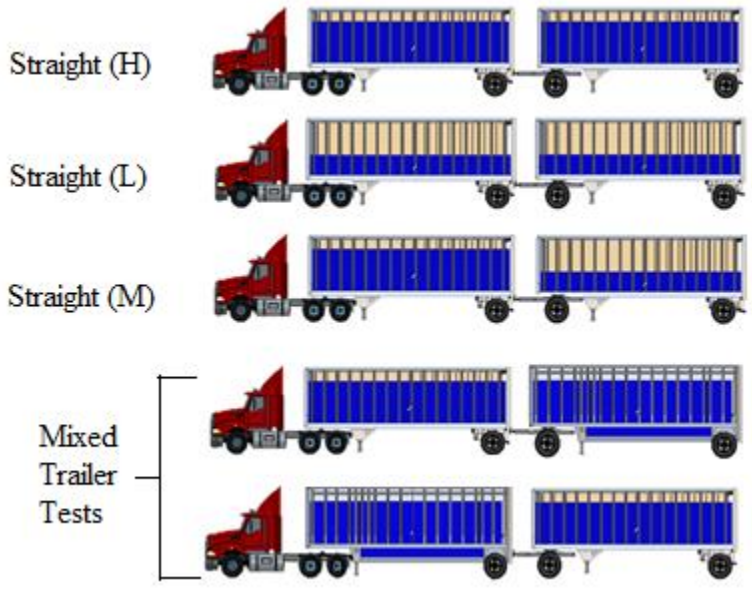

Figure 3-19. A-Double trailer combinations tested at TRC

3.4.2. Test Maneuvers

Four different maneuvers were performed to evaluate the stability of A-doubles during the high-speed testing study. Two of the maneuvers were quasi-steady-state maneuvers designed to observe the roll dynamics of the articulated vehicle and imitate a vehicle traveling through a constant radius turn or an idealized exit ramp. The other two maneuvers were dynamic, or directional, evasive maneuvers. They were designed to imitate a scenario where the driver has to avoid an obstacle in the vehicle's forward path. Thus, rather than being a measure of the steady-state rollover threshold, these maneuvers present a dynamic rollover threshold.

Two semi quasi-steady-state maneuvers were performed to observe the roll dynamics of the A-double configuration in a cornering maneuver. The first quasi-steady-state maneuver was the J-turn, in which the driver steered the vehicle. The J-turn followed a constant inside radius of 150ft with a 13 ft road width for 180°, as shown in Figure 3-20. After the driver ramps up to the required steering angle to maintain the intended curve, the tractor lateral acceleration slowly decreases throughout the turn due to the scrubbing of speed during a constant radius turn. Because the decrease in lateral acceleration throughout the turn is sufficiently slow, the quasi-steady-state assumption is upheld for the maneuver in the context of this study.

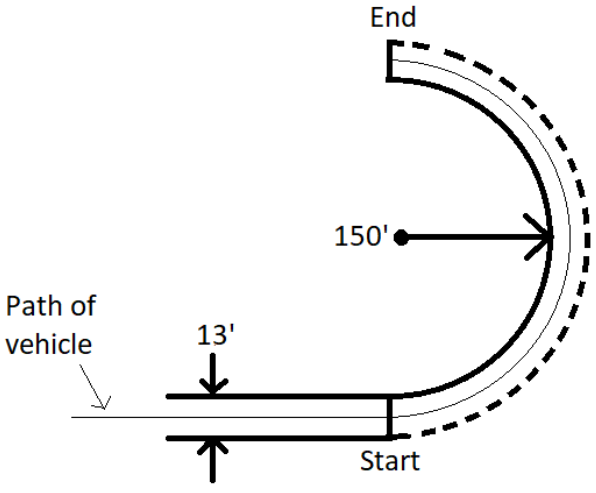

Figure 3-20. J-turn steering path.

The second quasi-steady-state maneuver was the robot-steered ramp-steer maneuver. The ramp-steer maneuver was designed to approximate the J-turn at a moderate speed of 30

mph. The CVeSS steering robot was used for this maneuver to provide more repeatable steering inputs to the vehicle between individual trials. The main difference between the driver-steered J-turn and the robot-steered ramp-steer is that the driver maintains a set path in the J-turn maneuver, while the robot holds a constant steering angle regardless during the ramp-steer maneuver of speed. Both the J-turn and the ramp-steer maneuver are speed-based maneuvers. As shown in Figure 3-21, the ramp time for the steering robot control was approximately 1.5 seconds, and the steering amplitude was about 215º. Once the steering wheel angle reaches the desired value, the lateral acceleration of the trailer is nearly constant as a result of the constant steering angle, upholding the quasi-steady-state assumption.

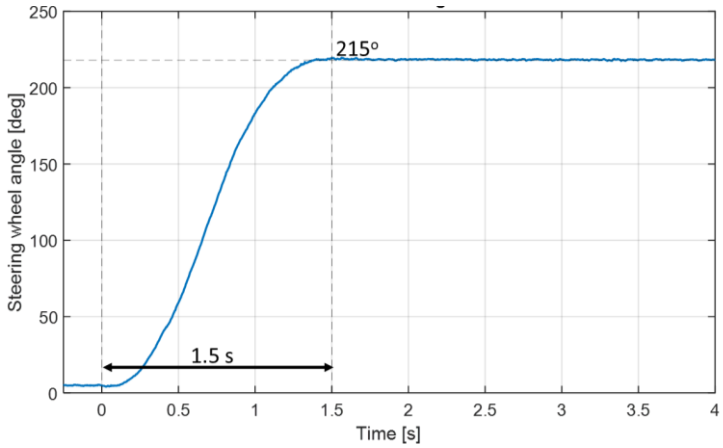

Figure 3-21. Ramp-Steer steering profile.

The first dynamic, evasive maneuver performed was the Double Lane Change (DLC) maneuver. As shown in Figure 3-22, the total length of the DLC was 340 ft. Upon reaching the starting gate, the driver quickly steered into the left lane within 126 ft and returned to the original lane within 115 ft. The path was designed according to recommendations from the NHSTA [45]. Each gate along the vehicle's path was marked with cones, with the requirement that if a cone was hit by the tractor the maneuver would be repeated.

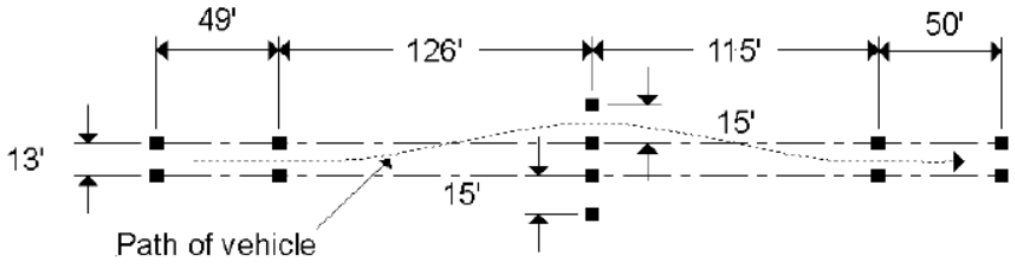

Figure 3-22. Double Lane Change (DLC) steering path [45]

The second dynamic maneuver was the Sine with Dwell (SWD) maneuver. Initially, four variations of this maneuver were performed: 0.25-Hz at 40 mph, 0.5-Hz at 40 mph, 0.25-Hz at 45 mph, and 0.5-Hz at 45 mph. However, after analyzing preliminary results, it was determined that the 40 mph tests did not have a sufficiently high entry speed to compare different trailer configurations and loading conditions, so those tests were discontinued. Additionally, the 0.5-Hz at 45 mph variation did not provide any additional results or conclusions from the DLC maneuver because the steering frequencies overlapped, so the tests with this variation were also discontinued. The 0.25-Hz SWD at 45 mph was used throughout the high-speed testing to analyze the effect of steering angle on the rollover characteristics of a vehicle. The maneuver consisted of a 0.25-Hz half-sine wave followed by a 2-second dwell. From a previous study, the maximum steering wheel angle of the tractor was determined to be 250^{o} by using a slowly increasing steer maneuver [46]. The maximum steering wheel angle represents the steering wheel angle at which the tractor lateral acceleration reaches 0.5 g. In this study, the steering wheel angle will be reported as a percentage of this maximum steering angle. Figure 3-23 displays the increasing steering wheel percentage on the steering profile of the SWD maneuver from 40% to 100% steering. The steering robot performed the steering of the SWD maneuver for high repeatability between tests. Because the vehicle's position varied at the end of the maneuver due to the changes in steering wheel angle, rather than using an end gate, this maneuver ended when the vehicle straightened out after the final steering input.

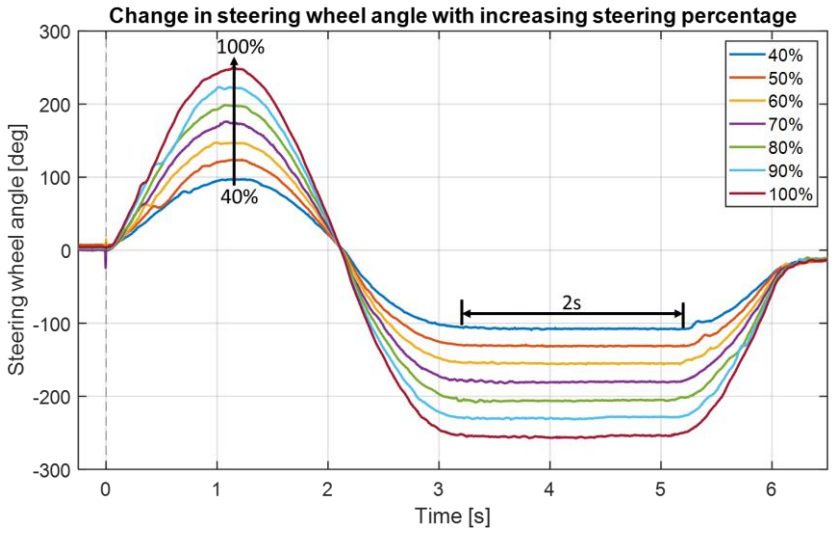

Figure 3-23. SWD steering profile from 40%-100% steering.

The procedure for each driver-steered maneuver – J-turn and DLC – is as follows. Each maneuver was performed with the vehicle coasting through the maneuver; the driver did not maintain throttle control through the maneuver. The driver was instructed to move through the starting gate at a predetermined speed, disengage the clutch just before passing through the starting gate, and follow the path until passing through the end gate of the maneuver or until the vehicle straightened out after the last steering input. During robot-steered maneuvers – ramp-steer and SWD – in addition to the procedure detailed above, the driver also relinquished steering control to the steering robot for the entire test duration. For the three speed-based maneuvers, the tractor entry speed was increased in 1-2 mph increments for each successive trial. After sufficiently hard outrigger contact was observed, the trial at that speed was repeated. If outrigger contact occurred in the repeated trial, the speed was lowered in 1 mph increments until outrigger contact no longer occurred. For the single steering-based maneuver, SWD, the steering percentage was increased by 5-10% for each successive trial. The same procedure for outrigger contacts as outlined above was followed, with the difference that the steering percentage was decreased by 5% until outrigger contact no longer occurred rather than decreasing the speed by 1 mph.

3.4.3. Test Environment

The high-speed testing study was performed at the Transportation Research Center (TRC) in East Liberty, Ohio on the Vehicle Dynamics Area (VDA). The VDA is 50 acres in size

with 2 loops and a large center pad with a 1% slope from north to south, as detailed in Figure 3-24 [47]. All test maneuvers were performed on the east side of the VDA with the vehicle traveling from north to south during the maneuver, with the 1% slope. When necessary, the North Loop was utilized for high-speed entry to the VDA. Additionally, the North Loop was also used for brake cooling after maneuvers in which the RSC and ESC engaged to prevent brake temperature differences from altering the results of the tests. All field tests were performed outdoors; therefore, the wind and temperature conditions were not controlled throughout the testing. No tests were performed during rain or in wet conditions. Under dry conditions, based on a previous study performed on the VDA, the coefficient of friction is expected to be in the range of 0.8-0.9 [48].

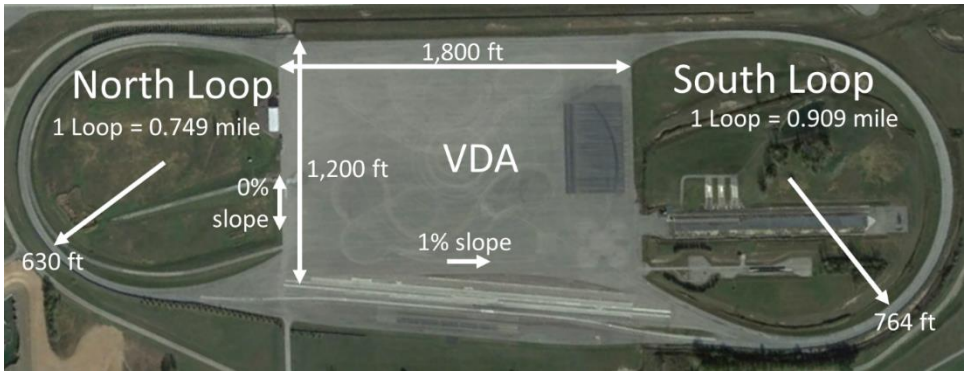

Figure 3-24. Transportation Research Center (TRC) Vehicle Dynamics Area (VDA) dimensions (Google Earth image, accessed March 2021).

3.4.4. Tests Performed

During the high-speed testing portion of the study, over 1,100 individual trials were performed, with approximately 946 of those trials being usable for data analysis. Some trials were unusable because of high sensor noise, instrument errors, test errors, or because the tuning on the steering robot was altered after the tests were completed. The high-speed testing study was broken up into five distinct sessions:

- Test Session 1 (Aug 24 – Aug 26): Shakedown & baseline testing
- Test Session 2 (Sep 14 – Sep 16): Heavy load
- Test Session 3 (Sep 17 – Sep 18): Light Load
- Test Session 4 (Oct 05 – Oct 09): Mixed Load, Mixed Trailer
- Test Session 5 (Oct 12 – Oct 13): Disc Brake Tests

The purpose of the first test session was to evaluate all instrumentation on the vehicle to ensure that the data collected was reasonable. During the second and third sessions, the goals were to test both trailer types under heavy and light loading conditions, respectively. The Straight (M) trailer combination and the two mixed trailer configurations were tested during the fourth session. Finally, during the fifth and last session, the high-speed maneuvers were repeated with disc brakes installed on the trailers in place of drum brakes.

Additional tests, such as straight-line braking and braking in-turn tests, were also performed at TRC. The tests are not relevant to this study; therefore, they will be omitted from this report. The complete test matrix is shown below in Table 3-7, with relevant tests highlighted. A more in-depth view of the test series performed at TRC can be found in Appendix B.

Table 3-7. Test matrix for high-speed testing at TRC.

Trailer Combination			Heavy load		Light load		Mixed load	
			ESC off	ESC on	ESC off	ESC on	ESC off	ESC on
Drum Brakes	Straight-Straight	RSC off	x		x		x	
		RSC on	x	x	x	x	x	x
	Drop-Drop	RSC off	x		x			
		RSC on	x	x	x	x		
	Mixed Trailer (Drop-Straight)	RSC off	x					
		RSC on	x	x				
	Mixed Trailer (Straight-Drop)	RSC off	x					
		RSC on	x	x				
Disc Brakes	Straight-Straight	RSC off		x				
		RSC on	x	x				

3.5. Test-Trailer RSC Properties

All test trailers were equipped with a 2S/2M combined ABS/RSC system that was commercially available in the United States. Using a pressure sensor, the RSC module obtained an estimate of the approximate axle load and used this value to estimate a rollover threshold for the trailer. The RSC system used lateral acceleration thresholds to determine

the proximity to rollover and used wheel speed sensors to calculate the longitudinal trailer speed and rate of acceleration. For this particular RSC module, there were two control schemes that are used to detect proximity to rollover, which will be referred to as RSC-I and RSC-II for the remainder of the report. When in danger of rolling over, the system applied the trailer brakes to slow down the vehicle and lower the lateral acceleration. The system was designed such that if the driver applied the trailer brakes at the same time as the RSC applied the trailer brakes, the larger of the two values would be used. The ABS functioned as usual and prevented tires from locking up during braking just as it would without the RSC system. Since this system has two wheel speed sensors (2S) and two modulators (2M), it could independently apply the trailer brakes on each side of the trailer. Besides this basic knowledge of the installed RSC system, the RSC module's inner workings and control schemes are unknown; therefore, the RSC system was treated as a black box controller.

To better show how the installed RSC system functions, brake pressure and RSC relay activation times for an example trial are shown for the DLC maneuver in Figure 3-25. The DLC maneuver was chosen because it had the most complex steering input; therefore, the roll response of the trailer was the most complex out of the four maneuvers. Since there are three distinct turns in the DLC maneuver – turning into the left lane, returning to the right lane, and straightening out in the original lane – there were three distinct locations during the turn in which a trailer may approach rollover conditions. There were two of these locations for the SWD maneuver, and for the J-turn and ramp-steer, the trailer only rolled over to the outside of the turn. As shown by the activation times and the brake pressures, when the system detected that the trailer was in danger of rolling over, the trailer brakes were applied to decrease longitudinal velocity and, thereby, lateral acceleration. During a left turn when the trailer was in danger of rolling over to the right, a low-pressure test pulse was applied to the left brakes to detect for possible wheel lift, and the right brakes were applied at high pressure. A high-pressure braking action was applied to the more heavily loaded outer wheel to generate the maximum braking force during the turn and most effectively brake the vehicle.

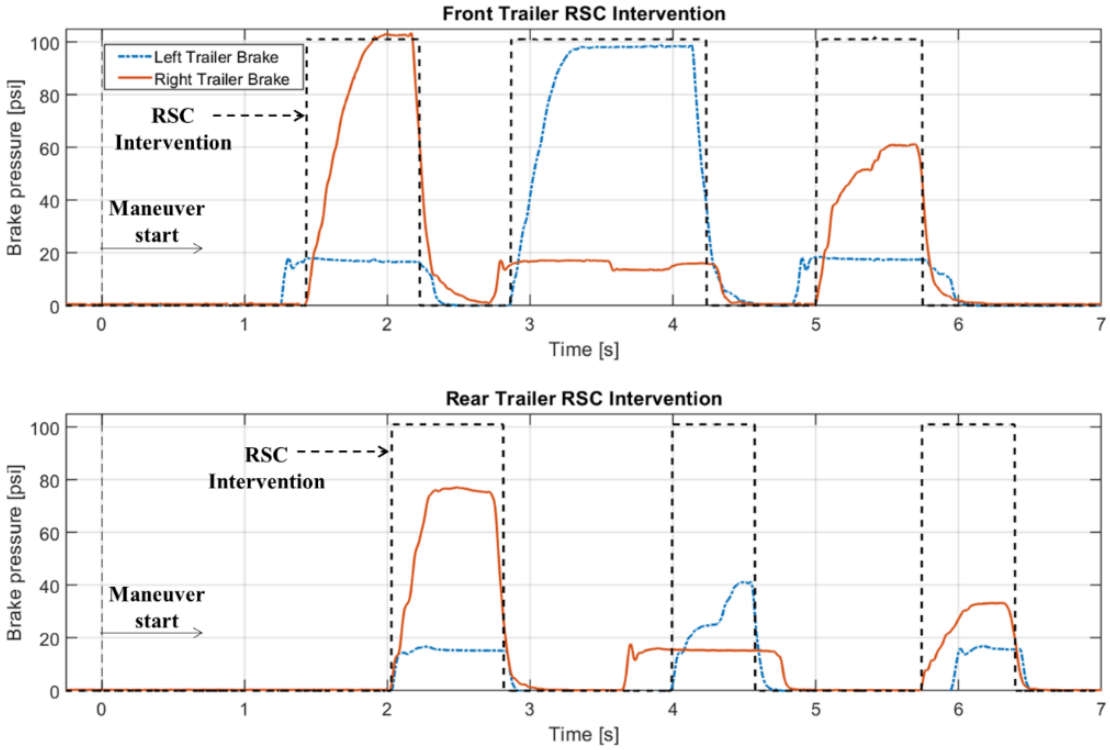

Figure 3-25. Time trace of brake chamber pressures of the front and rear trailers for the DLC maneuver at an entry speed of 44 mph with RSC intervention.

As shown in Figure 3-26, the RSC system was effective at lowering the vehicle speed. At 3.4 s, the approximate time of rollover for the stock vehicle in the trial shown, the RSC-equipped trailer had slowed down to approximately 40 mph, more than 2 mph less than the speed of the stock trailers. Because of the decrease in speed, the RSC-equipped trailer's lateral acceleration was lower than that of the stock trailer by approximately 0.05 g, as illustrated in Figure 3-27. As a result of the lower acceleration, the trailer with RSC did not roll over, while the trailer without RSC did. This result emphasizes that the decrease in trailer lateral acceleration from the RSC decreases the rollover probability of the trailers.

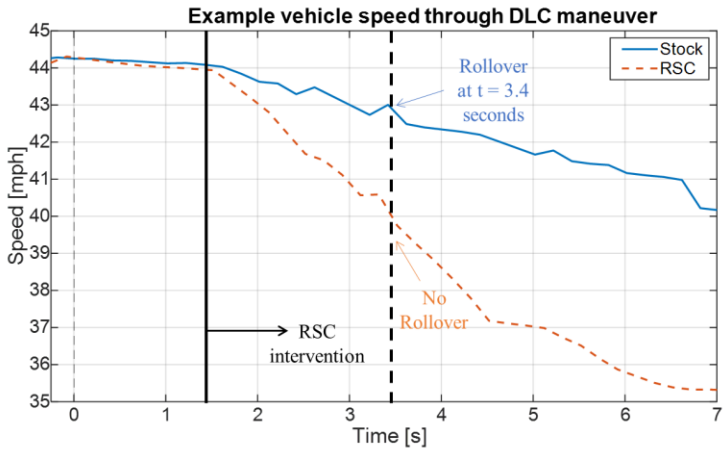

Figure 3-26. Comparison of forward velocity between stock and RSC-equipped trailers for the DLC maneuver at an entry speed of 44 mph.

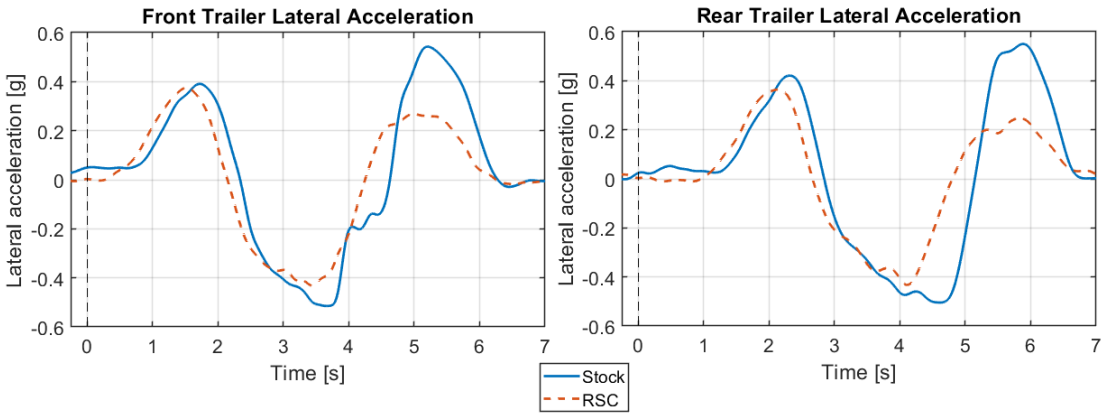

Figure 3-27. Lateral acceleration comparison between a stock and RSC-equipped trailer for the DLC maneuver at an entry speed of 44 mph.

3.6. Data Analysis Techniques

This section discusses the data processing techniques and the filters used to obtain the desired signals from the various sensors used in the study. The definition of rollover in terms of this study is also discussed.

3.6.1. Digital Filters

As mentioned in 3.1.7, the sample rate used by the NIcRIO data acquisition device during testing was 250 Hz, while the LiDAR was sampled at 50 Hz, and the GPS was sampled at 5 Hz. The NIcRIO data acquisition device is equipped with anti-aliasing filters, so no

additional analog filters were used to condition the signals before entering the NIcRIO. Data was then digitized and synchronized. For initial data screening, filtering was performed using a two-pass, 5th order, low-pass Butterworth filter with cut-off frequencies ranging from 3 to 25 Hz depending on the SNR of the sensor. A two-pass filter was used to avoid the phase-shift introduced by filtering since the results are temporally sensitive. For sensors more sensitive to vibration, such as the load cells and accelerometers, lower cut-off frequencies were used than sensors that were less sensitive to vibration, such as the pressure transducers and LiDAR. The final filtering stage for data processing was performed with a similar two-pass, 5th order low-pass Butterworth filter with cutoff frequencies listed in Table 3-8. Because the attenuation of undesired frequencies was acceptable with a 5th order filter, all low-pass filters used were 5th order. Additionally, the Butterworth filter was chosen because it is maximally flat in the passband and the stopband.

Table 3-8. 5th order, low-pass Butterworth filter cut-off frequencies for data screening and data processing.

Sensor	Screening f_c (Hz)	Processing f_c (Hz)	
		Quasi-Steady State Maneuvers	Dynamic Maneuvers
Triaxial Accelerometer (Tractor)	5	0.75	1.5
Triaxial Accelerometer (Trailers)	5	1.0	2.5
Single-Axis Accelerometer	5	1.0	2.5
Load Cell	3	2.0	2.0
String Potentiometer	10	1.0	4.0
Articulation Angle	-	5.0	5.0
Pressure Transducer	25	-	-

From time-domain and frequency-domain analysis, it was determined that the single-axis accelerometers had a lower SNR than the triaxial accelerometers, so the single-axis accelerometers were used where a redundancy existed. Different cut-off frequencies were used during the quasi-steady-state and the dynamic maneuvers because of the assumptions regarding the maneuver. Lower frequency filters were used on the quasi-steady-state maneuvers to remove the effects of small lateral oscillations of the trailer on the sensor measurements during the turns. Higher cut-off frequencies were used in the dynamic maneuvers because the lateral oscillations occurred at higher frequencies than in the quasi-steady-state maneuvers. Lower cut-off frequencies would smooth the data to an undesirable degree. The cut-off frequencies for the tractor acceleration measurements are lower than

on the trailers because a lower cut-off frequency was required to remove undesired oscillations from the data.

3.6.2. Rollover Definition

There are two stages of instability present in a typical rollover event: relative and absolute instability [24]. Relative instability is when wheel lift occurs on less than the total number of axles on the heavy vehicle. An occurrence of this is in the tractor semi-trailer configuration when the tires of the trailer lift off the ground, yet the tractor tires remain grounded. At this point, the trailer tires may either return to the ground or can experience absolute instability when the CG of the trailer aligns above the contact patch of the tire on the ground. When the CG is aligned above the contact patch, the trailer is in unstable equilibrium, similar to an inverted pendulum, at which the trailer will either rollover or return to the ground depending on the direction of the net moment on the trailer. Rather than defining rollover as when wheel lift occurs, as is typical in mathematical simulations, or when the outrigger contacts the ground, which is common in experimental testing, the outrigger wheel contact force measurement by the outrigger load cells is used to determine whether there was a high probability that a rollover would have occurred or whether there was a high probability that the trailer would have returned to the ground safely. From observations during testing, video data, and load cell data, it was determined that the approximate outrigger wheel contact force that differentiated rollover outrigger contacts from non-rollover outrigger contacts was 400 lbf. At a contact force of 400 lbf or greater, it appeared that the trailer possessed enough momentum to completely rollover and was experiencing absolute instability rather than relative instability.

To determine the rollover speed or steering percentage of the tested trailers in a specific combination and maneuver, the procedure outlined in Appendix C was followed. In cases where a rollover speed or steering percentage is referenced, this procedure was used to determine that speed or steering percentage. Rollover speeds do not represent the speed at the instant of rollover but instead represent the entry speed of the trial in which the trailer rolled over. The exact process of determining the rollover speed depended on the number of trials performed at particular entry speeds during a test series or the lack thereof. An

outrigger contact that was over 1,000 lbf was deemed exceptionally hard and was used as a secondary measure to examine the probability of rollover at different entry speeds.

4. Benefits of Trailer-based RSC on A-double Roll Dynamics Under Different Loading Conditions

In this chapter, the effect of trailer load on roll stability is analyzed using four high-speed testing maneuvers. In total, 3 vehicle loading conditions – heavy, mixed, and light – are compared. The tractor ESC system was disabled during the tests considered in this session. As discussed in 3.2.4, the weights of the heavily loaded and lightly loaded straight-rail trailers with the safety equipment installed are approximately 25,000 lb. and 17,500 lb., respectively. The total weight of the trailers under heavy, mixed, and light loading conditions is 50,000, 42,500, and 35,000 lb., respectively, excluding the weight of the dolly and the tractor, which is 23,000 lb. The center of gravity height for straight(H) is 77.8 in, and for straight(L) is 65.6 in measured from the road surface. It has been proven previously that CG height has a large effect on the roll stability of trailers; therefore, it is not the purpose of this study to prove that the heavier, higher CG trailers will roll over at lower entry speeds and lower lateral accelerations than the lighter, lower CG trailers [14]. Instead, this chapter will provide experimental data for an A-Double train that confirms this theory and expands upon the differences in roll dynamics that arise when the train is under different loading conditions. Furthermore, this chapter will compare the rollover thresholds, outrigger contact forces, and trailer rollover locations for the three loading conditions to emphasize the effect loading has on rollover nature of an A-double AHV. After discussing the effects of loading conditions on the roll dynamics of trailers in each maneuver, the effectiveness of RSC in increasing the rollover entry speed or rollover steering percentage of the trailers is examined.

4.1. A-double Roll Behavior under Different Loading Conditions

This section will compare the rollover propensity of straight-rail trailers under different loading conditions. The results are broken up by maneuver, starting with the quasi-steady-state maneuvers (J-turn and Ramp-steer) and finishing with the more complex dynamic maneuvers (DLC & SWD). For the three speed-based maneuvers, the entry speed into the maneuver rather than the instantaneous speed at rollover is used to compare the vehicle's rollover propensity under different loading conditions. For the single steering-based

maneuver, SWD, the steering wheel percentage is used rather than entry speed. The trailer roll dynamics under different loading conditions are compared throughout the section.

4.1.1. J-turn

For the J-turn maneuver, the total vehicle weight and rollover speed were inversely related. As the trailer cargo load was increased, the rollover speed decreased. During the high-speed study, the rollover speeds for the trailers under heavy, mixed, and light loading conditions were 33, 34, and 41 mph, respectively, as shown in Figure 4-1. As expected for a left-turn maneuver, all outrigger contacts occurred on the trailer's right side. Additionally, the rollover speed was governed by the front trailer rather than the rear trailer in all loading conditions. This occurs because the lateral acceleration of the front trailer was greater than that of the rear trailer throughout the turn. Since the vehicle's forward velocity was slowly decreasing due to friction, at the same spatial position in the J-turn the rear trailer was traveling at a lower speed than the front trailer; therefore, it had a lower acceleration than the front trailer at the same position. All trials with outrigger contacts for the J-turn used to determine the rollover entry speeds are listed in Table 4-1.

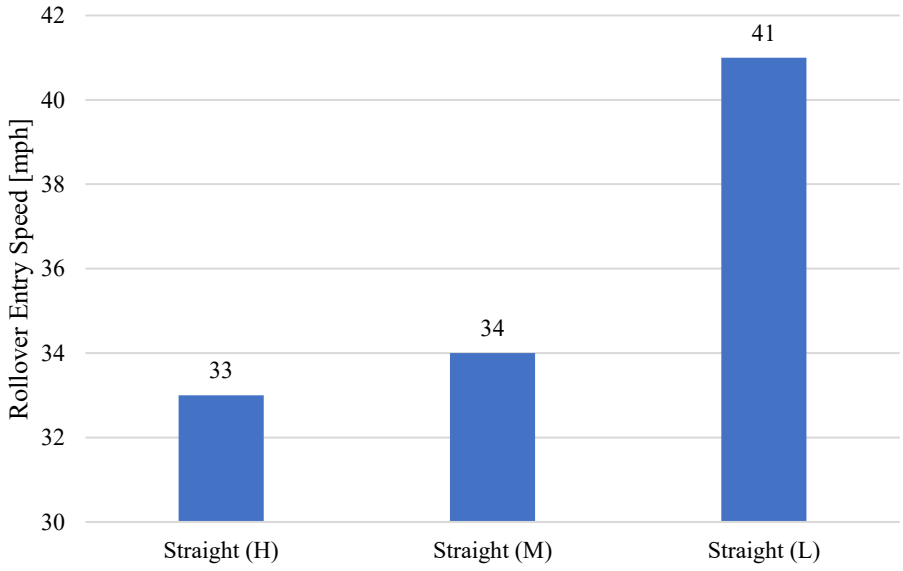

Figure 4-1. Rollover entry speed comparison of different trailer loading conditions for the J-turn maneuver.

Table 4-1. Relevant trials for entry rollover speed determination under different loading conditions during the J-turn.

Loading Condition	Entry Speed [mph]	Peak Outrigger Contact Force [lbf]			
		Front Left	Front Right	Rear Left	Rear Right
Heavy	30	0	0	0	0
	32	0	0	0	0
	33*	**0**	***406***	**0**	**0**
	34	0	***443***	0	0
Mixed	32	0	0	0	0
	33	0	0	0	0
	34*	**0**	***611***	**0**	**0**
	34*	**0**	***846***	**0**	**0**
Light	38	0	0	0	0
	40	0	0	0	0
	41*	**0**	***897***	**0**	**0**
	41*	**0**	***777***	**0**	**0**
	41*	**0**	***839***	**0**	**104**

rollover threshold = 400 lbf: green = below threshold, *red* = above threshold
*** rollover speed**

4.1.2. Ramp-Steer

Similar to the J-turn, for the ramp-steer maneuver, the trailer rollover speed was inversely related to the total vehicle weight and the rollover speeds were governed by the front trailer. The rollover speeds for the ramp-steer maneuver under heavy, mixed, and light loading conditions were 33, 35, and 45 mph, respectively, as shown in Figure 4-2.

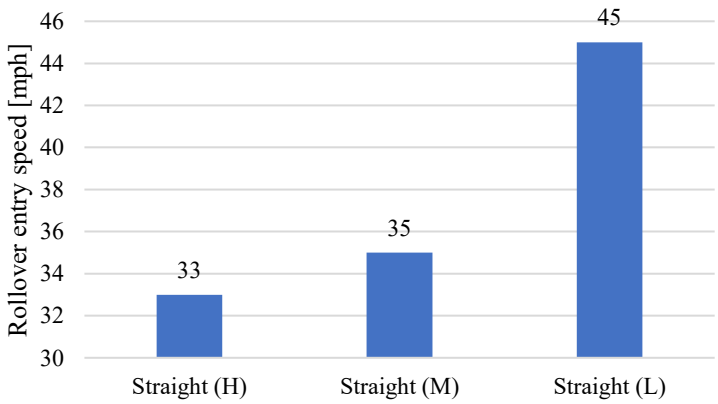

Figure 4-2. Rollover entry speed comparison of different trailer loading conditions for the ramp-steer maneuver.

Although the trends of the ramp-steer maneuver were the same as the J-turn, the exact rollover speeds differ because of the difference in the characteristics between the two maneuvers. Compared to the J-turn, there was no increase in rollover speed during ramp-

steer maneuver for heavily loaded trailers, a 1-mph increase for mixed loaded trailers, and a relatively large 4-mph increase for lightly loaded trailers. This increase occurred because the J-turn was a path-following, constant radius maneuver, while the ramp-steer was a constant steering angle maneuver. Because the ramp-steer maneuver maintained a constant steering angle at high speeds, the vehicle's turning radius increased, and the forward velocity required for the trailers to reach a sufficient lateral acceleration to exceed their lateral stability limit increased. The peak outrigger contact forces for relevant test trials are listed in Table 4-2.

Table 4-2. Relevant trials for entry rollover speed determination under different loading conditions during the ramp-steer maneuver.

Loading Condition	Entry Speed [mph]	Outrigger Contact Force [lbf]			
		Front Left	Front Right	Rear Left	Rear Right
Heavy	31	0	0	0	0
	32	0	0	0	0
	32	0	95	0	0
	33*	**0**	***844***	**0**	**0**
Mixed	30	0	0	0	0
	33	0	0	0	0
	34	0	0	0	0
	35*	**0**	***753***	**0**	**0**
	35*	**0**	***995***	**0**	**0**
Light	41	0	0	0	0
	43	0	0	0	0
	44	0	0	0	0
	45*	**0**	***591***	**0**	**214**
	45*	**0**	***730***	**0**	***555***

rollover threshold = 400 lbf: green = below threshold, *red* = above threshold
*** rollover speed**

Similar to the J-turn, all outrigger contacts occurred on the right side of the trailers during the ramp-steer; however, unlike the J-turn during the ramp-steer maneuver, the peak outrigger contact on the rear trailer exceeded the rollover threshold. Thus, it appears that during the lighter loading conditions, the rear trailer had a higher lateral acceleration in comparison to the front trailer than during heavier loading conditions. This effect appears to be greater during the ramp-steer maneuver because of the increased turning radius during the light loading conditions resulting from understeer.

4.1.3. Double Lane Change (DLC)

During the DLC maneuver, the total vehicle load was inversely related to the rollover speed; as the trailer load increased, the trailer rollover entry speed decreased. The rollover speeds for the Straight(H), Straight(M), and Straight(L) loading conditions were 40, 43, and 54 mph, respectively, as shown in Figure 4-3.

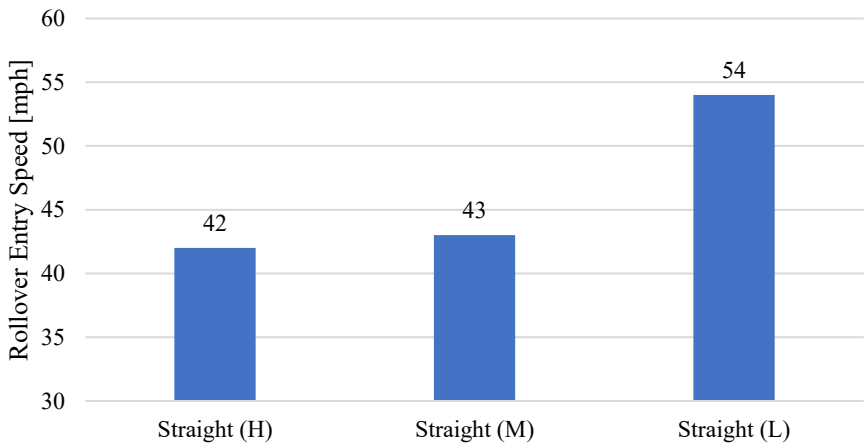

Figure 4-3. Rollover entry speed comparison of different loading conditions for the DLC maneuver.

Compared to the J-turn and the ramp-steer maneuver, the DLC maneuver was more complex and dynamic rather than quasi-steady-state. Because of the more complex steering input, there was more variability between trials. Furthermore, because the DLC has three distinct turns, there are three general areas of rollover rather than one. These rollover areas – locations A, B, and C – are illustrated in Figure 4-4, along with the first outrigger contact location under each loading condition. For all three loading conditions, the first outrigger contact occurred at location B, corresponding to the second turn of the maneuver. However, during the heavy and mixed loading conditions, the front trailer experienced outrigger contact, and during the light loading conditions, the rear trailer experienced outrigger contact. The light trailers' lower CG allowed the vehicle to reach a larger velocity before rollover, and the rearward amplification phenomenon increased at higher speeds due to higher steering frequencies. The increased lateral acceleration of the rear trailer caused the rear trailer to roll over sooner than the front trailer when both trailers were lightly loaded. This effect was not as strong in the heavily loaded conditions because the lower rollover entry speed did not require as quick of a steering frequency. Under mixed loading

conditions, the front trailer governed the rollover stability of the vehicle because the heavier, higher CG front trailer has a lower rollover lateral acceleration threshold than the lighter, lower CG rear trailer, causing the front trailer to roll over at lower speeds than the rear trailer. The peak outrigger contact force with the corresponding locations are listed in Table 4-3 for trials that were used to determine the rollover entry speed.

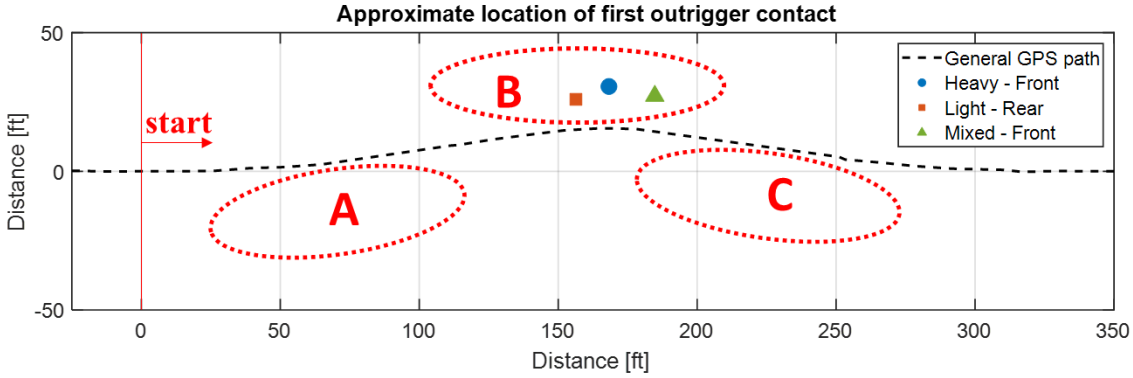

Figure 4-4. Outrigger contact location comparison in DLC maneuver for different loading conditions.

Table 4-3. Relevant trials for entry rollover speed determination under different loading conditions during DLC.

Loading Condition	GPS Entry Speed [mph]	Outrigger Contact Force [lbf]			
		Front Left	Front Right	Rear Left	Rear Right
Heavy	40	0	0	0	0
	40	0	0	0	0
	40	L(B)	0	*917 (B)*	0
	41	0	0	L(B)	0
	42*	***1018(B)***	**0**	***1208(B)***	**0**
	42*	***821(B)***	**0**	***1085(B)***	***2109(C)***
	42*	***1360(B)***	**0**	***1792(B)***	***2269(C)***
Mixed	42	0	0	0	0
	42	L(B)	0	0	0
	43*	***711(B)***	**0**	**0**	**0**
	44	*1071(B)*	0	0	0
	44	*1205(B)*	0	0	0
	44	*1388(B)*	0	0	0
	45	*1501(B)*	317 (A)	0	0
	46	*1197(B)*	0	0	0
Light	52	0	0	0	0
	54*	**0**	**0**	**0**	**0**
	54*	**0**	**0**	***1226(B)***	***1507(C)***
	56	0	0	*1881(B)*	*1142(C)*
	56	135(B)	0	*1848(B)*	*923(C)*

rollover threshold = 400 lbf: green = below threshold, *red* = above threshold
***rollover speed**

4.1.4. Sine with Dwell (SWD)

Unlike the previous three speed-based maneuvers, the SWD maneuver was a steering-based maneuver in which the independent variable was the amplitude of the steering input. The rollover steering percentage is used rather than the rollover entry speed to describe the roll stability threshold of the trailers for the SWD maneuver. The rollover steering percentages for the SWD maneuver are illustrated in Figure 4-5 and were as follows: 60% for heavy loading, 55% for mixed loading, and 90% for light loading.

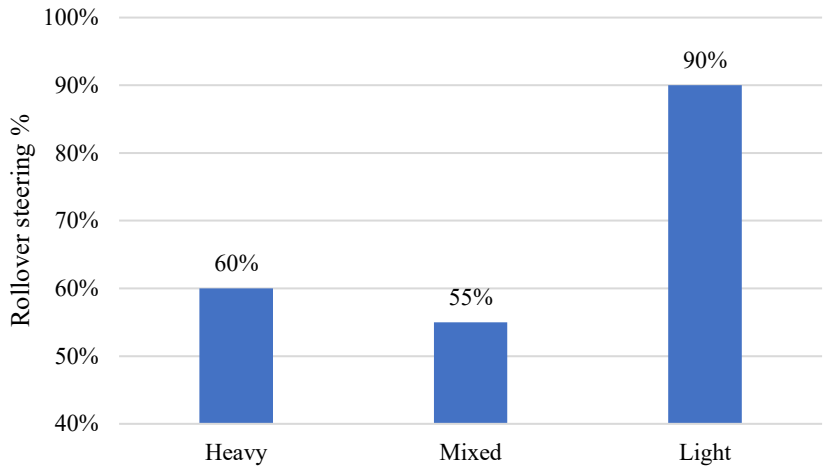

Figure 4-5. Rollover entry speed comparison during SWD maneuver for different loading conditions.

Like the DLC maneuver, the SWD maneuver had more than one possible outrigger contact location. Because there were two distinct turns in the SWD maneuver, there were two possible locations for outrigger contact, referred to as locations A and B. Locations A and B are illustrated in Figure 4-6 along with the first outrigger contact location for each loading condition. Under heavy loading conditions, there were two different locations of the first outrigger contact above the threshold in the two trials at the rollover steering percentage. In the first scenario, the front trailer rolled over to the left side at the apex of the SWD path at location B. In the second scenario, the rear trailer rolled over to the right as the trailer made its first turn at location A. Under mixed loading conditions, the front trailer rolled over to the left side at Location B, and under light loading conditions, the rear trailer rolled over to the left side at location B.

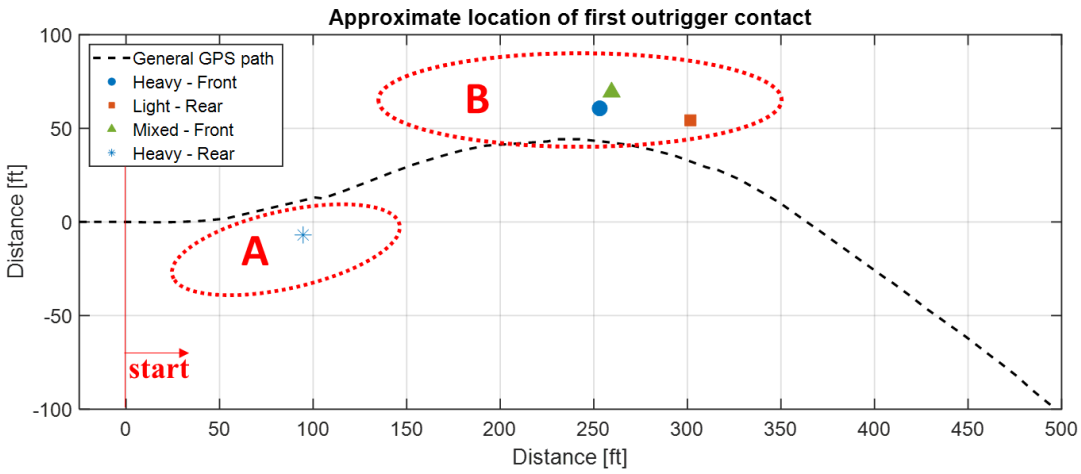

Figure 4-6. Outrigger contact location comparison in SWD for different loading conditions.

When the trailers were lightly loaded, the lower CG allowed the vehicle to reach a higher steering percentage before rollover, which increased the effects of rearward amplification. Consequently, the rear trailer reached its rollover lateral acceleration threshold before the front trailer and rolled over sooner. Although there were outrigger contacts on the front trailer, none were above the contact force threshold required to be categorized as a rollover. Rollover either occurred on the rear trailer or the front trailer under heavy loading conditions as both trailers reach the lateral acceleration threshold at approximately the same steering percentage. Under mixed loading conditions, the heavy front trailer rolled over first because it had a significantly lower CG than the lightly loaded rear trailer.

The outrigger contact force and location for relevant trails are listed in Table 4-4. The peak outrigger contact force explains why the vehicle rolled over at a lower steering percentage under mixed loading than the vehicle did under heavy loading. Comparing the two maneuvers at 60% steering, when the heavy front trailer is coupled with a light rear trailer, the left side outrigger contacts the ground with much greater force than when coupled with a heavy rear trailer. The average peak contact force on the front left outrigger at 60% steering wheel angle for heavy loading conditions was 642 lbf and a much larger 1,386 lbf for mixed loading conditions. A potential reason behind the difference in rollover speed was the difference in environmental conditions. During the mixed loading tests, strong winds were blowing SE, and during the heavy loading tests, winds were blowing NW. The heading of the trailer ranges from SE to S during the SWD maneuver. During the heavy loading tests there may have been strong winds resisting the rollover of the trailers, while

during the mixed loading tests, strong winds may have pushed the trailer in the direction of rollover. When comparing these two trials directly, the strong gusts of wind in opposing directions and their relationship to the vehicle's heading may have influenced the relationship between rollover speeds.

Table 4-4. Relevant trials for entry rollover steering percentage determination under different loading conditions during the SWD.

Loading Condition	Steering Percentage	Peak Outrigger Contact Force [lbf]			
		Front Left	Front Right	Rear Left	Rear Right
Heavy	55%	0	0	0	0
	60%*	***539(B)***	**0**	***486(B)***	**244(A)**
	60%*	***744(B)***	**0**	***718(B)***	***455(A)***
Mixed	50%	0	0	0	0
	55%*	**173(B)**	**0**	**0**	**0**
	55%*	***549(B)***	**0**	**0**	**0**
	60%	*1250(B)*	0	0	0
	60%	*1521(B)*	0	0	0
Light	80%	0	0	0	0
	85%	L	0		
	90%*	**294(B)**	**0**	**372(B)**	**0**
	90%*	**296(B)**	**0**	***706(B)***	**0**
rollover threshold = 400 lbf: green = below threshold, *red* = above threshold ***rollover steering percentage**					

4.2. Effects of RSC on Rollover of Straight-Rail Trailers in Different Loading Conditions

This section will compare the rollover propensity of trailers with and without roll stability control (RSC), under different loading conditions. Similar to the previous section, the results are broken up by maneuver, starting with the quasi-steady-state maneuvers and finishing with the more complex dynamic maneuvers. The goal of this section is to provide quantitative benefits for the inclusion of RSC devices on trailers.

4.2.1. J-turn

During the J-turn, the rollover entry speed for each trailer loading combination increased by utilizing RSC on both trailers. The increase in rollover entry speed for the Straight(H), Straight(M), and Straight(L) trailer combinations were 2, 2, and 4 mph, respectively, as shown in Figure 4-7. The trials that were used to determine the rollover entry speeds are shown in Table 4-5.

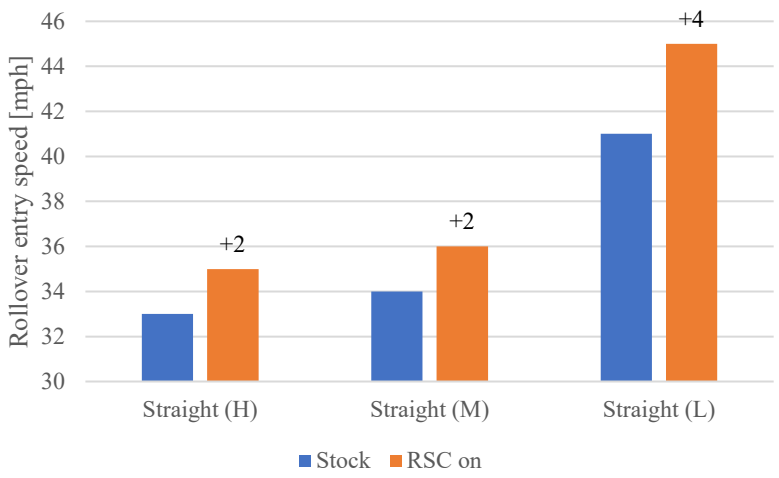

Figure 4-7. Rollover entry speed comparison for J-turn maneuver under various loading conditions.

Table 4-5. Relevant trials for entry rollover speed determination under different loading conditions during J-turn maneuver with RSC on.

Loading Condition	Entry Speed [mph]	Peak Outrigger Contact Force [lbf]			
		Front Left	Front Right	Rear Left	Rear Right
Heavy	34	0	0	0	0
	34	0	0	0	0
	34	**0**	543	**0**	**0**
	35*	**0**	**323**	**0**	**0**
	35*	**0**	***975***	**0**	**0**
	35*	**0**	***976***	**0**	**0**
	36	0	*1301*	0	0
	36	0	*1328*	0	0
	36	0	*1590*	0	0
Mixed	35	0	0	0	0
	36*	**0**	**L**	**0**	**0**
	36*	**0**	***899***	**0**	**0**
Light	42	0	0	0	0
	42	0	191	0	0
	43	0	244	0	0
	44	0	330	0	0
	45*	**0**	***488***	**0**	**0**
	45*	**0**	***806***	**0**	**0**

rollover threshold = 400 lbf: green = below threshold, *red* = above threshold
*** rollover speed**

The most significant increase was experienced by the Straight(L) combination because as the entry speed increased past a certain threshold, the driver could not maintain the intended path, and the vehicle understeered, as illustrated by the GPS paths in Figure 4-8. As the vehicle began to understeer, the turn radius increased, requiring a greater forward velocity to reach the rollover lateral acceleration threshold. Comparing the rollovers of the trailers

with RSC to the stock trailers, with RSC, there are no rear trailer outrigger contacts. During the stock trailer testing with the Straight(L) combination, a rear trailer contacted the ground during one of the trials. The lack of rear trailer outrigger contact in the J-turn shows the effectiveness of the RSC controller in decreasing the trailer lateral acceleration. This is especially apparent in the rear trailer. The additional decrease in speed resulted in a greater difference between the rear trailer lateral acceleration and the front trailer lateral acceleration at the same coordinates than in a vehicle without RSC.

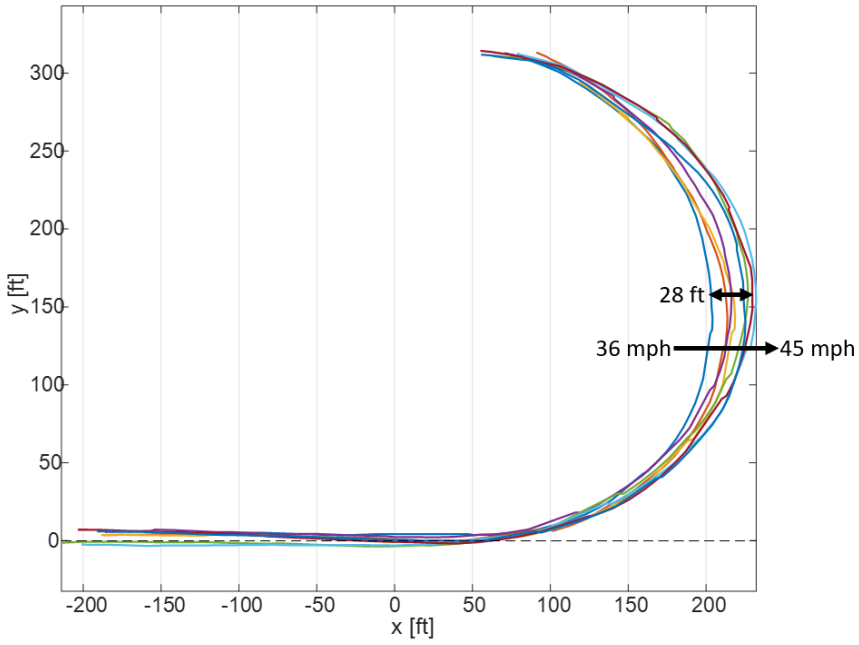

Figure 4-8. Increase in J-turn radius from 36-45 mph with RSC-equipped trailers

4.2.2. Ramp-Steer

Similar to the J-turn maneuver, the addition of RSC increased the rollover entry speeds of the trailers during the ramp-steer maneuver. During the Straight(H), Straight(M), and Straight(L) trailer combinations, the rollover entry speeds increased by 1, 2, and 5 mph, as shown in Figure 4-9. All trials with outrigger contacts that were used to determine the rollover entry speeds are shown in Table 4-6.

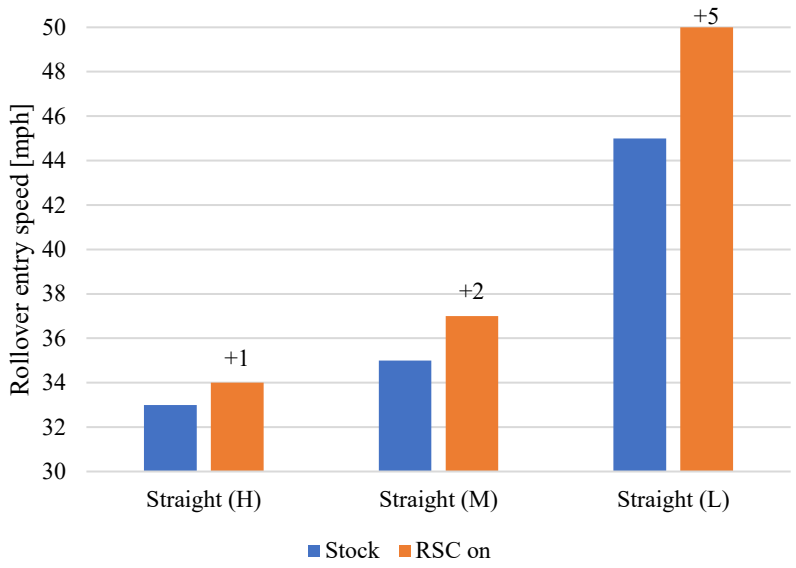

Figure 4-9. Rollover entry speed comparison during ramp-steer maneuver for different loading conditions.

Table 4-6. Relevant trials for entry rollover speed determination under different loading conditions during ramp-steer maneuver with RSC on.

Loading Condition	Entry Speed [mph]	Outrigger Contact Force [lbf]			
		Front Left	Front Right	Rear Left	Rear Right
Heavy	32	0	0	0	0
	33^	0	0	0	0
	34*	**0**	***622***	**0**	**0**
	34*	**0**	***725***	**0**	**0**
	34*	**0**	***1005***	**0**	**0**
Mixed	36	0	0	0	0
	37*	**0**	***910***	**0**	**0**
	37*	**0**	***912***	**0**	**0**
Light	48	0	387	0	0
	48	0	410	0	0
	49	0	308	0	0
	49	0	336	0	0
	50*	**-**	**-**	**-**	**-**

rollover threshold = 400 lbf: green = below threshold, *red* = above threshold
*** rollover speed**

The increase in rollover speed for the Straight(L) configuration was significantly higher than the increase for the other two trailer combinations. Because of the low CG of straight(L), the vehicle can reach higher speeds before a trailer rolls over, especially with the addition of RSC. Because the ramp-steer maneuver used a constant steering wheel angle, the vehicle experienced understeer at high speeds, increasing the turn radius and increasing the forward velocity required for the trailers to roll over. Similar to the J-turn

maneuver, there are no longer any rear outrigger contacts during the Straight(L) tests as there were during the stock trailer testing. This provides evidence that RSC is particularly helpful in decreasing the lateral acceleration of the rear trailer.

4.2.3. Double Lane Change (DLC)

The addition of RSC on the trailers extended the rollover entry speed required for rollover for all loading conditions in the DLC maneuver. As illustrated in Figure 4-10, the increase in rollover speed with the addition of RSC for the Straight(H), Straight(M), and Straight(L) trailer combinations were 4, 4, and 1 mph, respectively.

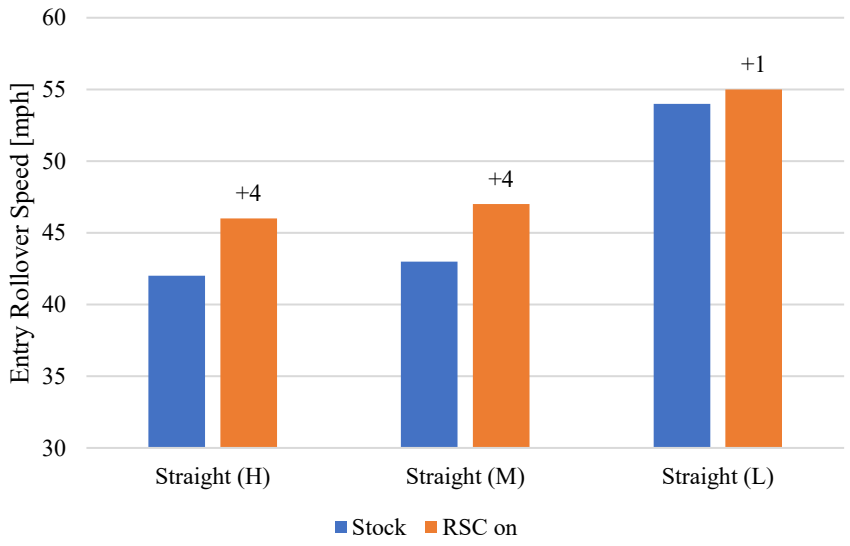

Figure 4-10. Rollover entry speed improvement of different trailer loading conditions for the DLC maneuver when both trailers are equipped with RSC.

All trials with outrigger contact that were used to determine the rollover entry speed during the DLC maneuver are shown in Table 4-7. The combination with the smallest increase in rollover entry speed for the DLC maneuver was Straight(L). This is the opposite of the trend observed in the J-turn and the Ramp-Steer, where the Straight(L) entry rollover speed increased the most of the three loading conditions.

Table 4-7. Relevant trials for entry rollover speed determination under different loading conditions during the DLC with RSC on.

Trailer Configuration and Loading Conditions	Entry Speed [mph]	Peak Outrigger Contact Force [lbf]			
		Front Left	Front Right	Rear Left	Rear Right
Straight(H)	45“	0	0	0	0
	46*^	**-**	**-**	**-**	**-**
	47	*406(B)*	0	*1635(B)*	0
	47	*640(B)*	0	*1825(B)*	L(C)
Straight-Straight (M)	46	0	0	0	0
	46	L(B)	0	0	0
	47*	***504(B)***	**0**	**0**	**0**
	48	*1371(B)*	0	0	0
	49	*1285(B)*	0	0	0
Straight-Straight (L)	**55***	**0**	**0**	***797(B)***	**0**
	56	0	0	*506(B)*	0
	57	0	0	*1270(B)*	0

green = below the rollover threshold (<400lb contact force)
red = above the rollover threshold (≥400lb contact force)
*** = rollover speed**
^ = no test performed

4.2.4. Sine with Dwell (SWD)

When utilizing the RSC system, the rollover steering percentage for the SWD maneuver increased from that of the stock vehicle in all three loading conditions. As shown in Figure 4-11, the rollover steering percentage increased by 5%, 15%, and by >10% in the Straight(H), Straight(M), and Straight(L) loading conditions, respectively. All trials with outrigger contacts used to determine the rollover steering percentages are shown in Table 4-8. The exact rollover steering percentage is unknown for the Straight(L) loading condition as the combination was only tested up to 100% of the steering wheel percentage. Since the Straight(L) vehicle completed the tests at 100%, it is known that the rollover steering percentage is greater than 100%. Unlike the other dynamic test, the DLC, the Straight(H) configuration did not have the highest increase in the rollover parameter. The largest increase in rollover steering percentage was either in the Straight(M) or Straight(L) combinations. This shows that RSC may not benefit heavily loaded trailers more than lightly loaded trailers during dynamic conditions. Comparing the first outrigger contact locations for the SWD with and without RSC, the addition of RSC led to first outrigger contacts earlier in the maneuver for both the Straight(H) and Straight(M) combinations.

Rather than rolling over at Location B as during the stock tests, the trailers rolled over at Location A when equipped with RSC. This observation provides evidence that the RSC module can sufficiently slow the trailers down such that no rollover occurs at Location B. At the rollover steering percentage, when the trailers are at Location A, the RSC has less time to react and cannot slow down the vehicle enough to prevent rollover due to the suddenness of the turn made by the tractor.

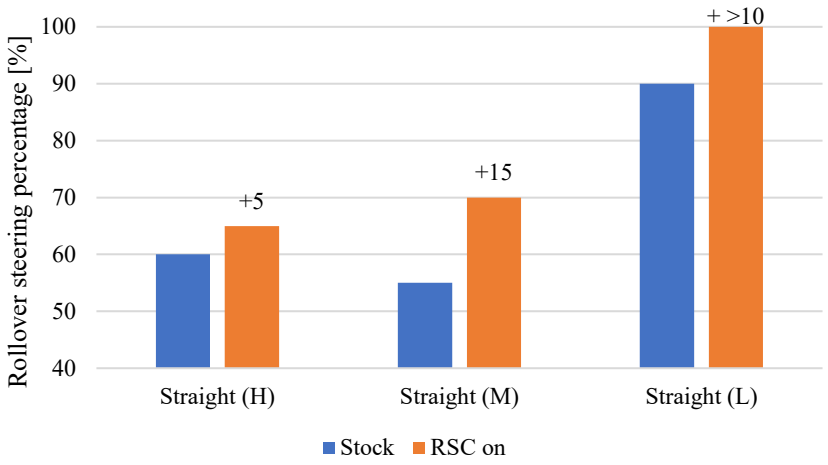

Figure 4-11. Rollover entry speed comparison of different trailer loading conditions for the SWD maneuver.

Table 4-8. Relevant trials for entry rollover steering percentage determination under different loading conditions during the SWD with RSC on.

Loading Condition	Steering Percentage	Peak Outrigger Contact Force [lbf]			
		Front Left	Front Right	Rear Left	Rear Right
Straight(H)	60%	0	0	L	0
	65%*	***1121(B)***	**162(A)**	***888(B)***	***641(A)***
	65%*	***1337(B)***	**219(A)**	***1530(B)***	***857(A)***
	65%*	***1182(B)***	***476(A)***	***1479(B)***	***868(A)***
Straight(M)	65%	0	0	0	0
	65%	L(B)	0	0	0
	65%	*869(B)*	0	0	0
	70%*	***825(B)***	***856(A)***	**0**	**0**
	70%*	***834(B)***	***683(A)***	**0**	**0**
Straight(L)	100%	0	0	0	0
rollover threshold = 400 lbf: green = below threshold, *red* = above threshold ***rollover steering percentage**					

4.3. Summary

The difference in cargo load between the straight(H) and straight(L) trailers generated a difference in the CG heights of the trailers. As a result of this difference, the rollover

threshold of straight(H) was lower than that of straight(L); therefore, straight(H) rolled over at lower entry speeds and lower steering percentages during the Straight(H) and Straight(M) tests than straight(L) did during the Straight(L) tests, as shown in Table 4-9.

Table 4-9. Rollover entry speeds and steering percentages under different loading conditions.

Maneuver	J-turn	Ramp-Steer	DLC	SWD
Straight (H)	33 mph	33 mph	42 mph	60 steer %
Straight (M)	34 mph	35 mph	43 mph	55 steer %
Straight (L)	41 mph	45 mph	54 mph	90 steer %

The results of the J-turn maneuver and the ramp-steer maneuver aligned closely. During the J-turn maneuver for the straight, mixed, and light loading conditions, the rollover speeds were 33, 34, and 41 mph, while the rollover speeds for the ramp-steer maneuver were 33, 35, and 45 mph. In both maneuvers, the front trailer governed the roll stability of the vehicle, rolling over to the right at the rollover speed. As a result of holding the steering wheel angle constant during the ramp-steer maneuver, the vehicle understeered at high speeds, increasing the turn radius. This is why the rollover entry speeds were higher for the ramp-steer maneuver than the J-turn.

For the DLC maneuver, the rollover speeds were 42, 43, and 54 mph. Like the J-turn maneuver, the Straight(H) combination rolled over at the lowest speed, and the Straight(L) combination rolled over at the highest speed. In both the J-turn and the DLC maneuver, however, the Straight(M) combination rolled over at greater speeds than the Straight(H) combination, even though a straight(H) rollover occurred in both. During the DLC maneuver, under heavy and mixed loading conditions, the front trailer governed the roll stability of the combination. When under light loading conditions, the rear trailer governed the roll stability of the vehicle as the effects of rearward amplification increased at the higher steering frequency.

The results of the SWD maneuver are unique from the speed-based maneuvers because the Straight(M) combination rolled over at a lower steering percentage than the Straight(H) combination. During the SWD maneuver, under light loading, the rear trailer governed the roll stability of the vehicle. Under mixed loading the front trailer governed the roll stability

of the vehicle. Under heavy loading, the first outrigger contact occurred on both trailers in different trails. Overall, it can be concluded that the Straight(L) will roll over at the highest entry speeds of the three loading conditions. Furthermore, the trailers under mixed loading will generally roll over at a higher speed than the heavy trailers. And lastly, the heavily loaded trailers are the most prone to rollover out of the three loading conditions.

Adding trailer-based RSC to both trailers had positive benefits for all 3 loading conditions in each of the four maneuvers, as shown in Table 4-10. For quasi-steady-state maneuvers, the use of RSC appeared to have the largest benefits in the lighter loading conditions. The largest increase in rollover entry speed was observed in the Straight(L) combination for both the J-turn and the ramp-steer maneuver. The large increase in rollover speed may have resulted from the increased turn radius from the understeer of the vehicle. As the radius of the turn increases, the forward velocity required to reach the lateral acceleration rollover threshold increases, so the entry speed must increase accordingly. The Straight(M) combination had the same improvement in entry rollover speed as the Straight(H) combination for the J-turn maneuver. Still, it increased an additional mph for the ramp-steer maneuver. This is likely a result of the decreased total load of the configuration.

Table 4-10. Rollover threshold improvement in trailers equipped with RSC from stock vehicle rollover thresholds under different loading conditions.

Maneuver	J-turn	Ramp-Steer	DLC	SWD
Straight (H)	2 mph	1 mph	4 mph	5 steer %
Straight (M)	2 mph	2 mph	4 mph	15 steer %
Straight (L)	4 mph	5 mph	1 mph	> 10 steer %

During the dynamic DLC maneuver, the increase in rollover speed when using RSC was largest in the Straight(H) and Straight(M) configurations, opposite of the results of the quasi-steady-state maneuvers. Lastly, the results of the dynamic SWD maneuver contradict those of the DLC maneuver. The largest increase was observed in the lighter trailer combinations, in Straight(M) and Straight(L) rather than Straight(H). During the SWD maneuver, however, the first outrigger contact location changed from the apex of the turn to the first turn of the maneuver. RSC was able to prevent rollover at the apex because it could sense the trailers were approaching rollover conditions; however, the RSC system

slow down the vehicle sufficiently during the sudden turn at the very start of the maneuver, especially at higher steering amplitudes. In conclusion, it appears that during quasi-steady-state maneuvers, RSC has the largest benefits for vehicles with lower GVWR. On the other hand, RSC had the largest benefits for vehicles with higher GVWR during the speed-based DLC maneuver. Lastly, during the steering-based SWD maneuver, RSC had the greatest benefits for vehicles with lighter GVWR.

5. Evaluation and Comparison of Lateral Acceleration and Trailer Roll Angle as Rollover Indicators in Heavy Vehicles

Clearly, as discussed in Chapter 4, trailer-based RSC is capable of increasing the initial forward velocity or steering amplitude at which a vehicle can enter a maneuver without rolling over. The RSC system used during the testing and most commercially available RSC systems use lateral acceleration to determine the proximity of the trailers to rollover. While lateral acceleration may provide a clear indication of a rollover, it has been suggested that the axle roll angle may provide a better indication of rollover in dynamic maneuvers [40]. This chapter will investigate this claim using data from the previously discussed high-speed testing to compare lateral acceleration and the trailer roll angle as rollover indicators for trailers in the A-double configuration. The unsprung mass roll angle was not measured during testing and is not discussed in this study.

The change in sprung mass position on the left and right sides of the trailer was measured by the string potentiometers and was used to determine the roll angle. The roll angle (φ) was calculated as follows:

$$\varphi = tan^{-1}\left(\frac{Q_x(\Delta z_R - \Delta z_L)}{d}\right) \tag{5.1}$$

where Q_x is the ratio between the string potentiometer distance to the suspension rotational axis and the trailer axle distance from the suspension rotational axis, $\Delta z_R - \Delta z_L$ is the difference between the sprung mass extension on the trailer's right side and the trailer's left sider as measured by the string potentiometers, and d is the lateral distance between the string potentiometer mounting points. The small angle assumption is made for the angle of the string potentiometer cable on the trailer structure. Lateral acceleration was measured by single-axis and triaxial accelerometers mounted at the heavily loaded trailer CG position, as discussed in 3.1.1.

5.1. Lateral Acceleration and Trailer Roll Angle at Rollover Limit

This chapter covers the lateral acceleration and axle roll angle values just prior to rollover for straight(H) and straight(L) trailers during the high-speed testing. To perform this analysis, the lateral acceleration and axle roll angle values at the time of outrigger contact (ToC) are used. During hard outrigger contact, large vibrations affect the lateral acceleration and roll angle measurements; therefore, the value at the rollover threshold of 400 lbf could not be used to extract data reliably. At the ToC, there is little to no correlation between the outrigger contact force and the lateral acceleration or roll angle data extracted. For repeatability and ease of processing, the ToC was defined as the minimum outrigger contact force value just prior to the peak outrigger contact force. If the determined time resulted in a large error between the determined roll indicator values and the expected values, video data was used to adjust the ToC to when the outrigger first contacted the ground.

To analyze differences between the lateral acceleration and roll angles at rollover conditions, hypothesis tests are performed. The hypothesis tests are used to determine whether or not there is a significant difference between the different scenarios presented, including coupled trailer type, coupled trailer loading, and maneuver type. In cases where there is a sufficient number of samples and the normality assumption can be made, a pooled t-test is performed. In cases where the sample size is small and the normality assumption cannot be made, the nonparametric exact Wilcoxon Rank Sum test is used. All hypothesis tests are performed at the 95% confidence level.

5.1.1. Effect of Coupled Trailer on Lateral Acceleration and Trailer Roll Angle at Rollover Limit

The effect of a coupled trailer with higher roll stability on the rollover threshold of a trailer with lower roll stability, when combined in an A-double configuration, is examined. There are three trailer combinations in the high-speed testing in which this effect can be examined: Straight(M) and the two mixed trailer combinations. The purpose of this section is to investigate whether each trailer can be considered as an individual unit when performing roll analysis when combined in an A-double configuration and to determine

the robustness of lateral acceleration and trailer roll angle as roll indicators in different trailer combinations.

The first comparison to be made is for different loading conditions. This comparison is made by comparing the lateral acceleration and trailer roll angle for the heavy-heavy condition with light-light and heavy-light conditions. Earlier, we referred to these as Straight(H), Straight(L), and Straight(M), respectively. Figure 5-1 illustrates that the difference between the median lateral accelerations at rollover is under 3% for mixed loading. The difference between the median axle roll angle at rollover is under 3% as well. As shown in Table 5-1, the results of the hypothesis tests support that there is no significant statistical difference between the mean trailer lateral acceleration or roll angle for a heavy trailer in the front when coupled to either a heavy or light trailer in the rear. The exact Wilcoxon Rank Sum test was used because the assumption of normality could not be made. This conclusion supports that the rollover threshold of an individual trailer is decoupled from the roll dynamics of the other trailer. In addition, this result allows for all instances where a heavily loaded straight rail trailer rolls over in the Straight(H) and Straight(M) combinations to be combined into a single index for additional analysis.

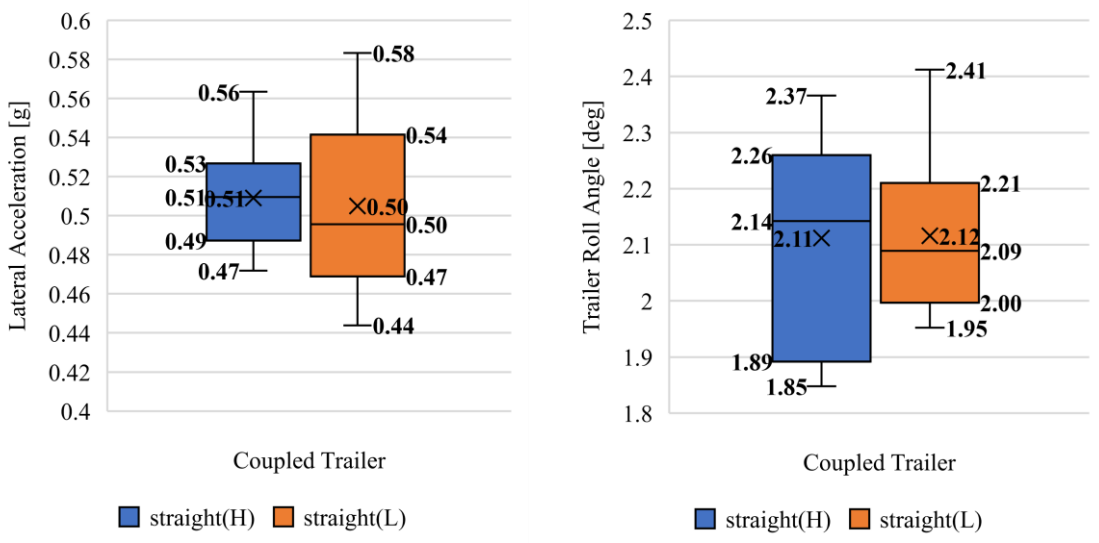

(a) (b)

Figure 5-1. Effect of coupled trailer load on (a) lateral acceleration and (b) trailer roll angle at the ToC for straight(H).

Table 5-1. Hypothesis test conclusions for the difference between lateral acceleration and trailer roll angle of Straight(H) (n = 17) and Straight(M) (n =13).

Parameter	Hypothesis Test	Null Hypothesis	Prob ≥ S	Conclusion
Lateral Acceleration	Exact Wilcoxon Rank Sum (one-sided)	H_{SH} and H_{SL} are identical	0.4184	Fail to Reject
Roll Angle	Exact Wilcoxon Rank Sum (one-sided)	H_{SH} and H_{SL} are identical	0.5	Fail to Reject

The second coupled trailer comparison to be made is whether or not a trailer of differing construction and higher roll stability affected the rollover dynamics of the other trailer in combination. The lateral acceleration and trailer roll angle at the time of outrigger contact for the straight(H) during the mixed-trailer combinations are compared to determine if the coupled trailer of a different type affects the rollover threshold of the straight(H). The couped drop-frame trailer has a CG height 7.1 in. lower than the straight-rail, an equal track width, and weighs 1,000 lbs. more. The suspension of the drop-frame trailer is an under-slung trailing-arm rather than a top-slung trailing arm, which has a ride height of 3.5 in. (10.5 in. lower than the straight-rail), 0.3 in. less jounce, and 2.1 in. less rebound than the straight-rail suspension. Figure 5-2 shows the distribution of the lateral acceleration and trailer roll angle just before rollover for a heavy straight-rail trailer when coupled with either another straight(h) or a drop(h) trailer.

The median lateral acceleration just prior to rollover between the two cases is approximately equal, differing by only 2%. The results of the hypothesis tests supported that there is no significant statistical difference between the mean lateral acceleration at rollover when straight(H) is connected to either another straight(H) or a drop(H). The hypothesis test for the trailer roll angle reached the opposite conclusion. The null hypothesis was rejected, supporting the alternative hypothesis that the mean trailer roll angle at rollover for straight(H) is greater when connected to a drop(H) than when connected to another straight(H). This result may indicate that the trailer roll angle has less robustness than lateral acceleration as a roll indicator when the combination of trailer types in the AHV differs. Because normality could be assumed for these trials and the number of samples was sufficiently large, a pooled t-test was performed. The details of the hypothesis tests are shown in Table 5-2. Because there is no significant statistical

difference between the mean lateral acceleration at rollover when a straight-rail is combined with either straight(H) or the drop(H), all instances where a heavy straight-rail trailer rolled over during the high-speed testing can be combined to provide a single rollover lateral acceleration index. While there was a significant statistical difference between the mean trailer roll angle when straight(H) was combined with a different trailer type as opposed to another straight(H), a single index will be used to represent the complete range in which straight(H) has a high probability of rolling over with the caveat that the connection with other trailer types may have an effect the trailer roll angle near or at rollover conditions.

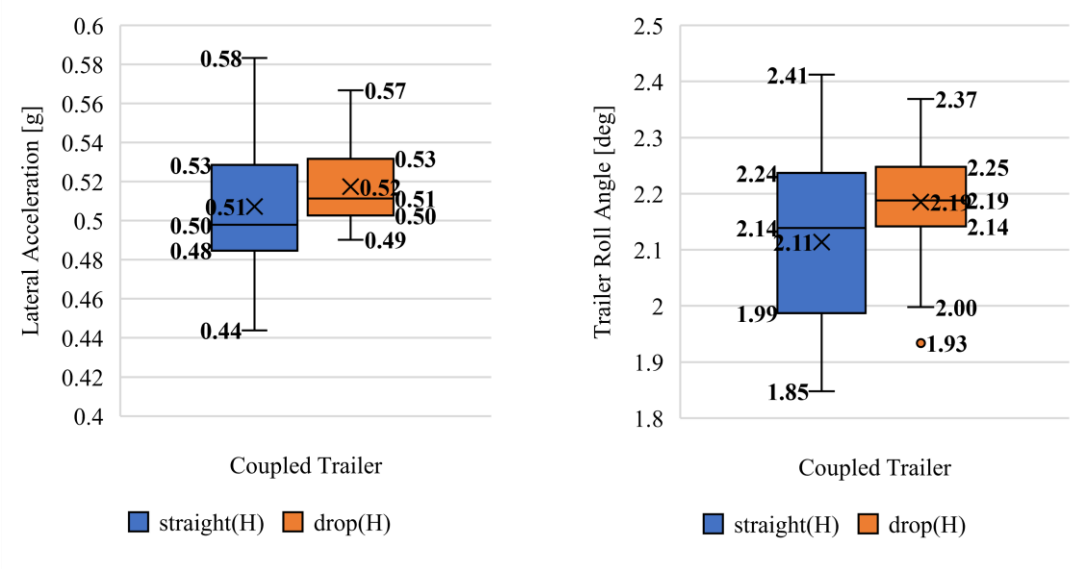

(a) (b)

Figure 5-2. Effect of coupled trailer type on (a) lateral acceleration and (b) trailer roll angle at the ToC for straight(H).

Table 5-2. Hypothesis test conclusions for the difference between lateral acceleration and trailer roll angle of straight(H) when coupled with either a straight(H) (n = 30) or drop(H) (n =21).

Parameter	Hypothesis Test	Null Hypothesis	Prob < t	Conclusion
Lateral Acceleration	Pooled t-test	$\mu_{Str} - \mu_{Diff} \geq 0$	0.1249	Fail to Reject
Roll Angle	Pooled t-test	$\mu_{Str} - \mu_{Diff} \geq 0$	0.0369	Reject Null Hypothesis, $\mu_{Str} < \mu_{Diff}$

5.1.2. Effect of Maneuver Type on Lateral Acceleration and Trailer Roll Angle at Rollover Limit

It is generally accepted that the dynamic rollover threshold of trailers is lower than the static or steady-state rollover threshold of trailers due to the increased momentum of the trailers [21]. While the damping in both the suspension and tires play a large part determining the dynamic rollover threshold, nonlinearities such as tire slip can also play an important role in the lateral acceleration at which a trailer rolls over. This analysis draws a comparison between trailer rollover thresholds during quasi-steady-state and dynamic maneuvers for straight(H) and straight(L).

The test results show that lateral acceleration and roll angle are generally lower during dynamic maneuvers than in quasi-steady-state maneuvers. As shown in Figure 5-3, during dynamic maneuvers, the median lateral acceleration is 6% lower than during quasi-steady-state maneuvers, and the median roll angle is 3% lower in dynamic maneuvers than in quasi-steady-state maneuvers. The pooled t-test hypothesis tests shown in Table 5-3 confirm the observation that in dynamic maneuvers, the lateral acceleration and trailer roll angle at rollover are lower than in quasi-steady-state maneuvers for heavy straight-rail trailers.

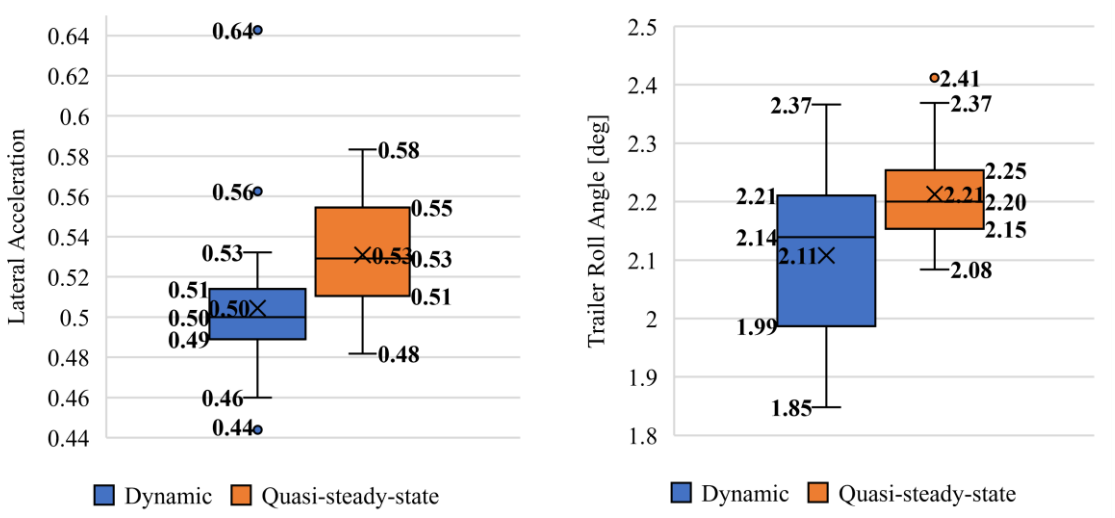

(a) (b)

Figure 5-3. Comparison of (a) lateral acceleration and (b) axle roll angle for straight(H) in dynamic and quasi-steady-state maneuvers.

Table 5-3. Hypothesis test conclusions for the difference between lateral acceleration and axle roll angle of heavy straight(H) in dynamic (n = 34) and quasi-steady-state (n =17) maneuvers.

Parameter	Hypothesis Test	Null Hypothesis	Prob < t	Conclusion
Lateral Acceleration	Pooled t-test	$\mu_{Dynamic} - \mu_{QSS} \geq 0$	0.0054	Reject Null Hypothesis, $\mu_{Dynamic} < \mu_{QSS}$
Roll Angle	Pooled t-test	$\mu_{Dynamic} - \mu_{QSS} \geq 0$	0.0054	Reject Null Hypothesis, $\mu_{Dynamic} < \mu_{QSS}$

Comparing the lateral acceleration of a straight(L) trailer at rollover during dynamic and quasi-steady-state maneuvers, as expected it appears that the lateral acceleration rollover threshold is lower than during quasi-steady-state maneuvers, as is illustrated in Figure 5-4. While there is a clear difference in the means and medians of the distributions, the standard deviation is much greater during quasi-steady-state maneuvers. During these maneuvers, the high lateral acceleration values may be attributed to the tractor experiencing understeer and the trailer tires slipping at the high speeds required for rollover. When comparing the trailer roll angle, the standard deviation of the trailer roll angle is much larger in the dynamic tests than during the quasi-steady-state tests. During the dynamic maneuvers, the sprung mass may have a greater response to the excitation than in the quasi-steady-state maneuvers. The sprung mass may have more lateral momentum during the dynamic maneuvers due to the increased steering frequency, creating a wider distribution of values and higher overall values. The hypothesis tests, described in Table 5-4, support that the lateral acceleration at rollover during dynamic maneuvers is significantly lower than the lateral acceleration at rollover during quasi-steady-state maneuvers for lightly loaded straight-rail trailers. No significant difference was found between the trailer roll angle during dynamic and quasi-steady-state maneuvers, as the null hypothesis was not rejected.

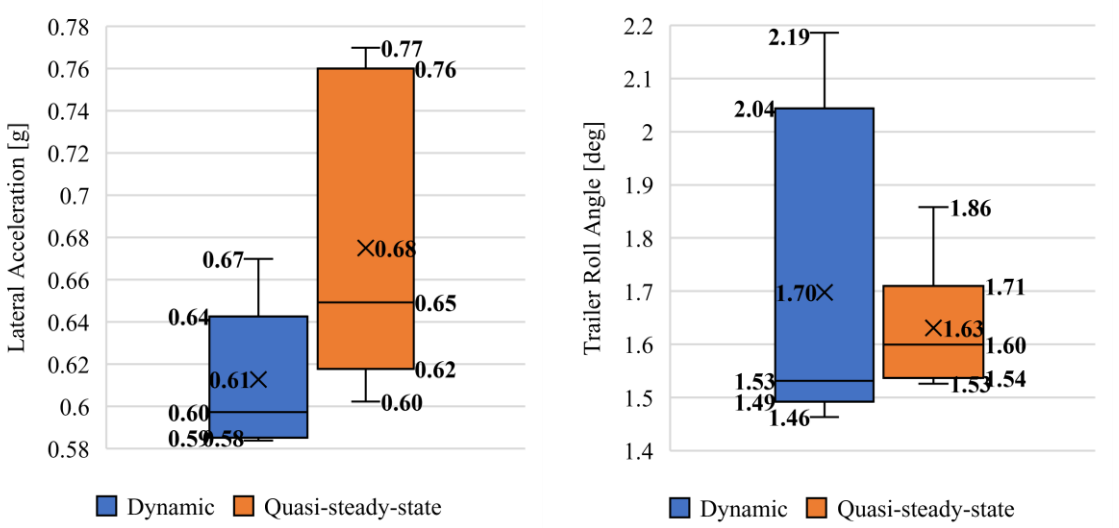

(a) (b)

Figure 5-4. Comparison of (a) lateral acceleration and (b) axle roll angle for straight(L) trailers in dynamic and quasi-steady-state maneuvers.

Table 5-4. Hypothesis test conclusions for the difference between lateral acceleration and trailer roll angle of straight(L) trailer in dynamic (n = 7) and quasi-steady-state (n = 6) maneuvers.

Parameter	Hypothesis Test	Null Hypothesis	Prob ≥ S	Conclusion
Lateral Acceleration	Exact Wilcoxon Rank Sum	$H_{Dynamic}$ and H_{QSS} are identical	0.0256	Reject Null Hypothesis, H_{QSS} is shifted right
Roll Angle	Exact Wilcoxon Rank Sum	$H_{Dynamic}$ and H_{QSS} are identical	0.3141	Fail to Reject

5.1.3. Effect of Trailer Loading and Trailer Type on Lateral Acceleration and Trailer Roll Angle at Rollover

This section compares the lateral acceleration and axle roll angle just prior to rollover for different trailer loading conditions. The two trailers considered are a heavily loaded straight-rail trailer and a lightly loaded straight-rail trailer. This information is presented as a comparison between the heavy and light straight-rail trailers. Even though there are differences in the values of lateral acceleration and trailer roll angle at rollover conditions for the different maneuver types, data from all rollovers is combined into a single range to achieve a more complete overview of the rollover range of the trailer.

When heavily loaded, the CG height for a straight-rail trailer is 77.8 in. When lightly loaded, the CG height decreases to 65.6 in. This difference in CG height and the 7,500 lb. difference in loading creates differences in the lateral acceleration required for rollover

between the heavily loaded and lightly loaded trailers. The decrease in trailer load decreases the CG and lowers the total weight of the sprung mass and the average jounce and rebound of the suspension. Because the trailer is equipped with a pneumatic suspension and the ride height is maintained, the suspension's roll stiffness decreases as the loading is increased. The trailer roll angle is not only a function of the suspension properties and lateral acceleration, but also the moment arm from the roll-center height [15]. As illustrated in Figure 5-5, the median lateral acceleration of a lightly loaded straight rail trailer at rollover is 22% larger than that of the heavily loaded trailer due to the lowered CG. Furthermore, the median trailer roll angle at rollover decreased by 27% from the changes in loading and resulting changes in suspension properties. The changes in suspension properties explain the additional 5% decrease in trailer roll angle. When the load was decreased, and the suspension ride height remained constant, as set by the load-leveling valve, the suspension roll stiffness was decreased. This further decreased the roll angle at which the lightly loaded trailers rolled over. For the same trailer type, the lateral acceleration required to rollover is larger with a decreased load, and the corresponding trailer roll angle is smaller than that of the trailer during heavy loading conditions.

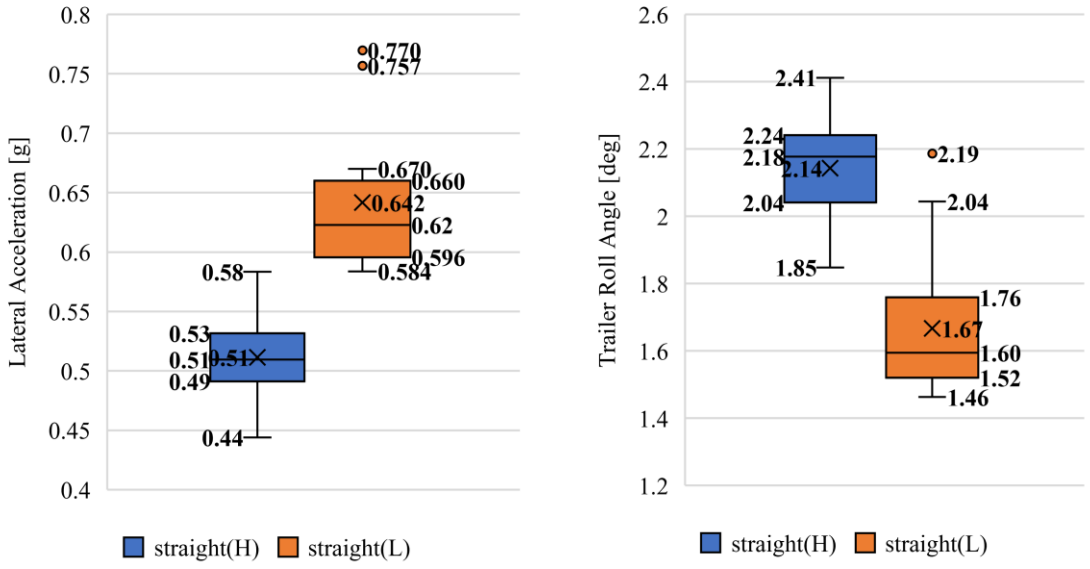

(a) (b)

Figure 5-5. Comparison of (a) lateral acceleration and (b) trailer roll angle at ToC between heavy and light loading conditions.

Comparing the experimentally determined median lateral acceleration and trailer roll angles to roll-plane model predictions, the experimentally derived rollover thresholds of the trailers exceed the predicted values, as shown in Table 5-5. This difference likely occurs because in the roll-plane models, the lateral acceleration and trailer roll angle limit values are determined at wheel-lift rather than the point of absolute instability. The experimental results were categorized as rollovers based on the contact force at the outrigger wheel rather than at wheel lift, so the definition of the critical lateral accelerations and trailer roll angles are less conservative than the roll-plane models. The two roll-plane models used are the rigid roll-plane model (SSF) Eq. (2.2) and the suspended mass roll plane model (SM) Eq. (2.7, 2.8). The roll gain Eq (2.6) used in the suspended mass model was derived from the median rollover threshold values for the roll indicators. By using the rollover threshold median values to determine roll gain, a more accurate prediction of the actual rollover thresholds can be made. The roll gains used for the calculations for the straight(H) and straight(L) trailers were 4.27 and 2.56 deg/g, respectively. The roll center height used in the suspended mass model is 25.5 in. The roll center height was the estimated height where the suspension was stiffest laterally and was verified using information from similar suspensions [15, 49]. The sprung mass center of gravity height was assumed to equal the overall center of gravity height.

Table 5-5. Comparison of experimentally-derived rollover threshold values and roll-plane model predictions for lateral acceleration and trailer roll angle.

		straight(H)	**straight(L)**
Lateral Acceleration [g]	Test Results (Median)	0.51	0.62
	Rigid Roll Model (SSF)	0.50	0.59
	% Difference (SSF)	1.6%	4.6%
	Suspended Mass Roll Model (SM)	0.48	0.58
	% Difference (SM)	6.3%	7.1%
Trailer roll angle [deg]	Test Results (Median)	2.18	1.60
	Suspended Mass Roll Model (SM)	2.04	1.48
	% Difference (SM)	6.3%	7.1%

5.2. Comparison of Lateral Acceleration and Trailer Roll Angle Time Response to Quasi-Steady-State and Dynamic Excitations

The change in roll angle is generally considered a reaction to a lateral acceleration excitation; therefore, the trailer roll angle response is expected to lag behind the lateral acceleration response to the same steering input. Because of this, in steady-state maneuvers, lateral acceleration is considered to provide a clearer indication of an impending rollover than the roll angle. The advantages of using lateral acceleration as a rollover indicator compared to the roll angle include easier installation and less complexity. When paired with an ability to estimate the loading and CG height of the trailer, the lateral acceleration can provide a reasonably accurate indication of an impending rollover. In this section, time-traces of the lateral acceleration and trailer roll angles at the rollover entry speeds are compared for the J-turn maneuver and the DLC maneuver. The rollover indicators are compared using these two maneuvers because they are controlled solely by the driver and represent more realistic on-road scenarios than the ramp-steer or the SWD maneuvers. For all trials shown, the lateral acceleration and trailer roll angles are normalized by their respective values at rollover during that particular trial.

During the lateral acceleration and trailer roll angle responses to the quasi-steady-state J-turn maneuver, as shown in Figure 5-6, the normalized trailer roll angle response appears to lag or remain in phase with the normalized lateral acceleration response until the point of rollover, as expected. An exception to this is that during the Straight (H) combination, the roll angle response appears to lead the lateral acceleration response for some time during the maneuver. Because zero-phase digital filtering was employed and the sensors were sampled simultaneously, no time shift was used to align the lateral acceleration and trailer roll angle responses. All trials shown are the rollover entry speeds for the J-turn and are shown until the time of outrigger contact. When multiple trials at the rollover speed were performed, the trial with the lateral acceleration and trailer roll angle closest to the median values for that particular trailer and with minimal lateral acceleration oscillation was chosen. Lateral acceleration oscillations near the final data points are due to either transient dynamics, large vibrations in the lateral acceleration data from outrigger contact, or a possible delay in the determined outrigger contact time from the actual outrigger contact time. In general, the trailer roll angle and the lateral acceleration of the trailer match

closely in the time-domain for quasi-steady-state maneuvers, as indicated by the relatively small difference between the two measurements. These results show that lateral acceleration and roll angle are closely related in quasi-steady-state maneuvers, and if used interchangeably as a roll indicator, both would provide similar results.

Despite being considered a response to increased lateral acceleration, the trailer roll angle also reasonably indicates impending rollover and may even have an advantage over lateral acceleration in dynamic maneuvers. As shown in Figure 5-7, although the normalized roll angle response appears to lag behind the normalized lateral acceleration response in the first turn of the dynamic DLC maneuver, the roll rate from the first turn of the maneuver to the second turn of the maneuver is greater than the lateral jerk in the same time frame. For the second turn, which was the most common location of rollover during the high-speed testing of the A-double trailer, the roll angle appears to provide a quicker indication of an impending rollover than lateral acceleration. When the trailer roll angle and lateral acceleration values are between 0.2 and 0.3 of the value at rollover during the counter-steer, the lateral acceleration signal is at a lower magnitude compared to its rollover value than the roll angle and the roll angle response appears to lead the lateral acceleration response. On the contrary, during the first turn of the maneuver, the roll angle clearly lags behind the lateral acceleration for most or all of the turn. This trend is upheld for each loading condition but is more apparent for a lower CG, such as Straight(L). All trials are at the rollover entry speeds for the DLC and are shown until the start of the outrigger rollover contact.

Straight(H)

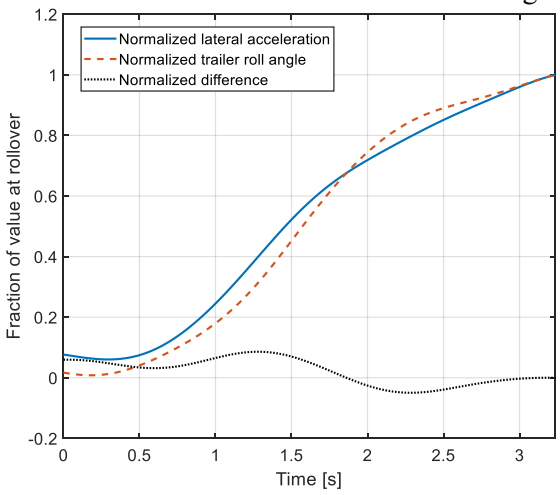

Fraction of value at rollover	Roll angle lead time (s)
0.1	-0.124
0.2	-0.144
0.3	-0.152
0.4	-0.140
0.5	-0.112
0.6	-0.064
0.7	0.028
0.8	0.160
0.9	0.152

Straight(M)

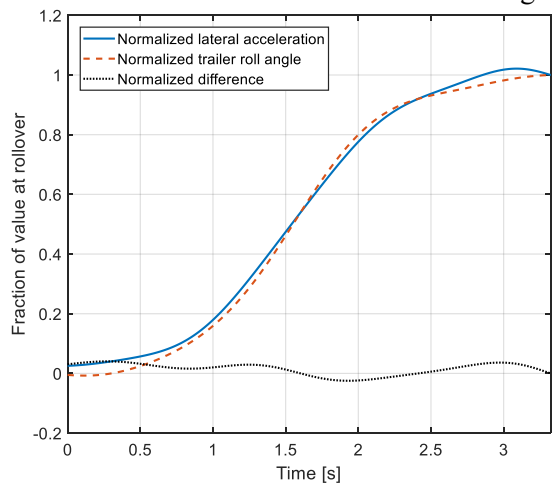

Fraction of value at rollover	Roll angle lead time (s)
0.1	-0.176
0.2	-0.56
0.3	-0.008
0.4	0.016
0.5	0.024
0.6	0.020
0.7	0.020
0.8	0.016
0.9	-0.008

Straight(L)

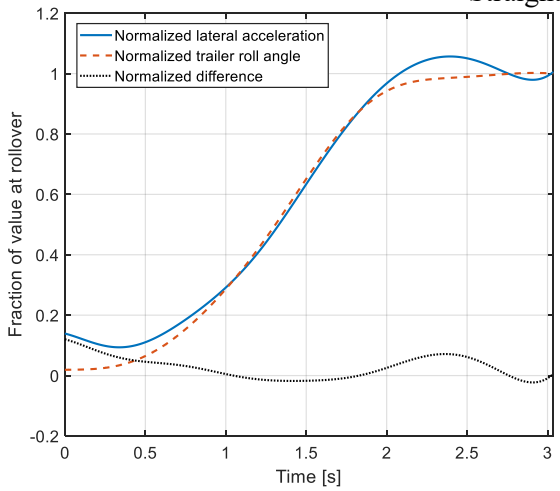

Fraction of value at rollover	Roll angle lead time (s)
0.1	-0.056
0.2	-0.048
0.3	-0.032
0.4	-0.032
0.5	0.012
0.6	0.016
0.7	0.040
0.8	0.048
0.9	0.028

Figure 5-6. Time response comparison of lateral acceleration and roll angle as fractions of the trial rollover value for each trailer combination during the quasi-steady-state J-turn maneuver.

Straight(H)

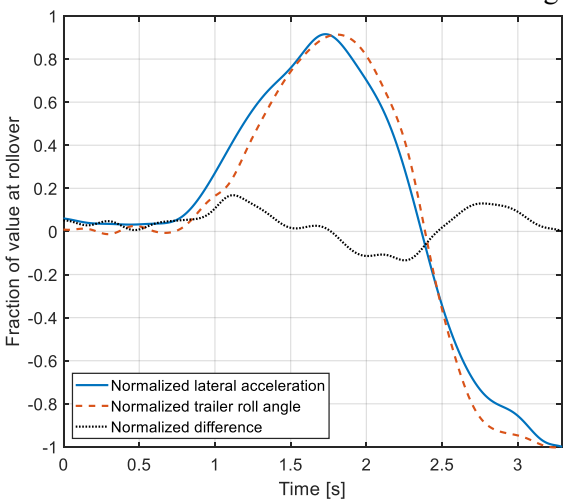

Fraction of value at rollover during counter-steer	Roll angle lead time during counter-steer (s)
0	-0.024
0.1	-0.016
0.2	-0.008
0.3	0
0.4	0.012
0.5	0.024
0.6	0.044
0.7	0.076
0.8	0.164
0.9	0.264

Straight(M)

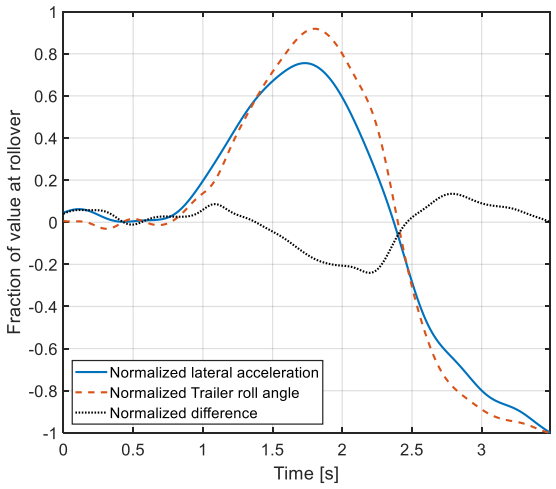

Fraction of value at rollover during counter-steer	Roll angle lead time during counter-steer (s)
0	-0.028
0.1	-0.012
0.2	-0.004
0.3	0.012
0.4	0.024
0.5	0.040
0.6	0.092
0.7	0.164
0.8	0.180
0.9	0.252

Straight(L)

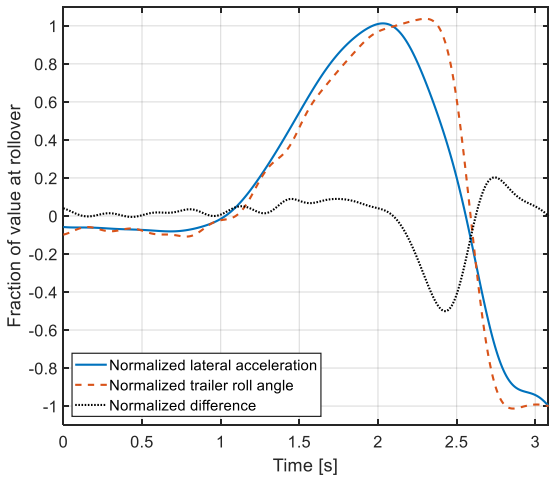

Fraction of value at rollover during counter-steer	Roll angle lead time during counter-steer (s)
0	-0.028
0.1	-0.016
0.2	-0.008
0.3	0.008
0.4	0.016
0.5	0.028
0.6	0.040
0.7	0.052
0.8	0.076
0.9	0.124

Figure 5-7. Time response comparison of lateral acceleration and roll angle as fractions of the trial rollover value for each trailer combination during the dynamic DLC maneuver.

The trailer roll angle appears to have an advantage over lateral acceleration for predicting an impending rollover during dynamic maneuvers; however, at intermediate fractions of the rollover value, the difference between the two values is small. Although there is a clear difference during Straight(L) tests, the roll angle only reaches 80% of the rollover value about 76 ms prior to lateral acceleration. While a quicker time response provides a clear advantage, there is another advantage to using roll angle. As a displacement measurement, the trailer roll angle generates a cleaner signal than lateral acceleration, the second derivative of displacement. With causal filtering, it may be easier to base real-time control schemes on the trailer roll angle rather than lateral acceleration because of the clarity of the signal. One advantage of using lateral acceleration as the rollover indicator is the ease of implementation. The lateral accelerometer used in the RSC system is typically internal to the module, protecting it from the environment, minimizing installation, and decreasing the system's complexity. To measure roll angle, unless the trailer is equipped with pneumatic suspension with independent air spring pressure (balanced suspension), an external sensor, such as a string potentiometer, is required. The use of an external sensor increases the complexity, maintenance, and difficulty of installation for an RSC device.

Investigating the differences between lateral acceleration and trailer roll angle at an increasing speed for the dynamic DLC maneuver, as illustrated in Figure 5-8, it appears that as the entry speed or steering frequency increased, the differences between the normalized lateral acceleration and trailer roll angle increased. While there is a significant difference at the rollover entry speed, the differences with respect to magnitude and time are observed at lower speeds as well. As the steering input becomes more aggressive or quicker with an increasing speed, during the second turn, the change in roll angle is visibly greater than the change in lateral acceleration at speeds as low as 34 mph. The consistently high roll rate compared to lateral jerk during counter-steer has the potential to provide a quicker indication of an impending rollover than the lateral acceleration, especially since the trailer is most prone to rollover at this location. Additionally, on average, during the DLC maneuver, roll angle has a larger magnitude compared to the rollover value than lateral acceleration, showing that even though roll angle and lateral acceleration are highly related, there are differences between the two, and they can fulfill different purposes as rollover indicators. These differences are investigated further in the following subsection.

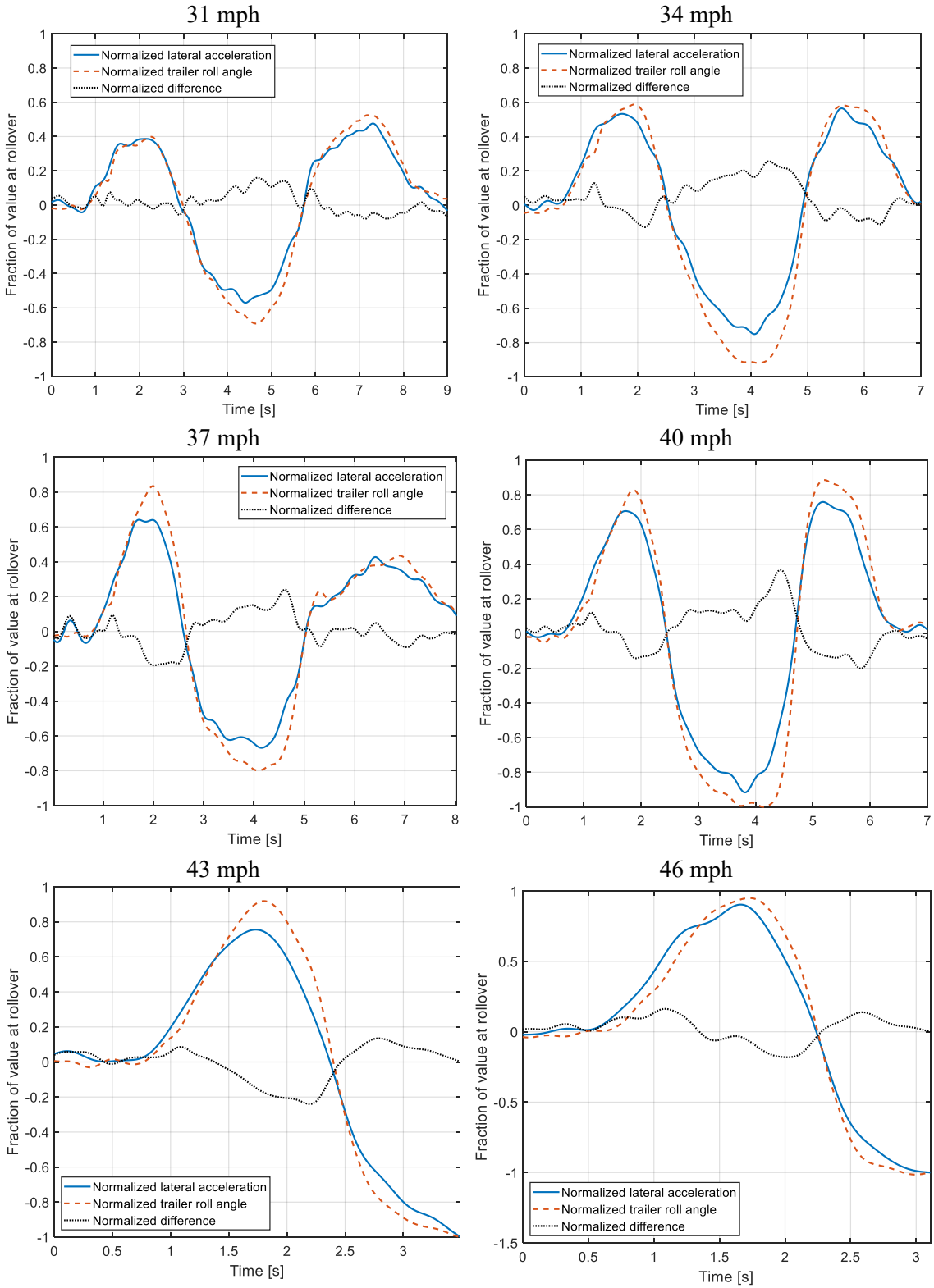

Figure 5-8. Time response comparison of lateral acceleration and roll angle as fractions of the value at rollover for the trial (or rollover median if no rollover) at increasing speeds for the Straight (M) combination during the dynamic DLC maneuver.

5.3. Comparison of Lateral Acceleration and Trailer Roll Angle Distributions at RSC Engagement

Lateral acceleration and trailer roll angle, although related, are distinct parameters that can be used to evaluate the roll stability of trailers. To examine the differences between lateral acceleration and trailer roll angle in the context of an RSC system, the values for each roll indicator are compared at the moment of RSC engagement. This section discusses the differences between lateral acceleration and trailer roll angle as RSC indicators for the quasi-steady-state and dynamic maneuvers separately.

In this section, the assumption is made that the estimated rollover threshold by the RSC system is equal to the median of the rollover ranges. It is assumed that the RSC module cannot discriminate between dynamic and quasi-steady-state maneuvers in real-time, so the threshold value used for both maneuver types is equal. Therefore, the median value represents a general estimate for the rollover threshold used by the RSC system. For straight(H) and straight(L), the median values of the lateral acceleration rollover ranges are 0.51 and 0.62 g, respectively. For the trailer roll angle, the median values are 2.18 and 1.60 deg, respectively. The lateral acceleration and trailer roll angle are normalized by the respective rollover median values for each distribution shown. While a distinction is not made between the maneuver type concerning the estimated rollover threshold value, a distinction is made between the experimental values of lateral acceleration and trailer roll angle during the tests; therefore, the results for each maneuver type are presented separately. Hypothesis tests are performed for cases where the difference between the distributions is small or non-obvious. Because of the large sample size, and approximate normality of the distributions, and (in relevant cases) approximately equal standard deviations, two-sample pooled t-tests were performed when necessary.

As mentioned in 3.5, the RSC systems used on the trailers possess two distinct lateral acceleration-related thresholds that initiate braking. The exact thresholds are unknown, as the RSC module is treated as a black box controller with information proprietary to the manufacturer. The two thresholds will be referred to as RSC-I and RSC-II. Looking at the distributions of the two different RSC thresholds, the RSC-I engagement does not appear directly related to a specific lateral acceleration threshold but, in general, increases with an

increasing entry speed during the high-speed testing. Since it is not directly related to a single value, the RSC-I engagement is a wide distribution of lateral acceleration and roll angle values. RSC-II engagement appears to be strongly correlated to a specific lateral acceleration threshold value. The standard deviation of the values is, in general, much smaller. Furthermore, there are fewer occurrences of activation, and the data appears to be concentrated at a particular mean lateral acceleration or trailer roll angle value.

5.3.1. Quasi-Steady-State Maneuvers

From the time comparisons in the previous chapter, it is expected that the values of trailer roll angle and lateral acceleration at the time of RSC engagement will follow similar distributions in the quasi-steady-state maneuvers when divided by the estimated rollover threshold. Because there was not a large delay or difference in amplitude between the lateral acceleration and roll angle in the time domain when normalized by the trial rollover indicator values, the expectation is that this also holds true for the values at the RSC activation times. Despite the small differences in the time-domain at the rollover speeds, in most cases, there are significant differences between the trailer roll angle distributions and the lateral acceleration distributions for the straight(H) and straight(L) trailers at both RSC-I and RSC-II engagement times for quasi-steady-state maneuvers.

As shown in Figure 5-9, the trailer roll angle distribution has a slightly larger mean and median than the lateral acceleration distribution for straight(H). Additionally, the roll angle distribution has a strong negative skew of -1.269, while the skew of the lateral acceleration distribution is only -0.209. Upon first observation, the distributions may look relatively similar; however, the one-sided t-test value of 0.024 confirms that the mean of the roll angle distribution is significantly greater than the mean of the lateral acceleration distribution. The same trends hold for straight(L) roll indicator distributions, as shown in Figure 5-10. There is a more considerable difference between the mean and medians of the two roll indicator distributions, with the mean and median of the roll angle distribution being 0.147 and 0.063 greater, respectively than the mean and median of the lateral acceleration distribution. The negative skew is much stronger in the roll angle distribution than the lateral acceleration, and the standard deviation of the roll angle distribution is greater than that of the lateral acceleration. It appears as though the decrease in loading

increased the difference between the consistency and central values of lateral acceleration and trailer roll angle as roll indicators for quasi-steady-state maneuvers.

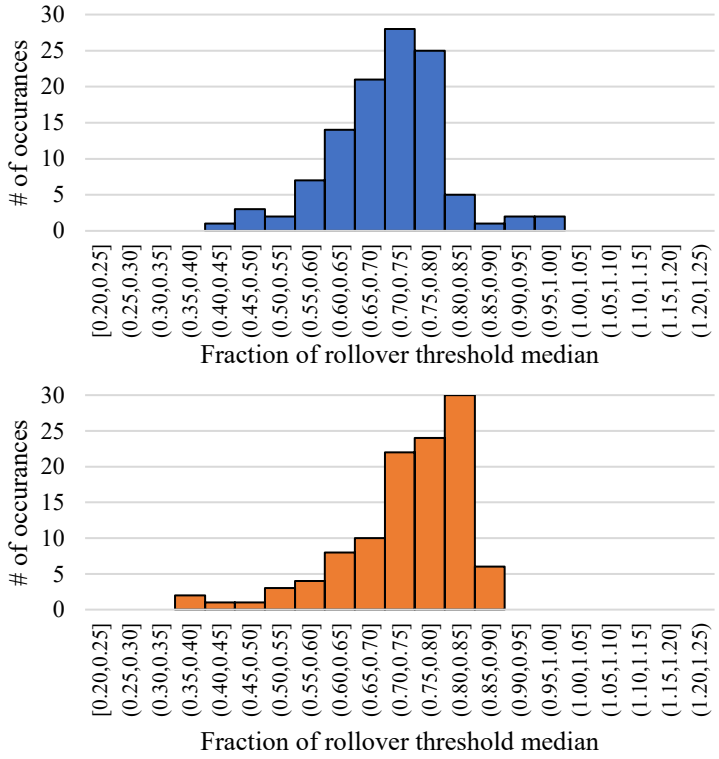

Median	0.720
Mean	0.708
Std	0.096
Skew	-0.209

(a)

Median	0.754
Mean	0.735
Std	0.105
Skew	-1.269

(b)

Figure 5-9. Distribution of (a) lateral acceleration and (b) trailer roll angle values at time of RSC-I engagement for straight(H) during quasi-steady-state maneuvers.

The standard deviations of the RSC-I roll indicator distributions are greater than the standard deviations of the RSC-II roll indicator distributions. This suggests that the control schemes governing the RSC-II engagement are more closely tied to a particular threshold value than the RSC-I control schemes. Comparing the roll indicator distributions for straight(H), shown in Figure 5-11, the lateral acceleration and roll angle distributions appear to be concentrated at approximately the same mode. The means and medians of the distributions are within 0.01 of the rollover threshold, so they are nearly equal. The major difference between the distributions is the skew. The lateral acceleration is positively skewed, with more values at lower fractions of its rollover value. At the same time, the roll angle distribution is negatively skewed, with more values at higher fractions of the rollover value. The one-sided t-test for the straight(H) distributions results in a test statistic of 0.27, failing to reject the null hypothesis; therefore, there is no significant statistical difference between the means of the two distributions despite a large difference in skew.

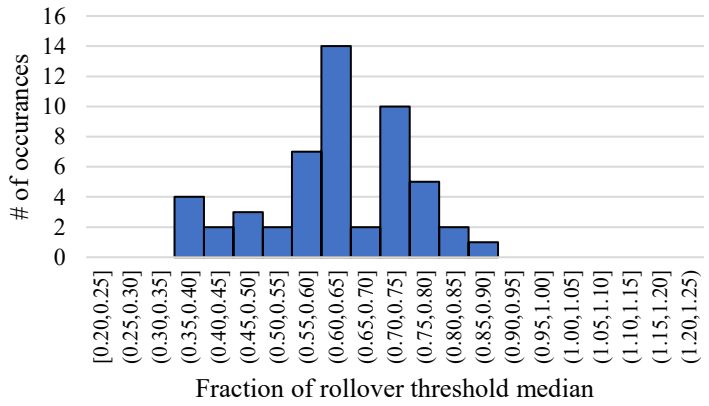

Median	0.619
Mean	0.624
Std	0.127
Skew	-0.470

(a)

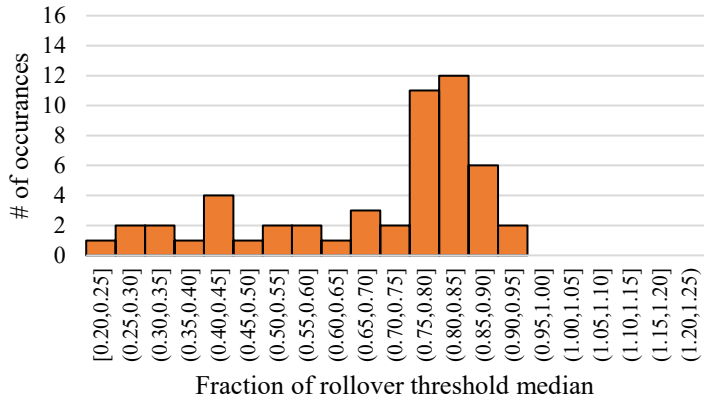

Median	0.766
Mean	0.687
Std	0.197
Skew	-0.925

(b)

Figure 5-10. Distribution of (a) lateral acceleration and (b) trailer roll angle values at time of RSC-I engagement for a straight(L) trailer during quasi-steady-state maneuvers

When comparing the lateral acceleration and trailer roll angle distributions of straight(L), the similarities between the two roll indicator values at the RSC-II engagement times with straight(H) are no longer present, as shown in Figure 5-12. The means and medians of the two distributions differ by 0.126 and 0.139, respectively, and the skews of the distributions are opposite, with the lateral acceleration distribution having a moderate positive skew and the roll angle distribution having a moderate negative skew.

While quasi-steady-state maneuvers are nearly aligned in the time domain, in actuality, the values of the roll angle and the lateral acceleration vary throughout the maneuver, leading to a difference in the respective values when RSC-I and RSC-II engage. Even the lower standard deviation RSC-II engagement distributions have significant differences. This data bolsters the claim that while trailer roll angle and lateral acceleration are related, they cannot be used interchangeably, and roll angle data cannot always be used to validate lateral-acceleration-based RSC systems.

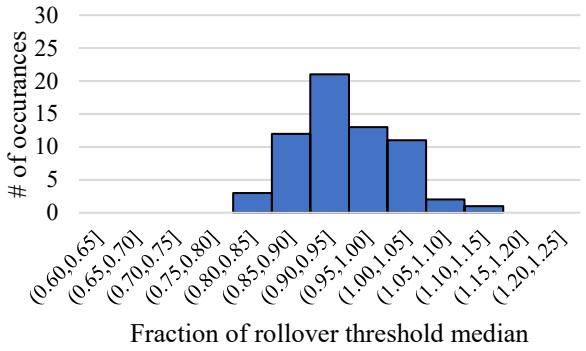

Median	0.943
Mean	0.947
Std	0.062
Skew	0.551

(a)

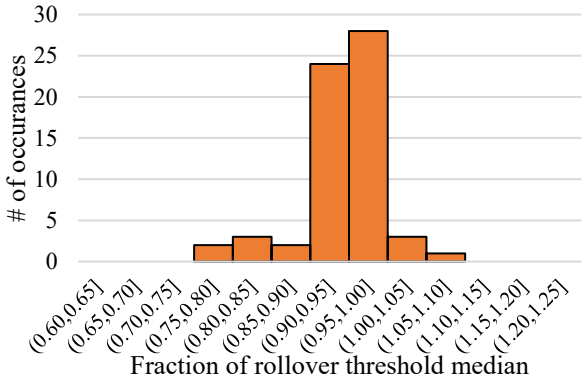

Median	0.950
Mean	0.941
Std	0.054
Skew	-1.310

(b)

Figure 5-11. Distribution of (a) lateral acceleration and (b) trailer roll angle values at time of RSC-II engagement for straight(H) during quasi-steady-state maneuvers.

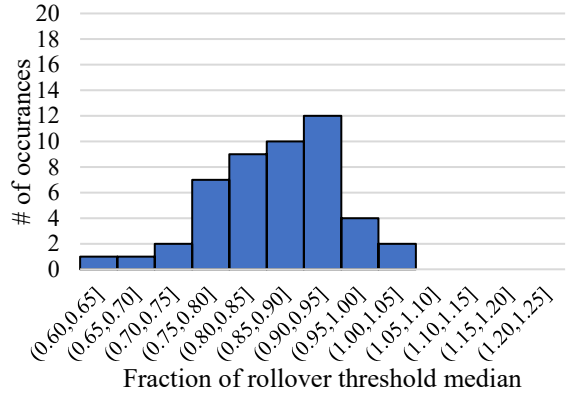

Median	0.869
Mean	0.861
Std	0.089
Skew	0.669

(a)

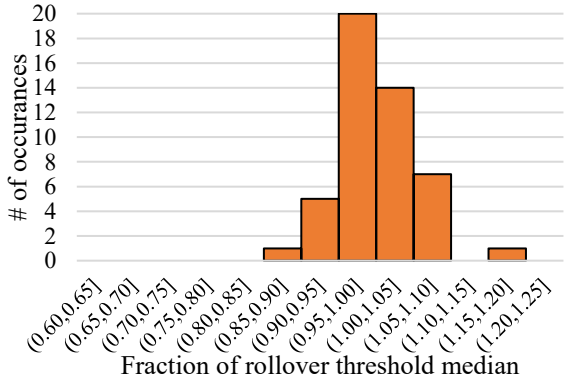

Median	0.995
Mean	1.000
Std	0.049
Skew	-0.517

(b)

Figure 5-12. Distribution of (a) lateral acceleration and (b) trailer roll angle values at time of RSC-II engagement for a straight(L) during quasi-steady-state maneuvers.

5.3.2. Dynamic Maneuvers

The lateral acceleration and trailer roll angle distributions at RSC-I activation times for straight(H) are shown in Figure 5-13. Comparing the two distributions, the lateral acceleration distribution follows a normal distribution more closely while the roll angle is more negatively skewed. The roll angle populates the higher percentages of the rollover threshold when RSC-I activate, as indicated by the larger mean and median. Although the two distributions appear similar, the one-sided t-test test statistic is equal to 0.0024, confirming that the means of the two distributions have a significant statistical difference.

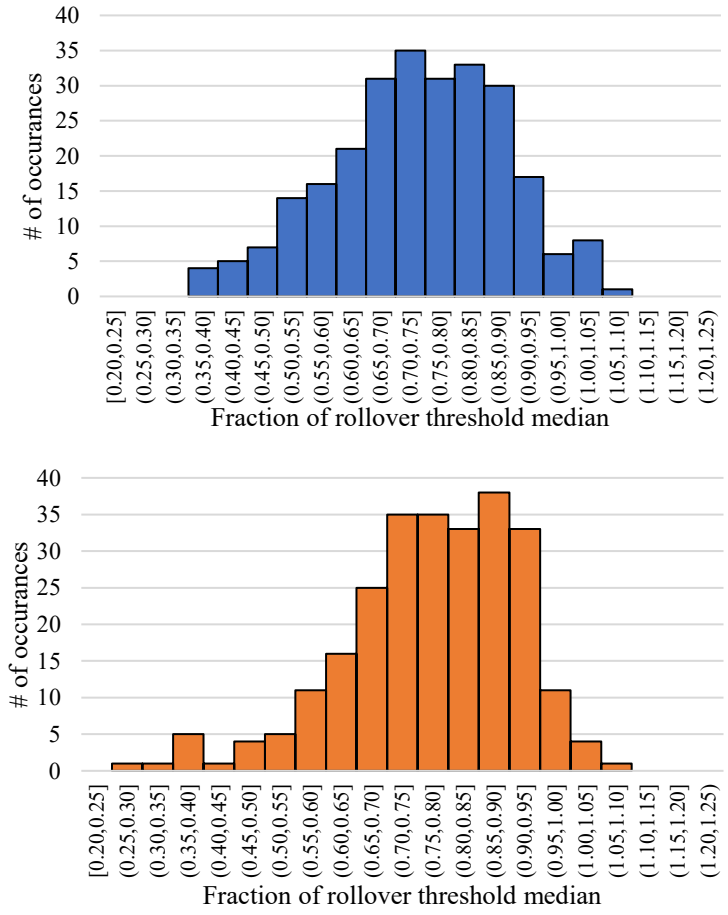

Median	0.745
Mean	0.738
Std	0.145
Skew	-0.311

(a)

Median	0.785
Mean	0.773
Std	0.141
Skew	-0.748

(b)

Figure 5-13. Distribution of (a) lateral acceleration and (b) trailer roll angle values at time of RSC-I engagement for straight(H) during dynamic maneuvers.

Analyzing the lateral acceleration and trailer roll angle distributions at RSC-I activation for straight(L) in Figure 5-14, both distributions are approximately normal. Unlike the straight(H), the lateral acceleration and roll angle distributions have nearly equal means and medians. A one-sided t-test was performed to verify this observation. The resulting test

statistic was 0.332, confirming that there is no significant statistical difference between the means of the two distributions. The concentration of values near the mean and median in the lateral acceleration distribution is greater than the roll angle distribution, as indicated by the smaller standard deviation. The closeness of the roll angle and lateral acceleration distributions for straight(L) compared to straight(H) suggest that as the loading is decreased on a particular trailer, the difference between lateral acceleration and roll angle as roll indicators during dynamic maneuvers decreases also. At RSC-I engagement times, the lateral acceleration and roll angle values are approximately the same fraction of the rollover value. This trend was not observed for the quasi-steady-state maneuvers in which the lateral acceleration and trailer roll angle distributions did not align.

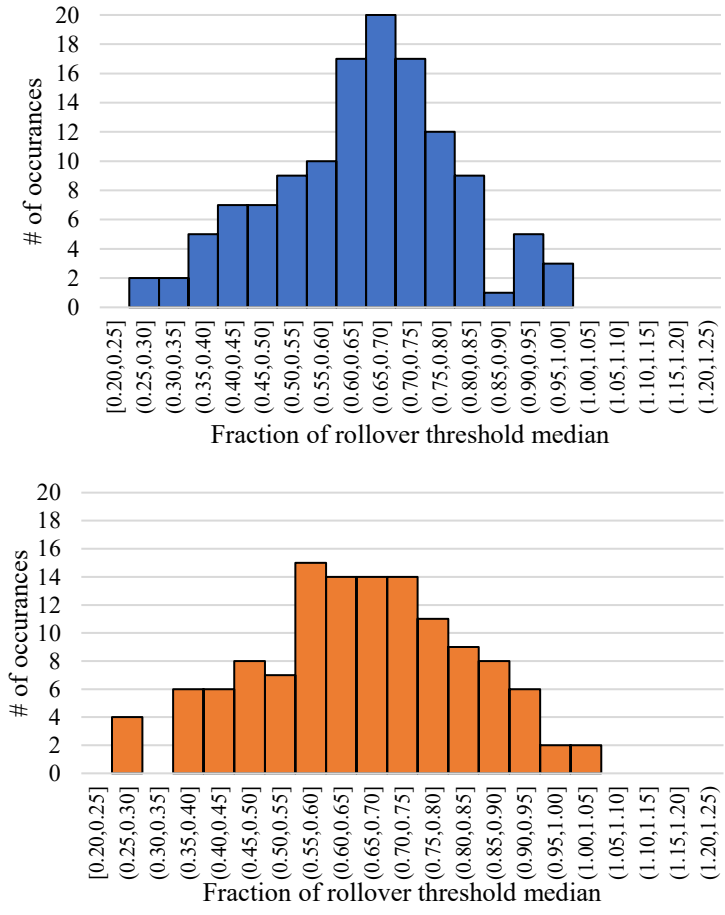

Median	0.662
Mean	0.648
Std	0.153
Skew	-0.200

(a)

Median	0.666
Mean	0.657
Std	0.172
Skew	-0.185

(b)

Figure 5-14. Distribution of (a) lateral acceleration and (b) trailer roll angle values at time of RSC-I engagement for a straight(L) during dynamic maneuvers

The results indicate that the lateral acceleration and roll angle distributions are more similar at RSC-I engagement during dynamic maneuvers than during quasi-steady-state

maneuvers; however, evidence has shown that while related, the roll angle and lateral acceleration are not identical as the distribution means were proved different for the straight(H) trailer.

As illustrated in Figure 5-15, although the control schemes for RSC-II are different than that of RSC-I, the same trends between the lateral acceleration and roll angle distributions appear for straight(H). At the time of RSC-II engagement, on average, the trailer roll angle values are a higher fraction of their respective rollover value than lateral acceleration is. The mean and median of the trailer roll angle are 0.038 and 0.031 greater than the lateral acceleration distribution.

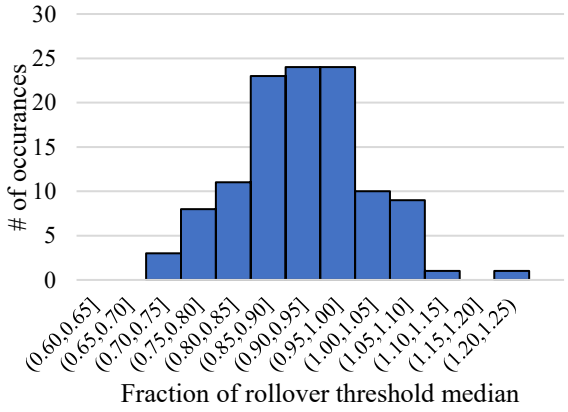

Median	0.917
Mean	0.925
Std	0.091
Skew	0.202

(a)

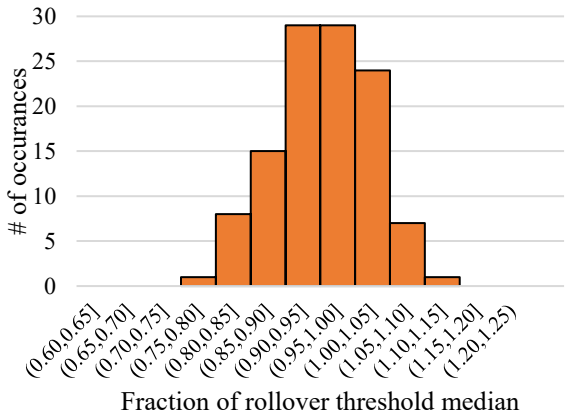

Median	0.955
Mean	0.956
Std	0.068
Skew	-0.288

(b)

Figure 5-15. Distribution of (a) lateral acceleration and (b) trailer roll angle values at time of RSC-II engagement for straight(H) during dynamic maneuvers.

In contrast to the RSC-I engagement, there is a significant difference between the lateral acceleration and trailer roll angle distributions for straight(L) at RSC-II engagement times for dynamic maneuvers, as shown in Figure 5-16. The roll angle distribution is centered to the right of the lateral acceleration distribution, having a mean 0.037 larger and median

0.075 larger. Additionally, the roll angle distribution is moderately skewed to the right, while the lateral acceleration distribution has a slight skew to the left. The large difference between the roll indicators contradicts the results from the straight(L) RSC-I engagement distributions. It provides evidence that the lateral acceleration and roll angle cannot be used interchangeably to verify data. Additionally, the concept of roll gain in trailer roll dynamics does not accurately portray the roll dynamics of trailers for all time, especially close to the rollover value, as shown by the differences in the RSC-II distributions which are centered around values near the median rollover threshold value.

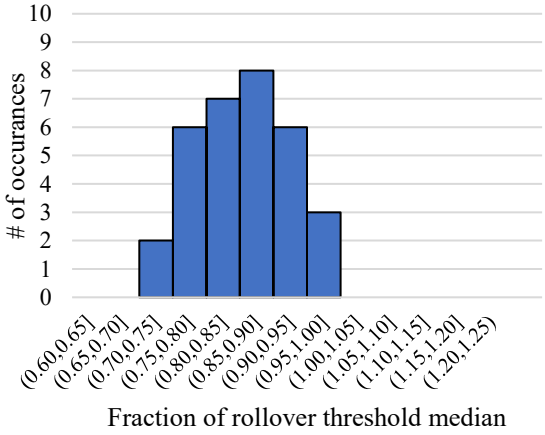

Median	0.861
Mean	0.855
Std	0.072
Skew	-0.208

(a)

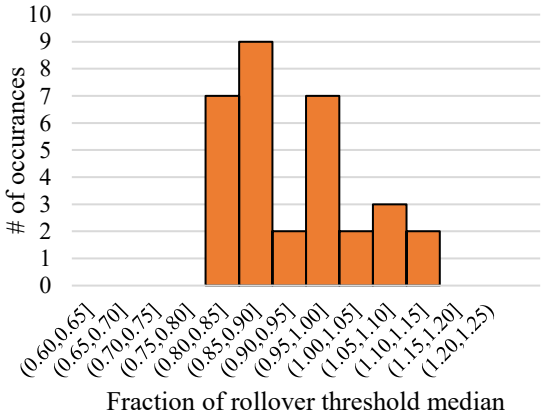

Median	0.898
Mean	0.930
Std	0.091
Skew	0.542

(b)

Figure 5-16. Distribution of (a) lateral acceleration and (b) trailer roll angle values at time of RSC-II engagement for a straight(L) during dynamic maneuvers.

5.4. Summary

The first section of this chapter performed hypothesis tests to determine if a coupled trailer has an effect on the roll dynamics of the other trailer. When investigating the effects of a coupled straight(L) on straight(H)'s lateral acceleration and trailer roll angle values, it was

determined that there was no significant statistical difference between the means of two distributions. When investigating the effects of a coupled trailer of a different type on straight(H)'s lateral acceleration and trailer roll angle values, it was determined that there was no significant statistical difference between the means of the two lateral acceleration distributions, but the mean of the roll angle distribution when straight(H) was connected to another straight(H) was greater than when it was connected to the different trailer. This could suggest that the trailer roll angle is less robust than lateral acceleration to a change in trailer combinations.

The next comparison made was between trailer rollover thresholds during quasi-steady-state and dynamic maneuvers for the straight(H) and straight(L) trailers. For straight(H), it was found that the mean lateral acceleration and mean roll angle were greater in dynamic maneuvers than in quasi-steady-state maneuvers. For straight(L), the lateral acceleration during quasi-steady-state maneuvers is shifted right of the roll angle distribution, but the null hypothesis was not rejected for the difference between the roll angle distributions. All hypothesis tests are summarized in Table 5-6.

Table 5-6. Hypothesis test results for comparisons between coupled trailer type and maneuver type on lateral acceleration and trailer roll angle rollover thresholds.

Comparison	Trailer	Roll Indicator	Hypothesis Test Result
Trailer Coupled with straight(H)	straight(L)	Lateral Accel	fail to reject $H_0 = H_{SH}$ and H_{SL} are identical
		Roll Angle	fail to reject $H_0 = H_{SH}$ and H_{SL} are identical
	drop(H)	Lateral Accel	fail to reject $H_0 = \mu_{SH} \geq \mu_{Diff}$
		Roll Angle	reject H_0: $\mu_{SH} < \mu_{Diff}$
Dynamic vs. Quasi-Steady-State	straight(H)	Lateral Accel	reject H_0: $\mu_{Dynamic} < \mu_{QSS}$
		Roll Angle	reject H_0: $\mu_{Dynamic} < \mu_{QSS}$
	straight(L)	Lateral Accel	reject H_0: H_{QSS} is shifted right
		Roll Angle	fail to reject $H_0 = H_{QSS}$ and H_{Dyn} are identical

In addition to completing hypothesis tests, the median values of lateral acceleration and trailer roll angle values at the ToC were calculated. The overall median values, as well as the median values for quasi-steady-state and dynamic maneuvers are shown in Table 5-7. The experimentally derived rollover threshold values show that the decrease in loading from straight(H) to straight(L) increases the lateral acceleration but decreases the trailer roll angle at rollover. The difference in median lateral acceleration at rollover increased by 22% from straight(H) to straight(L), but the difference in suspension properties from the

reduced load resulted in a median trailer roll angle at rollover for the straight(L) that was 27% less than that of straight(H). The large discrepancy between trailer roll angle between the trailer types reveals that it may be necessary to have prior knowledge of the suspension properties to enact a roll stability controller based on sprung mass body roll.

Table 5-7. Median lateral acceleration and trailer roll angle rollover threshold values from experimental testing for straight(H) and straight(L) trailers.

Roll Indicator	Maneuver Type	straight(H)	straight(L)
Median Lateral Acceleration [g]	Quasi-Steady-State	0.53	0.65
	Dynamic	0.50	0.61
	Combined	0.51	0.62
Median Trailer roll angle [deg]	Quasi-Steady-State	2.20	1.60
	Dynamic	2.14	1.53
	Combined	2.18	1.60

While the roll angle is generally considered a response to an increased lateral acceleration, comparing the time-traces of lateral acceleration data to trailer roll angle data shows that this assumption does not always hold true. In quasi-steady-state maneuvers, such as the J-turn and the ramp-steer, the normalized lateral acceleration and normalized trailer roll angle values are approximately equal for the entirety of the maneuver. The difference between the two values is typically small, not exceeding 10% of the rollover threshold value. In dynamic maneuvers, on the other hand, the differences in the time traces between the trailer mass roll angle and lateral acceleration increase, reaching approximately 20% of the rollover threshold. The trailer roll angle clearly lags behind the lateral acceleration for the entirety of the 1st turn in the DLC maneuver; however, the lateral acceleration appears to lag behind the roll angle during the second turn of the maneuver. The roll rate during the second turn of the maneuver is far greater than the lateral jerk rate. Because of this, the trailer roll angle may be able to provide a more accurate and timely estimation of an impending rollover than lateral acceleration measurements would. Lastly, when comparing the lateral acceleration and trailer roll angle at different speeds, at lower speeds, the values are close to equal, but the values diverge, and the error grows as the speed increases.

The differences in the roll indicator distributions at both the RSC-I and RSC-II engagement times during both quasi-steady-state and dynamic maneuvers show that despite being related, there are significant differences between the lateral acceleration and roll angle

values with respect to their rollover values at the same moment in time. Controller designers should be wary of this, recognizing that the trailer roll angle cannot necessarily validate lateral acceleration data or vice versa. In the context of an RSC module that operates based on lateral acceleration thresholds, the standard deviation of the trailer roll angle at RSC intervention times is typically different than that of the lateral acceleration. Additionally, the skew of the trailer roll angle distributions is typically much greater in magnitude than the skew of the lateral acceleration distribution. These results indicate that for a lateral acceleration-based controller, the trailer roll angle values at RSC intervention generally have a different distribution than lateral acceleration and that the roll indicators cannot always be used interchangeably.

6. Conclusions & Recommendations

An experimental analysis was performed with Class 8 33-ft A-double trailers to evaluate the roll dynamics of articulated heavy vehicles and to determine the effectiveness of trailer-based RSC in mitigating roll instability. In addition, a comparison between lateral acceleration and trailer roll angle as rollover indictors in trailer-based RSC was conducted. This chapter presents the findings from these studies and gives recommendations for future work to elaborate on and build on the results.

6.1. Conclusions

To evaluate the roll dynamics of the test vehicle and the effectiveness of trailer-based RSC systems, high-speed testing was conducted at the Transportation Research Center (TRC) in East Liberty, Ohio. During the high-speed testing, 2 quasi-steady-state (J-turn and Ramp-Steer) and 2 dynamic (DLC and SWD) maneuvers were performed to evaluate the test vehicle's roll stability with and without RSC. The J-turn, Ramp-Steer, and DLC maneuvers were evaluated in terms of entry speed, while the SWD maneuver was evaluated in terms of steering percentage. The focus of this study was on the comparison of straight-rail trailers under three different loading conditions: heavy, mixed, and light. The heavy and light loading conditions contained either both heavily loaded or lightly loaded trailers, respectively. The mixed condition included a heavy front and a light rear trailer.

Of the three loading conditions, the lightly loaded trailers rolled over at the highest entry speed or steering percentage during all four maneuvers. In general, the mixed loading resulted in a higher entry speed than the heavily-loaded condition, with the exception of the SWD maneuver. Out of the three loading conditions, the heavily-loaded trailers rolled over at the lowest speeds. The results show that connecting a light trailer to the rear of a heavy trailer raised the maximum allowable entry speed but decreased the maximum allowable steering amplitude.

The trailer-based RSC system proved to be effective at increasing the maximum allowable speed or steering wheel angle for each loading condition in each maneuver. During the quasi-steady-state maneuvers, the RSC generated a greater improvement in rollover entry

speed for lighter loads than heavier loads. During the J-turn, the improvements in entry speed for the Straight(H), Straight(M), and Straight(L) loading conditions were 2, 2, and 4 mph, respectively. The increase during the ramp-steer maneuver was 1, 2, and 5 mph, respectively. A possible reason for the large increase during the light-loading conditions was the increased turn radius due to understeer at high speeds. The results of the DLC maneuver showed that RSC was most effective at increasing the rollover entry speed for the heavily-loaded and mixed-loaded trailers. The improvements for the Straight(H), Straight(M), and Straight(L) loading conditions for the DLC maneuver were 4, 4, and 1 mph, respectively. During the SWD, the results did not match the other dynamic maneuver, as the increase in steering percentage was less for the Straight(H) combination than the Straight(L) combination. For the SWD maneuver, the increase in rollover steering percentage for the Straight(H), Straight(M), and Straight(L) loading conditions was 5%, 15%, and >10%, respectively. The results show that RSC is especially effective in decreasing the lateral acceleration of the rear trailer. This was particularly evident in dynamic maneuvers where rearward amplification is most apparent.

The trailer-based RSC effectively mitigates trailer roll instability by applying the trailer brakes when it senses that the trailer is approaching its rollover limit. The RSC system used in the high-speed testing intervenes when the system's pre-set lateral acceleration threshold is exceeded. The results, however, indicate that the trailer roll angle would provide a quicker indication of rollover than lateral acceleration in dynamic maneuvers. Additionally, roll angle may provide a cleaner signal than lateral acceleration for use in real-time controllers. Despite this, lateral acceleration is easier to measure in practice and does not require instrumentation external to the system, lowering overall complexity.

Comparing the lateral acceleration and trailer roll angle began with evaluating the effects of trailer coupling on its rollover threshold. The rollover threshold of a straight(H) trailer connected to a straight(L) or drop(H) indicated no significant difference in lateral accelerations compared to a straight(H) connected to a straight(H). But, a significant difference was found between the trailer roll angle when connected to a drop(H) of nearly equal loading but a lower CG and different suspension architecture. When comparing the lateral acceleration and trailer roll angle between quasi-steady-state maneuvers and

dynamic maneuvers, there are similar trends. For straight(H), the lateral acceleration and trailer roll angle rollover thresholds are lower in dynamic maneuvers than quasi-steady-state maneuvers. For straight(L), the lateral acceleration rollover threshold is also lower in dynamic maneuvers than quasi-steady-state maneuvers. However, no definitive conclusion can be drawn for the trailer roll angle for straight(L). The results generally support the notion that the rollover threshold in dynamic maneuvers (e.g., lane-change maneuvers) is lower than in quasi-static maneuvers (e.g., exit ramps) because of the inertial and damping effects.

As expected, it was determined that the lateral acceleration rollover threshold (0.51g) for straight(H) was the lower among the two trailers that were tested, while straight(L) had the higher threshold (0.62g). The trailer with the greater roll angle at rollover was straight(H) at 2.18 deg, with the lesser being straight(L) at 1.60 deg. The significant difference found between trailer roll angle when comparing conditions with higher CG (such as a loaded trailer) to lower CG (such as a light or unloaded trailer) indicates that the trailer roll angle changes more widely with trailer loading than trailer lateral acceleration does. As indicated by the decrease in suspension roll stiffness, the suspension properties also significantly affect the trailer roll angle, whereas they do not affect lateral acceleration. In practice, this indicates that a priori knowledge of the suspension properties is required to estimate the roll angle rollover limit to determine the most suitable RSC activation value.

The time response for lateral acceleration and trailer roll angle due to quasi-steady-state and dynamic excitations are different. During the quasi-steady-state J-turn maneuver, the lateral acceleration and trailer roll angle responses appear to be similar in both magnitude and phase. Therefore, using the roll angle will yield nearly the same RSC activation response as lateral acceleration, which is commonly used in production systems. However, during the dynamic DLC maneuver, the lateral acceleration leads the trailer roll angle during the initial steering but lags during the counter-steer. The counter-steer is when the rollover occurs most often; hence, for dynamic steering maneuvers, such as DLC, the roll angle would provide a quicker indication of a pending rollover, even though it requires a priori knowledge of the trailer suspensions response to a dynamic input, as discussed earlier.

Finally, when comparing the distributions of lateral acceleration and trailer roll angle at RSC activation time, the distributions are distinct in most cases. In general, when RSC activates, whether RSC-I or RSC-II, the roll angle is closer to the trailer rollover limit than the lateral acceleration; therefore, the mean and the median of the trailer roll angle distributions is typically higher than that of the lateral acceleration distributions. Furthermore, the trailer roll angle distributions tend to be more skewed and have different standard deviations than the lateral acceleration. The results prove that the trailer roll angle and lateral acceleration are distinctly different roll indicators. Therefore, the approach for calibrating and tuning an RSC system that uses lateral acceleration as the roll indicator cannot be adopted for one that uses the roll angle. For the latter, new measures such as an awareness of the trailer's suspension response to body roll must be included.

6.2. Recommendations

The first half of this study mainly focused on the differences in rollover threshold of A-doubles when the trailers were in different loading combinations. The trailer's rollover thresholds were analyzed when they were heavily loaded, lightly loaded, or mixed. Although the three load cases represent typical fleet operation conditions, they do not entirely analyze the effects of loading on the effectiveness of RSC. Other loading conditions should be developed and tested to investigate how the longitudinal and lateral CG positions affect trailer-based RSC effectiveness. Additionally, testing should be performed with other types of trailers (e.g., drop frames, flatbeds, tankers, etc.) to determine the effect of trailer constructions on the RSC activation. An investigation on tankers with varying amounts of liquid or torsionally-compliant flatbed trailers with different loading conditions would be of particular interest.

The second half of the study focused on comparing lateral acceleration and trailer roll angle as indicators for RSC systems. While both values were measured in real-time, the commercially available RSC systems use lateral acceleration thresholds. To build upon this study, high-speed testing is needed with RSC systems in which the trailer roll angle is used as a rollover indicator to more definitively assess any benefits that such a system may offer. Measures such as the increase in maneuver entry speed or steering percentage can be used for comparing lateral-acceleration-based and roll-angle-based RSC systems. If such an

analysis agrees with the findings from this study, then potentially, a hybrid approach may be adopted in which the RSC intervention is based on both lateral acceleration and roll angle thresholds.

References

[1] Federal Motor Carrier Safety Administration, 2020, “Large Truck and Bus Crash Facts 2018,” FMCSA Report No. FMCSA-RRA-19-018. https://www.fmcsa.dot.gov/safety/data-and-statistics/large-truck-and-bus-crash-facts-2018

[2] Federal Motor Carrier Safety Administration, 2007, “Unit Costs of Medium and Heavy Truck Crashes,” FMSCA Report No. FMCSA-RRA-07-034. https://www.fmcsa.dot.gov/sites/fmcsa.dot.gov/files/docs/UnitCostsTruck%20Crashes2007.pdf

[3] Baker, D., Bushman, R., Berthelot, C., 2001, “Effectiveness of Truck Rollover Warning Systems. Transportation Research Record: Journal of the Transportation Research Board,” *Transportation Research* Record 1779(), 134–140. doi:10.3141/1779-18

[4] National Highway Traffic Safety Administration, 2015, “Federal Motor Vehicle Safety Standards; Electronic Stability Control Systems for Heavy Vehicles,” Docket No. NHSTA-2015-0056 RIN 2127-AK97

[5] Woodrooffee, J., Blower, D., Gordon, T., Green, P. E., Liu, B., Sweatman, P., 2009, “Safety Benefits of Stability Control Systems For Tractor-Semitrailers,” NHSTA Report No. DOT HS 811 205

[6] Grīslis, A., 2010, "Longer Combination Vehicles and Road Safety," Transport, 25(3), pp. 336-343. https://doi.org/10.3846/transport.2010.41

[7] U.S. Department of Energy, 2012, “Vehicle Weight Classes and Categories,” https://afdc.energy.gov/data/10380

[8] Federal Highway Administration, 2014, “Traffic Monitoring Guide,” https://www.fhwa.dot.gov/policyinformation/tmguide/tmg_2013/vehicle-types.cfm

[9] Bureau of Transportation Statistics, 2021 “Moving Goods in the United States,” https://data.bts.gov/stories/s/Moving-Goods-in-the-United-States/bcyt-rqmu

[10] Federal Highway Administration, 2019, “Federal Size Regulations for Commercial Motor Vehicles,” https://ops.fhwa.dot.gov/freight/publications/size_regs_final_rpt/

[11] Jin, Z., Li, B., Li, J., 2019, *Dynamic Stability and Control of Tripped and Untripped Vehicle Rollover*, Morgan & Claypool

[12] Winkler, C. B., Ervin, R. D., 1999, “Rollover of Heavy Commercial Vehicles,” The University of Michigan Transportation Research Institute, UMTRI-99-19

[13] Law, E. and Janajreh, I., 2004, "Effects of Tire and Vehicle Design Characteristics on Rollover of Tractor Semi-Trailers," SAE Technical Paper 2004-01-1739, 2004, https://doi-org.ezproxy.lib.vt.edu/10.4271/2004-01-1739.

[14] Ervin, R. D., 1983, “The Influence of Size and Weight Variables on the Roll Stability of Heavy Duty Trucks,” *SAE Transactions*, 1983, Vol. 92, Section 830693-831395 (1983), pp. 629-654, https://www.jstor.org/stable/44647636

[15] Laird, L. A., 1988, “Measurement of Heavy Vehicle Suspension Roll-Stability Properties, and A Method to Evaluate Overall Stability Performance,” *SAE Transactions*, Vol. 97, Section 5 (1988), pp.842-885, https://www,jstor.org/stable/44724585

[16] Chen, B., Peng, H., 2005, “Rollover Warning for Articulated Heavy Vehicles Based on a Time-to-Rollover Metric,” Journal of Dynamic Systems, Measurement and Control. 127. 406-414. 10.1115/1.1988340.

[17] Gertsch, J., Shim, T., 2008 “Interpretation of roll plane stability models,” *Int. J. Vehicle Design,* Vol.46, No. 1, pp. 72-93

[18] Chen, Y., Peterson, A.W., Zhang, C. and Ahmadian, M., 2019, “A simulation-based comparative study on lateral characteristics of trucks with double and triple trailers”, *Int. J. Vehicle Safety*, Vol. 11, No. 2, pp.136–157.

[19] Chen, Y., Ahmadian, M., and Peterson, A., 2015, "Pneumatically Balanced Heavy Truck Air Suspensions for Improved Roll Stability," SAE Technical Paper 2015-01-2749, 2015, doi:10.4271/2015-01-2749.

[20] García L. O.,Wilson F. R., Innes, J. D., 2003. “Heavy Truck Dynamic Rollover: Effect of Load Distribution, Cargo Type, and Road Design Characteristics.” *Transportation Research Record: Journal of the Transportation Research Board* 1851 (1): 25–31. https://doi.org/10.3141/1851-03.

[21] Dahlberg, E., 2000, "A Method Determining the Dynamic Rollover Threshold of Commercial Vehicles." *SAE Transactions* 109, pp.789-801. http://www.jstor.org/stable/44650818.

[22] Hyun, D., Langari, R., 2003 “Modeling to Predict Rollover Threat of Tractor-Semitrailers,” *Vehicle System Dynamics* 39:6, pp. 401-414, DOI: 10.1076/vesd.39.6.401.14596

[23] Preston-Thomas, J., Woodrooffe, J., 1990, “A Feasibility Study of a Rollover Warning Device for Heavy Trucks”

[24] Liu, P. J., Rakheja, S., Ahmed, A. K. W., 1997, “Detection of Dynamic Roll Instability of Heavy Vehicles for Open-Loop Rollover Control,” SAE Technical Paper 973263, 1997, https://doi.org/10.4271/973263.

[25] Yu, H., Güvenç L., Özgüner, Ü., 2008, “Heavy duty vehicle rollover detection and active roll control,” *Vehicle System Dynamics*, 46:6, 451-470, DOI:10.1080/00423110701477529

[26] Fancher, P., Winkler, C., 2007, “Directional performance issues in evaluation and design of articulated heavy vehicles,” Vehicle System Dynamics, 45:7-8, 607-647, DOI: 10.1080/00423110701422434

[27] Mikulcik, E. C., and L. G. Jensen. 1990, “Low Speed Off Tracking of Multiple-Axle Road Vehicles.” *SAE Transactions* Vol. 99, Section 2: Journal of Commercial Vehicles (1990): 163–72. http://www.jstor.org/stable/44469385.

[28] Ontario, 2021, “O. Reg. 413/05: Vehicle Weights and Dimensions – For Safe, Productive and Infrastructure-friendly Vehicles,” *Highway Traffic Act, R.S.O. 1990, c. H.8,* https://www.ontario.ca/laws/regulation/050413

[29] Federal Highway Administration, 2017, “Review of Practices to Implement Cost-Effective Roadway Infrastructure Improvements to Reduce the Number and Severity of Crashes Involving Commercial Motor Vehicles,” https://safety.fhwa.dot.gov/cmv_rtc/ch3.cfm

[30] Olson, P., 1989, “Driver Perception Response Time,” SAE Technical Paper 890731, 1989, https://doi.org/10.4271/890731.

[31] Chandrasekharan, S., Guenther, D., Heydinger, G., Salaani, M. et al., 2009, “Development of a Roll Stability Control Model for a Tractor Trailer Vehicle,” *SAE Int. J. Passeng. Cars – Mech. Syst.* 2(1):670-679, 2009, https://doi-org.ezproxy.lib.vt.edu/10.4271/2009-01-0451.

[32] WABCO, 2019, “ESCsmart™”, https://www.wabco-auto.com/WabcoWeb/media/Library/Assets/WABCO-pictures/Documents%20(PDF)/Brochures/WABCO_ESCsmart_FactSheet_TRUCK_EN_RGB_WEB-(1).pdf?ext=.pdf

[33] Imine, H., Fridman, L. M., Madani, T., 2012 "Steering Control for Rollover Avoidance of Heavy Vehicles," in *IEEE Transactions on Vehicular Technology*, vol. 61, no. 8, pp. 3499-3509, Oct. 2012, doi: 10.1109/TVT.2012.2206837.

[34] Tan Vu, V., Sename, O., Dugard, L., Gaspar, P., 2017, “Enhancing roll stability of heavy vehicle by LQR active anti-roll bar control using electronic servo-valve hydraulic actuators”, *Vehicle System Dynamics*, DOI: 10.1080/00423114.2017.1317822

[35] Sampson, D.J.M., Cebon, D., 2003, “Achievable roll stability of heavy road vehicles,” *Proceedings of the Institution of Mechanical Engineers, Part D: Journal of Automobile Engineering*. 2003;217(4):269-287. doi:10.1243/09544070360613237

[36] Dunwoody, A. B., Froese, S., "Active Roll Control of a Semi-Trailer." *SAE Transactions* 102 (1993): 999–1004. http://www.jstor.org/stable/44723003.

[37] Bendix, 2015, “Bendix® TABS-6™ Advanced Multi-channel Trailer ABS Module” SD-13-47672, https://atelierjp.ca/wp-content/uploads/2016/07/Manuel-dentretien-RSS-BENDIX.pdf

[38] Haldex, 2008, “Haldex TRS Installation / Service Manual for 4S/2M and 2S/2M Systems,” L30040 5/08 Rev. 5

[39] WABCO, 2015, “Trailer EBS-E,” https://www.wabco-auto.com/WabcoWeb/media/Library/Assets/WABCO-pictures/Documents%20(PDF)/Brochures/Trailer-EBSE_8200100073_web_English.pdf?ext=.pdf

[40] Rakheja, S., Piche, A., 1990, "Development of Directional Stability Criteria for an Early Warning Safety Device," *SAE Transactions* 99, pp. 877-89. http://www.jstor.org/stable/44469456.

[41] Senalik, A. and Medanic, J., "Feasibility of Modifying an Existing Semi-Trailer Air Suspension Into an Anti-Rollover System," SAE Technical Paper 2001-01-2733, 2001, https://doi-org.ezproxy.lib.vt.edu/10.4271/2001-01-2733.

[42] Huang H., Yedavalli R. K., Guenther, D. A., 2012, “Active roll control for rollover prevention of heavy articulated vehicles with multiple-rollover-index minimisation,” *Vehicle System Dynamics*, 50:3, 471-493, DOI: 10.1080/00423114.2011.597863

[43] NHSTA, DOT, Federal Motor Vehicle Safety Standards No. 121; Air Brake Systems, FMVSS 121

[44] NHSTA, DOT, Federal Motor Vehicle Safety Standards No. 121; Air Brake Systems, FMVSS 105

[45] NHTSA, 2011, "Tractor Semi-Trailer Stability Objective Performance Test Research – Roll Stability," NHSTA Report No. DOT HS 811 467

[46] Hou, Y., 2017, “Roll and Yaw Stability Evaluation of Class 8 Trucks with Single and Dual Trailers in Low- and High-speed Driving Conditions,” Ph.D. dissertation, Virginia Polytechnic Institute and State University, Blacksburg, VA

[47] Transportation Research Center, “28. Vehicle Dynamics Area,” https://www.trcpg.com/virtual-facility-tour/vehicles-dynamics-area/

[48] Snyder A., Jones B., Grygier, P., and Garrott, R., "NHTSA Light Vehicle ABS Performance Test Development," *Transportation Research Center Inc NHTSA/NVS,* vol. 312, 2005.

[49] Winkler, C.B., Karamihas, S. M., and Bogard, S. E., 1992, “Roll-Stability Performance of Heavy-Vehicle Suspensions,” *SAE Transactions,* 1992, Vol. 101, Section 2: Journal of Commercial Vehicle (1992), pp. 652-664, https://www.jstor.org/stable/44719839

Appendix A. Analog Sensor Calibration Curves

This appendix contains the calibration curves for all analog sensors installed on the test vehicle.

Table A-1. Calibration curves for sprung mass travel string potentiometers. All string potentiometers have a range of 10 in.

Model (Trailer)	Location	S/N	Calibration Curve y = displacement (in) x = output voltage (V)	R^2
VP-510 (Drop-frame)	Front-Left	31050012	y = 0.9989x + 0.1679	1.0
	Front-Right	30050468	y = 0.9714x + 0.1924	1.0
	Rear-Left	31050010	y = 0.9719x + 0.1981	1.0
	Rear-Right	30030372	y = 0.9819x + 0.1878	0.9999
JX-P510 (Straight-Rail)	Front-Left	50030319	y = 0.9955x + 0.1969	1.0
	Front-Right	50030317	y = 0.9984x + 0.1766	1.0
	Rear-Left	50030318	y = 0.9985x + 0.1772	1.0
	Rear-Right	50030321	y = 0.9986x + 0.1996	1.0
	Spare	50030320	y = 1.0013x + 0.1824	1.0

Table A-2. Calibration curves for triaxial and single-axis accelerometers

Model	Location	S/N	Axis	Sensitivity (mV/g)	Offset (mV)
3713F1110G (Triaxial) ±10g	Front Drop-frame	LW9828	x	132.9	10.4
			y	132.9	6.4
			z	132.9	9.2
	Rear Drop-frame	LW9827	x	133.0	7.1
			y	132.9	7.1
			z	133.0	9.5
	Front Straight-rail	LW9547	x	132.5	8.7
			y	132.5	8.0
			z	133.6	9.9
	Rear Straight-rail	LW9830	x	132.9	10.5
			y	133.3	8.8
			z	133.0	9.8
	Tractor	LW9759	x	132.6	10.5
			y	132.8	7.5
			z	132.9	10.0
3741F1210G (Single-axis) ±10g	Rear Drop-frame & Front Straight-rail*	14410	y	270.0	0.2
	Rear Straight-rail	14409	y	270.0	2.0
*Single-axis accelerometer moved from rear drop-frame to front straight-rail on 10/06/20					

The Honeywell pressure transducers are ratiometric sensors with an input range of 0-250 psi and an input voltage range of 4.75-5.25V. The pressure below converts the output voltage and the excitation voltage into voltage for the Honeywell sensors:

$$P = \frac{V_o - 0.1V_i}{0.8V_i} \times (250\ psi) \qquad (A.1)$$

The OMEGA pressure transducers have an output proportional to the measured pressure, as defined by the equation below:

$$P = \frac{200\ psi}{5\ V} \times (V_o) \qquad (A.2)$$

Table A-3. Curve-fits for all pressure transducers relative to the reference transducer

Brand/Model	**#**	**S/N**	**Curve-fit** y = equivalent reference pressure x = measured pressure	**R-squared**
Honeywell PX2EN1XX250PSAAX	reference	1932410027	y = 0.9946 x + 0.3914	1
	1	1225700097	y = 0.9987 x + 0.4150	1
	2	1424710213	y = 0.9794 x - 0.8805	1
	3	1424710201	y = 0.9871 x + 0.1930	1
	4	1225700100	y = 0.9962 x + 0.9042	1
	5	1932410100	y = 0.9929 x + 0.6217	1
	6	1932400077	y = 0.9910 x + 0.9261	1
	7	1424710198	y = 0.9969 x + 0.2017	1
	8	1424710202	y = 0.9978 x + 0.2363	1
	9	1424710194	y = 0.9962 x + 0.6249	1
	10	1424710203	y = 0.9965 x + 0.2396	1
	11	1225700030	y = 0.9969 x + 0.6637	1
	12	1424710188	y = 0.9971 x + 0.2607	1
	13	1424710187	y = 0.9956 x + 0.5589	1
	14	1932510230	y = 0.9924 x + 0.5137	1
	15	1932410083	y = 0.9953 x + 0.4655	1
	16	1932900052	y = 0.9976 x + 0.7787	1
	17	1932310116	y = 0.9966 x + 0.7023	1
	18	1932310126	y = 0.9952 x + 0.7882	1
	19	1932310148	y = 0.9856 x + 0.6637	1
	20	1932300158	y = 0.9934 x + 1.5438	1
	21	1932300157	y = 0.9967 x + 0.7902	1
OMEGA PX329-200G5V	22	091413D194	y = 0.9973 x - 0.6394	1
	23	042614D073	y = 0.9941 x - 0.6974	1
	24	091413D177	y = 0.9957 x - 0.3317	1
	25	111111D111	y = 0.9932 x - 0.9410	1
	26	092913D230	y = 1.0337 x - 5.0371	1

The load cells are ratiometric sensors with a maximum rated tensile load of 200,000 lbf. The load cells were provided with their sensitivity values, shown in

$$F = \frac{F_{max} V_o}{V_i S} \qquad (A.3)$$

Table A-4. Sensitivity of load cells provided by the manufacturer

S/N	**Sensitivity** [mV/V]
F90522131	1.5668
F90522132	1.5384
F90522133	1.5491
F90522134	1.5134
F90522135	1.5437
F90522136	1.5533
F90522137	1.5673
F90603102	1.5549

Appendix B: Tests Performed at TRC

In this section, tables containing all test series performed in the high-speed study at TRC are given. Tables will be organized by test session and will each contain a single day of testing.

Test Session 1: Shakedown & Baseline

Table B-1. Tests performed at TRC on August 26, 2020.

Date: Wednesday, August 26, 2020 Testing duration: 5.5 hours Weather: Sunny, 85º/88º, Wind: 8-12 mph SSW						
Test series	**Maneuver**	**Loading condition**	**RSC**	**ESC**	**# of tests**	**Total test #**
1	J-turn	Heavy	Off	Off	8	117
2	Ramp-steer (Tuning)*	Heavy	Off	Off	11	
3	0.5 Hz SWD (Tuning)*	Heavy	Off	Off	9	
4	40 mph - 0.5 Hz SWD*	Heavy	Off	Off	4	
5	45 mph - 0.5 Hz SWD*	Heavy	Off	Off	5	
6	40 mph – 0.25 Hz SWD*	Heavy	Off	Off	8	
7	45 mph – 0.25 Hz SWD*	Heavy	Off	Off	5	
8	40 mph – 0.25 Hz SWD*	Heavy	Off	Off	7	
9	45 mph – 0.25 Hz SWD*	Heavy	Off	Off	8	
10	40 mph – 0.5 Hz SWD*	Heavy	Off	Off	4	
11	45 mph – 0.5 Hz SWD*	Heavy	Off	Off	5	
12	DLC	Heavy	Off	Off	13	
13	40 mph – 0.5 Hz SWD*	Heavy	Off	Off	8	
14	45 mph – 0.5 Hz SWD*	Heavy	Off	Off	6	
15	40 mph – 0.25 Hz SWD*	Heavy	Off	Off	5	
16	45 mph – 0.25 Hz SWD*	Heavy	Off	Off	6	
17	Ramp-steer*	Heavy	Off	Off	5	
* Data not used for analysis; SWD = sine with dwell; DLC = double lane change						

Test Session 2: Heavy Load

Table B-2. Tests performed at TRC on September 14, 2020.

Date: Monday, September 14, 2020 Testing duration: 5.5 hours Weather: Partially cloudy, 63°/75°, Wind: 6-11 mph WNW						
Test series	**Maneuver**	**Loading condition**	**RSC**	**ESC**	**# of tests**	**Total test #**
1	J-turn	Heavy	On	Off	7	110
2	Ramp-steer	Heavy	On	Off	9	
3	Ramp-steer	Heavy	Off	Off	4	
4	SWD (robot tuning)*	Heavy	Off	Off	17	
5	40-mph 0.5-Hz SWD	Heavy	Off	Off	6	
6	45-mph 0.5-Hz SWD	Heavy	Off	Off	6	
7	40-mph 0.25-Hz SWD	Heavy	Off	Off	6	
8	45-mph 0.25-Hz SWD	Heavy	Off	Off	5	
9	J-turn	Heavy	On	Off	6	
10	J-turn	Heavy	On	On	8	
11	Ramp-steer	Heavy	On	On	6	
12	Ramp-steer	Heavy	On	Off	5	
13	40-mph 0.5-Hz SWD	Heavy	On	Off	7	
14	45-mph 0.5-Hz SWD	Heavy	On	Off	6	
15	40-mph 0.25-Hz SWD	Heavy	On	Off	6	
16	45-mph 0.25-Hz SWD	Heavy	On	Off	6	
* Data not used for analysis; SWD = sine with dwell; DLC = double lane change						

Table B-3. Tests performed at TRC on September 16, 2020.

Date: Wednesday, September 16, 2020 Testing duration: 2.0 hours Weather: Sunny, 70°, Wind: 3 mph SE						
Test series	**Maneuver**	**Loading condition**	**RSC**	**ESC**	**# of tests**	**Total test #**
1	40-mph 0.5-Hz SWD	Heavy	On	On	6	37
2	45-mph 0.5-Hz SWD	Heavy	On	On	6	
3	40-mph 0.25-Hz SWD	Heavy	On	On	6	
4	45-mph 0.25-Hz SWD	Heavy	On	On	6	
5	DLC	Heavy	On	On	7	
6	DLC	Heavy	On	Off	6	

Test Session 3: Light Load

Table B-4. Tests performed at TRC on September 18, 2020.

Date: Friday, September 18, 2020 Testing duration: 5.5 hours Weather: Sunny, 53º/60º, Wind: 10-11 mph NNW						
Test series	**Maneuver**	**Loading condition**	**RSC**	**ESC**	**# of tests**	**Total test #**
1	40-mph 0.5-Hz SWD	Light	On	Off	6	
2	45-mph 0.5-Hz SWD	Light	On	Off	7	
3	40-mph 0.5-Hz SWD	Light	On	On	6	
4	45-mph 0.5-Hz SWD	Light	On	On	7	
5	40-mph 0.25-Hz SWD	Light	On	On	6	
6	45-mph 0.25-Hz SWD	Light	On	On	7	
7	40-mph 0.25-Hz SWD	Light	On	Off	6	
8	45-mph 0.25-Hz SWD	Light	On	Off	7	
9	Ramp-steer	Light	On	Off	9	
10	DLC	Light	On	Off	8	
11	J-turn	Light	On	Off	8	156
12	J-turn	Light	On	On	8	
13	DLC	Light	On	On	10	
14	Ramp-steer	Light	On	On	8	
15	DLC	Light	Off	Off	8	
16	45-mph 0.5-Hz SWD	Light	Off	Off	10	
17	45-mph 0.25-Hz SWD	Light	Off	Off	9	
18	Ramp-steer	Light	Off	Off	6	
19	J-turn	Light	Off	Off	6	
20	40-mph 0.5-Hz SWD	Light	Off	Off	6	
21	40-mph 0.25-Hz SWD	Light	Off	Off	8	

Test Session 4 (Oct 05 – Oct 08): Mixed Load, Mixed Trailer

Table B-5. Tests performed at TRC on October 5, 2020.

Date: Monday, October 5, 2020 Testing duration: 1.5 hours Weather: Cloudy, 43°, Wind: 2 mph E						
Test series	**Maneuver**	**Loading condition**	**RSC**	**ESC**	**# of tests**	**Total test #**
1	J-turn*	Mixed	Off	Off	8	34
2	Ramp-steer*	Mixed	Off	Off	9	
3	45-mph 0.25-Hz SWD*	Mixed	Off	Off	5	
4	DLC*	Mixed	Off	Off	12	
*Data not used for analysis (large accelerometer noise); SWD = sine with dwell; DLC = double lane change						

Table B-6. Tests performed at TRC on October 6th, 2020.

Date: Tuesday, October 6, 2020 Testing duration: 5.0 hours Weather: Sunny, 56°/68°, Wind: 10-16 mph SE						
Test series	**Maneuver**	**Loading condition**	**RSC**	**ESC**	**# of tests**	**Total test #**
1	J-turn	Mixed	Off	Off	8	115
2	Ramp-steer	Mixed	Off	Off	7	
3	45-mph 0.25-Hz SWD	Mixed	Off	Off	6	
4	DLC	Mixed	Off	Off	14	
5	J-turn	Mixed	On	On	10	
6	DLC	Mixed	On	On	12	
7	J-turn	Mixed	On	Off	9	
8	DLC	Mixed	On	Off	15	
9	Ramp-steer	Mixed	On	Off	8	
10	45-mph 0.25-Hz SWD	Mixed	On	Off	8	
11	45-mph 0.25-Hz SWD	Mixed	On	On	8	
12	Ramp-steer	Mixed	On	On	10	

Table B-7. Mixed trailer tests performed at TRC on October 7th, 2020.

Date: Wednesday, October 7, 2020 Testing duration: 5.0 hours Weather: Sunny, 58°/68°, Wind: 12-22 mph SE							
Test series	**Maneuver**	**Trailer Combination**	**Loading condition**	**RSC**	**ESC**	**# of tests**	**Total test #**
1	J-turn	Drop-Straight	Heavy	On	Off	12	99
2	DLC	Drop-Straight	Heavy	On	Off	15	
3	J-turn	Drop-Straight	Heavy	On	On	9	
4	DLC	Drop-Straight	Heavy	On	On	8	
5	Ramp-steer	Drop-Straight	Heavy	On	On	10	
6	45-mph 0.25-Hz SWD	Drop-Straight	Heavy	On	Off	7	
7	45-mph 0.25-Hz SWD	Drop-Straight	Heavy	On	On	7	
8	Ramp-steer	Drop-Straight	Heavy	On	Off	8	
9	J-turn	Drop-Straight	Heavy	Off	Off	7	
10	Ramp-steer	Drop-Straight	Heavy	Off	Off	5	
11	DLC	Drop-Straight	Heavy	Off	Off	6	
12	45-mph 0.25-Hz SWD	Drop-Straight	Heavy	Off	Off	5	
SWD = sine with dwell; DLC = double lane change							

Table B-8. Mixed trailer tests performed at TRC on October 8th, 2020.

Date: Thursday, October 8, 2020 Testing duration: 4.5 hours Weather: Sunny, 47°/62°, Wind: 0-7 mph NNW							
Test series	**Maneuver**	**Trailer Combination**	**Loading condition**	**RSC**	**ESC**	**# of tests**	**Total test #**
1	J-turn	Straight-Drop	Heavy	On	Off	6	76
2	DLC	Straight-Drop	Heavy	On	Off	7	
3	J-turn	Straight-Drop	Heavy	On	On	6	
4	DLC	Straight-Drop	Heavy	On	On	10	
5	Ramp-steer	Straight-Drop	Heavy	On	On	7	
6	45-mph 0.25-Hz SWD	Straight-Drop	Heavy	On	Off	7	
7	45-mph 0.25-Hz SWD	Straight-Drop	Heavy	On	On	6	
8	Ramp-steer	Straight-Drop	Heavy	On	Off	5	
9	J-turn	Straight-Drop	Heavy	Off	Off	6	
10	Ramp-steer	Straight-Drop	Heavy	Off	Off	5	
11	DLC	Straight-Drop	Heavy	Off	Off	5	
12	45-mph 0.25-Hz SWD	Straight-Drop	Heavy	Off	Off	6	
SWD = sine with dwell; DLC = double lane change							

Test Session 5 (Oct 12): Trailer Disc Brakes

Table B-9. Tests performed at TRC on October 12, 2020.

Date: Monday, October 12, 2020 Testing duration: 4.5 hours Weather: Cloudy, 64°/68°, Wind: 9 mph SE						
Test series	**Maneuver**	**Loading condition**	**RSC**	**ESC**	**# of tests**	**Total test #**
1	J-turn	Heavy	On	Off	5	80
2	DLC	Heavy	On	Off	9	
3	J-turn	Heavy	On	On	6	
4	DLC	Heavy	On	On	8	
5	Ramp-steer	Heavy	On	On	7	
6	45-mph 0.25-Hz SWD	Heavy	On	Off	6	
7	45-mph 0.25-Hz SWD	Heavy	On	On	8	
8	Ramp-steer	Heavy	On	Off	6	
9	Ramp-steer	Heavy	Off	On	6	
10	DLC	Heavy	Off	On	7	
11	45-mph 0.25-Hz SWD	Heavy	Off	On	6	
12	J-turn	Heavy	Off	On	6	

Appendix C: Method of Determining Probability of Rollover

This section contains the table for determining the rollover entry speed or rollover steering percentage based on outrigger contact force for a given trailer configuration. Table C-1 delineates the process followed to determine such speeds/steering percentages.

Table C-1. Procedure for determining rollover speed and rollover steering percentage based on the outrigger wheel contact force across a number of trails.

Number of Trials	No Outrigger Contact	Outrigger Contact < 400lbf	Outrigger Contact >= 400lbf & <1000 lbf	Outrigger Contact > 1000lbf	Rollover Threshold ?
0*	-	-	-	-	Maybe**
1	0	1	0	0	No
1	0	0	1	0	Maybe**
1	0	0	0	1	Yes
2	1	1	0	0	No
2	1	0	1	0	Maybe**
2	1	0	0	1	Yes
2	0	2	0	0	No
2	0	1	1	0	Maybe**
2	0	0	2	0	Yes
2	0	0	1	1	Yes
2	0	0	0	2	Yes
3	2	1	0	0	No
3	2	0	1	0	No
3	2	0	0	1	No
3	1	2	0	0	No
3	1	1	1	0	No
3	1	1	0	1	No
3	1	0	2	0	Yes
3	1	0	1	1	Yes
3	1	0	0	2	Yes
3	0	3	0	0	No
3	0	2	1	0	No
3	0	2	0	1	No
3	0	1	2	0	Yes
3	0	1	1	1	Yes
3	0	1	0	2	Yes
3	0	0	3	0	Yes
3	0	0	2	1	Yes
3	0	0	1	2	Yes
3	0	0	0	3	Yes

* In cases where there was no test performed at a particular speed, the outrigger contacts at the speeds 1 mph below and 1 mph above were used to determine the rollover speed.
** In cases where the rollover threshold is determined as "Maybe", the outrigger contacts at the speeds 1 mph below and 1 mph above were used to determine if the speed is or is not the rollover speed.